Stony Brook University

The Role of FGF signaling in neural and mesodermal fate choice in the zebrafish

A Dissertation Presented

By

Eric Londin

To

The Graduate School

In Partial fulfillment of the

Requirements

For the Degree of

Doctor of Philosophy

In

Genetics

Stony Brook University

December 2007

Stony Brook University

The Graduate School

Eric Londin

We, the dissertation committee for the above candidate for the

Doctor of Philosophy degree,

hereby recommend acceptance of this dissertation.

Dr. Howard I. Sirotkin, Assistant Professor, Department of Neurobiology and Behavior, State University of New York at Stony Brook (Dissertation Advisor)

Dr. Maurice Kernan, Assistant Professor, Department of Neurobiology and Behavior, State University of New York at Stony Brook (Chairperson of Defense)

Dr. Gerald H. Thomsen, Associate Professor, Department of Biochemistry and Cell Biology, State University of New York at Stony Brook

Dr. Bernadette Holdener, Associate Professor, Department of Biochemistry and Cell Biology, State University of New York at Stony Brook

Dr. Ken-Ichi Takemaru, Assistant Professor, Department of Pharmacology, State University of New York at Stony Brook

Dr. Nathalia Glickman Holtzman, Assistant Professor, Department of Biology, Queens College

This Dissertation is accepted by the Graduate School

Lawrence B. Martin, Dean of the Graduate School

Abstract the of the Dissertation

The Role of FGF signaling in neural and mesodermal fate choice in the zebrafish

By

Eric Londin

Doctor of Philosophy

In

Genetics

Stony Brook University

2007

The ectoderm gives rise to both neural and epidermal tissues. An important step in the specification of the neural plate is the inhibition of bone morphogenetic proteins (BMP) in the dorsal ectoderm by extracellular BMP antagonists originating from the organizer. However, even in the absence of the organizer, zebrafish embryos still develop well-patterned neural tissue suggesting that other signals are involved in neural induction. Here, the role of fibroblast growth factor (FGF) signaling is examined in zebrafish neural development. FGFs first act in the blastula to inhibit transcription of *bmp* mRNA, and later during gastrulation, FGF signals induce Chordin expression. These results show a clear role for FGF in formation of the neural plate. In addition to neural induction, FGF signaling has long been known to be essential in patterning of the mesoderm. Both neural and mesodermal patterning are occurring in similar time and space to each other, raises question of how the

two functions of FGF signaling are regulated. Recent insights into the regulation of FGF signaling came with the identification of the FGF regulated transcription factor Churchill (*chch*). Examination of *chch's* function reveals that *chch* is required to limit mesoderm formation. Through the use of cell transplantation experiments, *chch* inhibited cells were found to exhibit an increased migratory behavior. Furthermore these cells migrate out of the epiblast and into the germ ring, but blocking Nodal signaling prevents these cell movements. Additionally, *chch* limits the transcriptional response to Nodal signals. These results suggest that *chch* regulates both cell movements and mesodermal gene expression. The mechanism of *chch's* function may come through the Smad interacting protein 1 (*Sip1*) gene. *Sip1* has been shown to have roles in inhibiting TGF-β signaling, induction of neural gene expression and inhibition of mesodermal gene expression and regulating cell movements. Taken together, the results presented here show a role for FGF signaling in neural and mesodermal patterning.

Table of Contents

List of figures

List of tables

Acknowledgements:

I would like to thank the following people for their support and assistance:

My wife and best friend, Jessica Dutton. Thank you for your never-ending support and helping me through some hard times.

My parents. Thank you for always supporting and believing in me in helping me achieve my goals.

My advisor, Howard Sirotkin, for having had a mentor who constantly encouraged me throughout the last few years. I am thankful for the skills and knowledge that you taught me which will help me further my career.

My thesis committee, Maurice Kernan, Bernadette Holdener, Ken-Ichi Takemaru, Gerald H. Thomsen and Nathalia Glickman Holtzman. Thank you for your advice, insights and direction

My current and former labmates, Jack Niemiec, Laurie Mentzer, Kieth Gates Fatma Kok and Rich Grady. Thank you for all of your help, support, advice and insights made my work possible.

The direction and staff of the Genetics graduate program, in particular, Kate Bell.

Chapter 1: Background and Significance

The mechanism by which a fertilized egg develops into a patterned embryo is a question that has been studied for over a century. Early embryology studies focused on the structure of the embryo and the formation of the early germ layers. These studies identified positions of precursors for different tissues and organs within the developing embryo. More modern studies have been able to use cellular, molecular and genetic techniques to provide insights into the mechanisms determining patterning of the embryo. Together, classical and modern embryological studies provided a wealth of information about the formation and patterning of an embryo, but many question still remain to be answered. For my thesis work presented here, I have utilized the zebrafish as an animal model to study the mechanisms involved in patterning of the nervous system.

1.1 Zebrafish as an animal model for embryonic development:

Over the past 20 years, zebrafish have emerged as a powerful model system for studying vertebrate development. The ability to generate a large amount of easily accessible embryos (Streisinger et al., 1981) and the optical transparency of the embryo has allowed for the development of a wide variety of developmental tools such as time-lapse imaging, fate-mapping and cell transplantations (Kimmel, 1989). In addition, the embryos are experimentally accessible for molecular techniques including microinjection of *in vivo* transcribed mRNA, plasmid DNA constructs, and morpholinos. Whole mount *in situ* hybridization to examine localization of mRNAs during development can all be performed. The rapid development of the embryo occurs allows for robust expression of injected transcripts and transgenic fish can be generated by microinjection of plasmid constructs (Udvadia and Linney, 2003). Forward and reverse genetic screens have been performed to identify mutants in all aspects of early development from early embryonic patterning to latter organogenesis (Driever et al., 1996; Haffter et al., 1996).

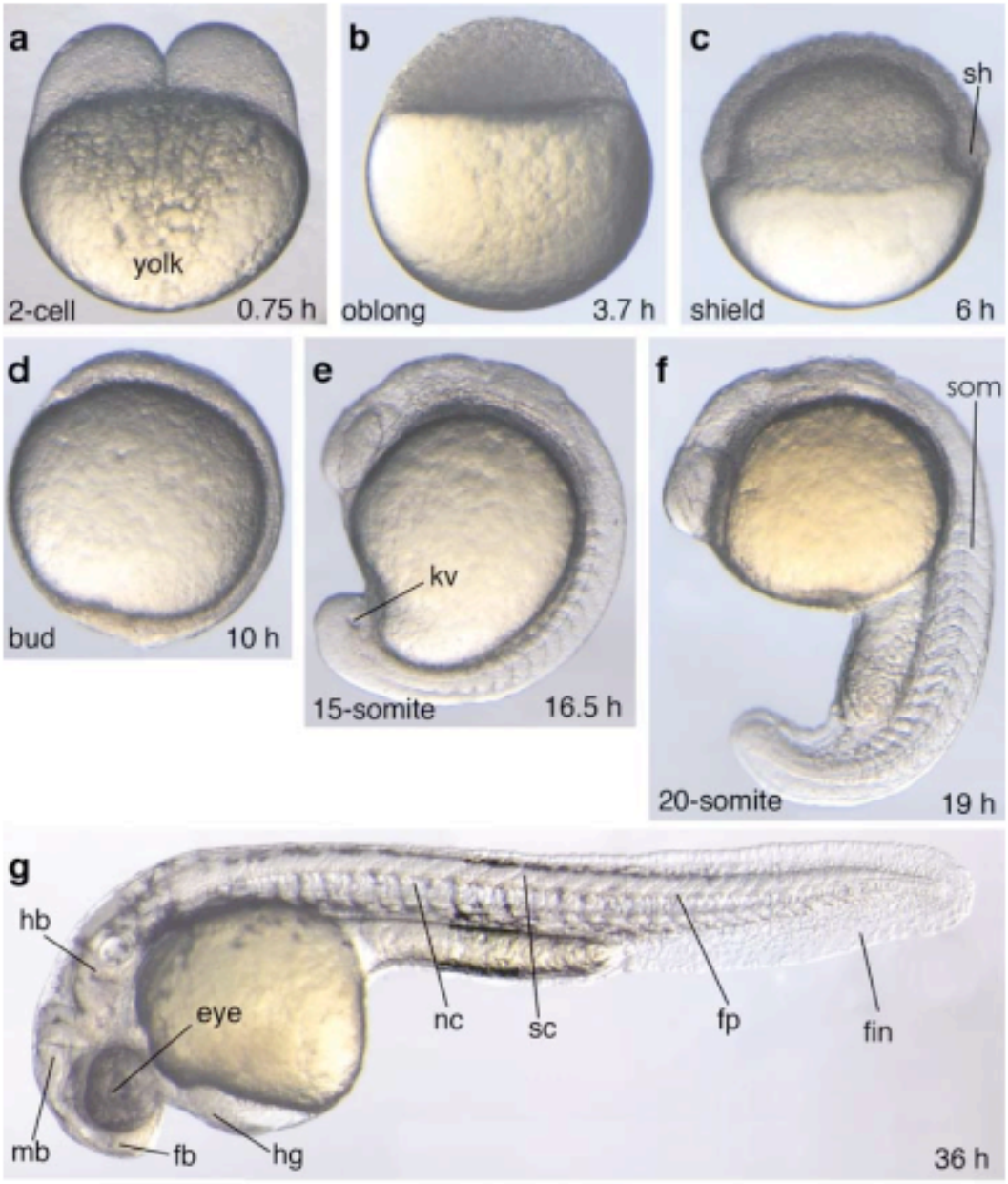

Figure 1.1. Zebrafish Embryogenesis. Living embryos are shown at the indicated stages and hours (h) of development. Embryos are oriented with the animal pole to the top (a-f) and dorsal to the right (c-f), anterior to the left (g) and dorsal to the top. Abbreviations: sh, shield; kv, Kupffer's vesicle; som, somite; hg, hatching gland; fb, forebrain; mb, midbrain; hb, hindbrain; nc, notochord; sc, spinal cord; fp, floor plate. Figure adapted from (Schier and Talbot, 2005).

During the first three hours of zebrafish development, rapid cell division occurs with a pile of cells forming on top of the yolk. These cell divisions result in a large number of cells while the total volume of the embryo does not change (Figure 1.1). These cells form the embryo proper, while the cells in the yolk make up the extraembryonic structures. At three hours of development, the cell cycles lengthen and the mid-blastula transition (MBT) occurs, which is the time that zygotic transcription begins to occur (Kimmel et al., 1995). Prior to this time, development is controlled by maternally deposited mRNAs and proteins.

After four hours of development, the cells of the embryo begin to intercalate and spread over the yolk in a process called epiboly. The cells of the embryo continue to converge and extend over the yolk during gastrulation. This convergence of cells towards the dorsal side of the embryo results in the formation of the shield (zebrafish Spemann organizer) and for the first time, specific polarity of the embryo can be identified (Figure 1.1). At this time, the embryo has become divided into three germ layers; endoderm which gives to the gastrointestinal tract and its associated structures; ectoderm which gives rise to epidermis and the nervous system; and mesoderm which gives rise to bone, muscle, connective tissue, urogenital track and the circulatory system. This is also the time that dorsal-ventral patterning has become apparent. By the end of gastrulation, the cells have spread over the yolk (Kimmel et al., 1995).

Following the gastrulation period, after 10 hours of development, begins the segmentation period. Here, different sets of cell movements take place, which culminates with somite development. The primary organs become visible, a prominent tail bud forms, and the elongation of the embryo occurs (Figure 1.1). The anterior-posterior (AP) and dorso-ventral (DV) axes become clearly visible. By the end of this period of development (24 hpf) there are morphologically distinct cell types and the first body movements take place (Kimmel et al., 1995) (Figure 1.1).

1.2 Embryonic fate maps:

Upon induction of the germ layers during gastrulation, a fate map demarcating the position for different tissues and organs can be defined (Kimmel et al., 1990). The precursor cells of the different germ layers are arranged along the animal-vegetal axis. The ectoderm cells are

located animally in the embryo and more marginally located are an intermingled mix of mesodermal and endoderm cells called the mesendoderm.

In zebrafish, a cells position during early cleavage stages does not determine the fates of its descendant cells. Furthermore, the plane of cell divisions during early cleavage stages does not predict their position along the future dorsal-ventral (DV) axis (Helde et al., 1994). In addition, most of these pre-gastrula stage cells are not committed to particular fates, further preventing the fate of a cell from being predicted (Ho and Kimmel, 1993). But, by early gastrula stages cell fates can be predicted based upon the position within the embryo.

The DV axis of the embryo contains precursor cells for mesoderm, ectoderm and endoderm cell types. In the ectodermal region, non-neural ectoderm or epidermis is derived from the ventral animal region of the embryo (Figure 1.2). Conversely, neural derivatives are more dorsally located. Within this region, the forebrain and midbrain precursors are more animally located while hindbrain and spinal cord derivatives are more laterally located (Woo and Fraser, 1995). Similarly, different mesodermal precursors are also located along the DV axis. In the mesodermal region, the most dorsally located cells are compromised of the shield and gives rise to axial mesoderm structures including the notochord and prechordal plate, while more laterally located cells give rise to the heart and trunk somites. Blood and pronepheros are derived from marginal cells ventral from the shield (Figure 1.2). Tail mesodermal cells are also derived from the ventral mesodermal region of the embryo. The various endodermal precursors are also located along the DV axis, here, the pharynx derivatives are located dorsally while stomach, intestine and liver are ventrally located (Warga and Kimmel, 1990).

While cell positions within the embryo are important in determining their final fate, embryological regions in the embryo have been identified that are sufficient to induce specific fates in neighboring cells. The dorsal margin contains factors essential for dorsal, anterior and lateral cell types while repressing ventral and posterior fates (Figure 1.2) (Saude et al., 2000; Schier, 2003). Conversely, the ventral margin can induce posterior structures (Agathon et al., 2003; Woo and Fraser, 1997).

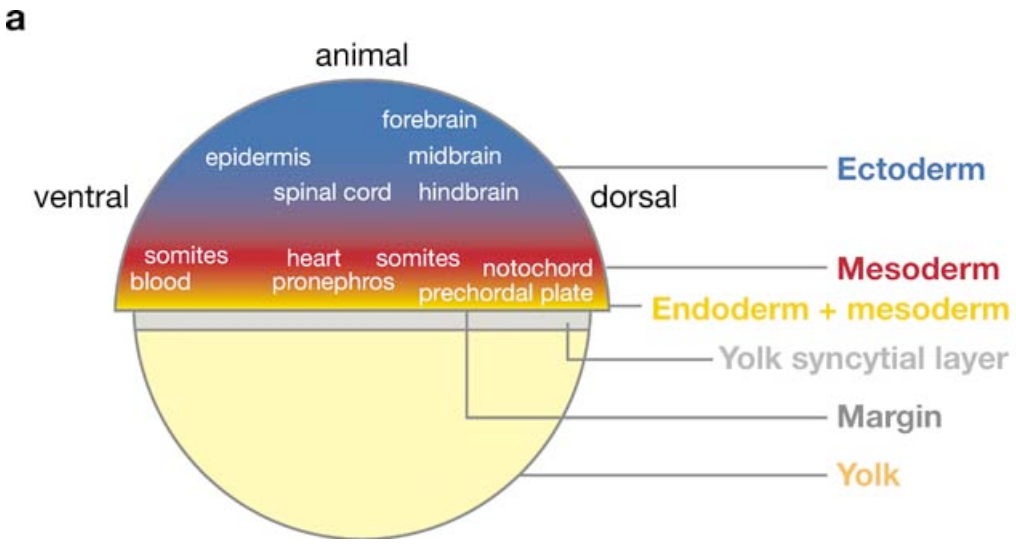

Figure 1.2. Fate map of the zebrafish embryo during early gastrulation. At 50% epiboly the germ layers are arranged along the animal-vegetal axis with the ectoderm (blue) at the most animal pole, mesoderm (red) is located vegetally near the margin and a mix of endoderm and mesoderm (yellow) also known as the mesendoderm, is at the margin. The specific fates of the germ layers are arranged along the dorsal-ventral axis. In the ectodermal region, neural fates are dorsally located and epidermal fates are ventrally located. In the mesendodermal region, axial mesodermal fates are dorsally located and posterior structures are ventrally located (Schier and Talbot, 2005).

1.3 Germ layer formation:

The response of a cell to various signaling pathways and molecules will determine their final fate. During gastrulation, the blastoderm cells are specified and move to generate an embryo with the three germ layers as well as anterior-posterior and dorsal-ventral polarity. The different types of cell movements that occur during gastrulation place the cells into contact with different signaling pathways and molecules helping to determine their final fate. Upon movement to different regions of the embryo, the cell interactions with various signaling pathways such as Nodal, bone morphogenetic proteins (BMP) and fibroblast growth factors (FGF) will further help determine the its fate. Here, the process of gastrulation as well as some of the important signaling pathways involved in germ layer formation will be reviewed.

1.3.1 Gastrulation cell movements in cell movements:

Gastrulation is a set of cell movements that results in the formation of a subdivided embryo with three distinct germ layers and clear polarity along the anterior-posterior and dorso-ventral axis (Leptin, 2005). Four types of cell movements occur during gastrulation (epiboly, internalization, convergence and extension movements), which result in the properly patterned embryo.

Gastrulation begins after the embryo has reached the end of blastulation. At this time, the embryo has a mass of cells (the blastoderm) on top of the yolk, and the process of epiboly begins. During epiboly, the deep cells of the blastoderm move outward to intermix with more superficial cells (Warga and Kimmel, 1990). This mixture of cells moves vegetally over the surface of the yolk eventually encapsulating it. Ultimately, one side of the blastoderm becomes thicker, becoming the dorsal side of the embryo (Solnica-Krezel and Driever, 1994). Once epiboly has covered 50% of the yolk, the morphological process of internalization begins which results in the formation of mesoderm and endoderm. Accumulated cells at the marginal zone create a thickened ring of cells around the yolk called the germ ring. Beginning dorsally, then around all points of the margin, cells internalize and migrate towards the animal pole forming an internal layer of cells (Montero and Heisenberg, 2004; Warga and Kimmel, 1990). Both the overlapping and non-involuting ectoderm

continue to undergo epiboly resulting in a separation of mesodermal and ectodermal cell layers during gastrulation (Figure 1.3).

Beginning at the same time as internalization, are the movements of convergence extension (CE). Convergence refers to a mediolateral narrowing of the embryo by the movement of cells towards the dorsal side of the embryo, while extension is the elongation of the anterior-posterior axis of the embryo also on the dorsal side (Warga and Kimmel, 1990). Dorsally located cells exhibit increased amounts of movements while ventrally located mesoderm does not move dorsally or extend toward the animal pole but rather moves towards the vegetal pole and contributes to the tail bud (Myers et al., 2002a; Myers et al., 2002b) (Figure 1.3).

Various signaling pathways and molecules including the Nodal and FGF signaling pathways regulate the complex cell movements during gastrulation. For example, Nodal signaling regulates internalization and specification of the mesoderm. In mouse and zebrafish Nodal signaling mutants, prospective mesoderm and endoderm fail to internalize (Feldman et al., 1998; Gritsman et al., 1999; Zhao et al., 2003), instead these cells become incorporated into the neuroectoderm. Nodal signaling must be restricted prior to the start of gastrulation to prevent excessive internalization of mesodermal cells (Bertocchini and Stern, 2002; Perea-Gomez et al., 2002). FGF signaling mutants in mice and *Xenopus* show defects in specification and internalization of mesoderm (Amaya et al., 1991; Yamaguchi et al., 1994). Here, FGFs downregulate *E-cadherin* expression, preventing epiboly movements (Babb and Marrs, 2004; Kane et al., 2005).

Gastrulation is a complex process resulting in the formation of a patterned embryo where the three germ layers become distinct. These cell layers will eventually give rise to every tissue and organ formed in the adult.

1.3.2 Signaling pathways involved in germ layer formation:

Three signaling pathways important for germ layer formation are Nodal, BMPs, and FGFs. Each of these signaling pathways have unique functions in germ layer formation, but there is also a significant amount interaction between the pathways (Figure 1.4).

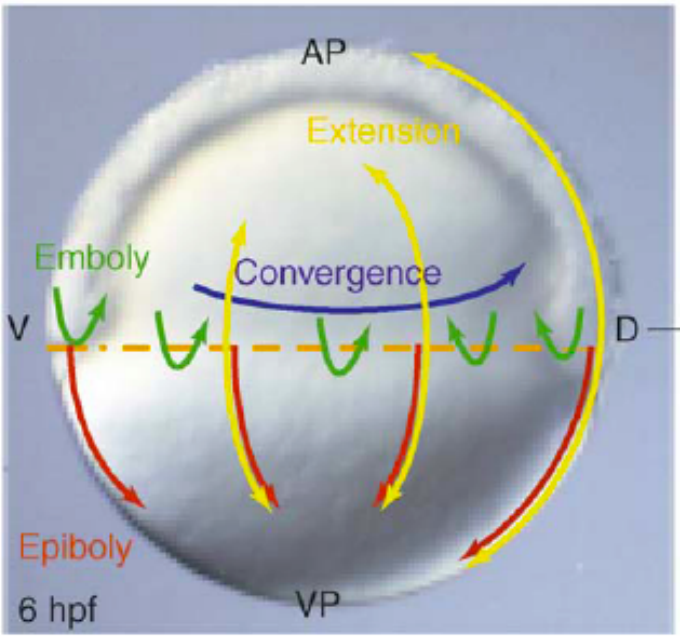

Figure 1.3. Gastrulation movements in zebrafish. Gastrulation movements at shield stage. Shown as dorsal to the right, ventral to the left, anterior to the top and ventral to the bottom. The yolk cell is domed at the animal pole forming an inverted cup shape. The four gastrulation movements are shown with epiboly (red arrows), emboly (internalization) (green arrows), convergence (blue arrows), and extension (yellow arrows). The blastoderm cells undergo epiboly towards the vegetal pole, the prospective mesendodermal cells internalize at the margin. Cells converge towards the dorsal side and extend along the animal-vegetal axis. The net result of these movements is to transform a blastula stage embryo into an embryo containing head and trunk rudiments. Figure modified from (Solnica-Krezel, 2006).

Transforming Growth Factors-ß (TGF- ß) Signaling: Both Nodal and BMP signaling are apart of the transforming growth factor ß (TGF- ß) signaling pathway. The pathways are activated by binding of the ligand to the extracellular domain of the type II receptor, which induces a conformational change, resulting in the phosphorylation and activation of the type I receptor. Once activated, the receptor transduces the signal to the appropriate Smad proteins. There are three classes of Smad proteins: (i) the receptor-activated Smads, Smad1, Smad2, Smad3, Smad5 and Smad8; (ii) the co-mediator Smad, Smad 4; and (iii) the inhibitory Smads, Smad6 and Smad7. The Nodal signaling pathway predominately signals through Smad2 and Smad3, while the BMP pathway signals through Smad1, Smad5 and Smad8 (Figure 1.4). Once activated, the receptor Smads form a complex with Smad4 and translocates to the nucleus where they can stimulate gene expression of target genes (Feng and Derynck, 2005; Kitisin et al., 2007) (Figure 1.4). In the Nodal signaling pathway an additional co-receptor, EGF-CFC, is required for signaling to occur (Gritsman et al., 1999).

Nodal signaling plays a central role in development and has been shown to be important in axis formation, mesoderm and endoderm induction, neural patterning and left-right development. At the start of gastrulation, Nodal signals specify mesoderm and endodermal fates, and in fact, in the absence of Nodal signaling, progenitor cells acquire inappropriate fates (Carmany-Rampey and Schier, 2001; Feldman et al., 2000). For instance, dorsal marginal cells give rise to hindbrain and midbrain fates instead of notochord and prechordal plate. Instead of internalizing mesoderm or endoderm, Nodal inhibited cells stay on the surface of the embryo and become incorporated into the neuroectoderm (Carmany-Rampey and Schier, 2001; Feldman et al., 2000). With the exception of the tail somites, Nodal signaling is required for the induction of all mesoderm cell types (Feldman et al., 1998; Gritsman et al., 1999).

While Nodal signaling is required for mesoderm formation, different levels of Nodal signals induce different cell fates. Higher levels of Nodal will induce *goosecoid (gsc)* while *brachyury* requires lower levels of Nodal signals for its proper induction, although there is a vegetal shift in the location of mesodermal progenitors (Dougan et al., 2003). Higher levels of Nodal signals induce dorsal fates rather than ventral fates (Dougan et al., 2003). Similarly, high levels of Nodal signals are also required for endoderm induction (Schier et al., 1997;

Thisse et al., 2000), and are absent when Nodal signaling is lost. Taken together, different levels of Nodal signaling activity can induce different fates.

In addition to being required for mesoderm and endoderm formation, neural patterning requires repression of Nodal signals, which need to be blocked within the prospective neuroectoderm (Piccolo et al., 1999). Mutations in the Nodal pathway lead to the absence of medial floor plate and ventral forebrain and cyclopic embryos (Schier et al., 1997; Strahle et al., 1997).

Sharing a similar signaling pathway as Nodal, bone morphogenetic proteins (BMP) are also involved in determination of ventral mesoderm and epidermal cell fates. BMP signals are required for dorsal-ventral patterning during early gastrulation whereas by mid-gastrulation regulate tail development (Pyati et al., 2005). Zebrafish BMP mutants fail to develop tails suggesting a requirement for development of posterior fates (Kishimoto et al., 1997). Graded BMP signals along the dorsal-ventral axis pattern the mesoderm (Neave et al., 1997; Nikaido et al., 1997) and ventral-lateral margin fates such as blood, heart, and tail somites, are formed from a BMP gradient.

Within the ectoderm, the neural-ectoderm is inhibited where BMP is expressed. A BMP gradient within the ectoderm corresponds to the neural-epidermal boundary. The ventral ectoderm contains the highest amount of BMP signals and induces epidermis, while the dorsal ectoderm has inhibited BMP signals, and differentiates into to the neuroectoderm (Barth et al., 1999). Taken together, both BMP and Nodal signals have complex roles in germ layer formation.

Fibroblast Growth Factor (FGF) Signaling: Another signaling pathway important during development is the fibroblast growth factor (FGF) signaling pathway. The binding of a FGF ligand to its receptor results in the dimerization and phosphorylation of the cytoplasmic domain of the receptor. This phosphorylation activates the G-protein Ras, and subsequently activates Raf (Figure 1.4). Raf activates Mek resulting in the phosphorylation and activation of MAP kinase (Mapk). Once activated, Mapk enters the nucleus where it activates transcription factors, ultimately resulting in the transcription of target genes (Bottcher et al., 2004).

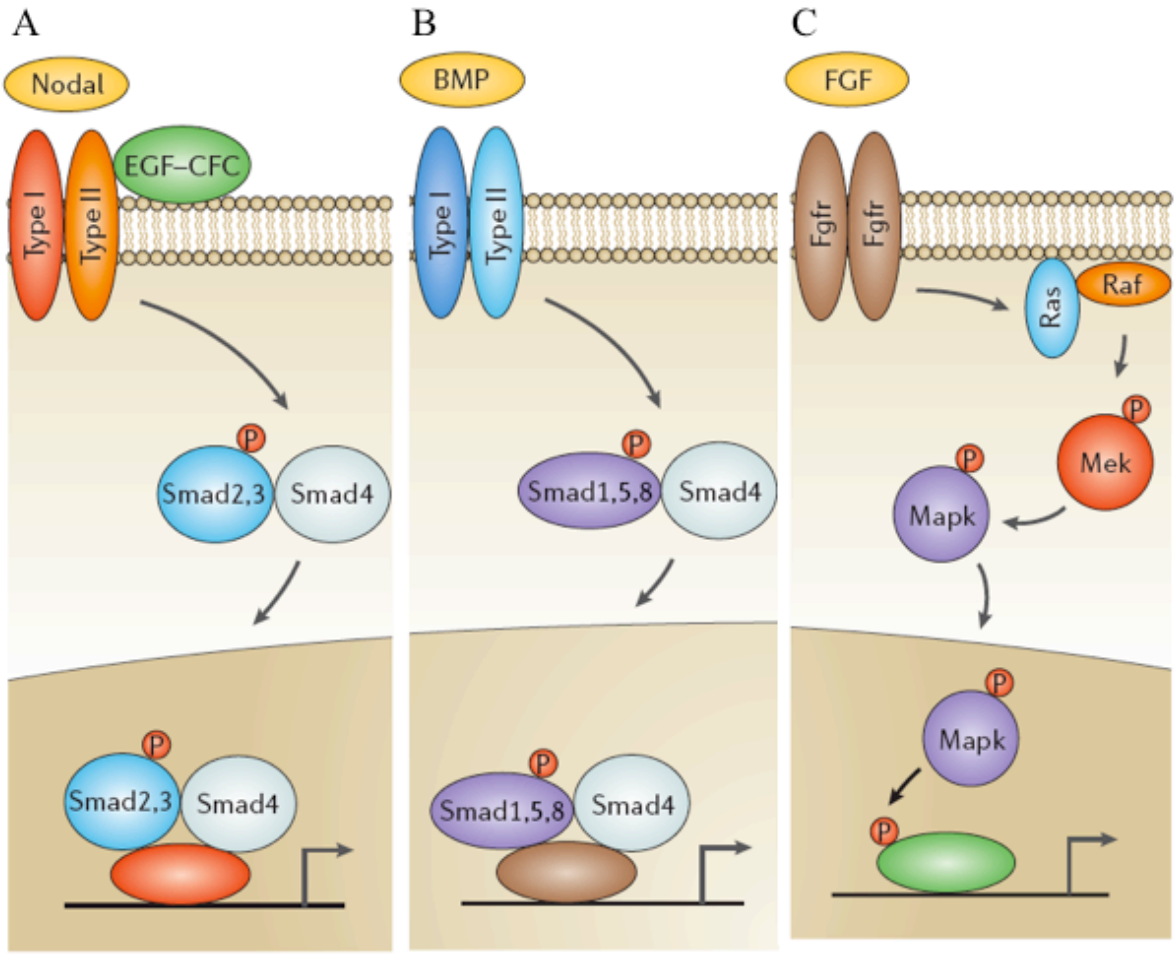

Figure 1.4. Schematic representations of the Nodal, BMP and FGF signaling pathways. The Nodal (A) and BMP (B) signaling pathways are activated by with the ligand binding to the type II receptor which phosphorylates and activates the type I receptor. The activated receptor phosphorylates Smad proteins (Smad2/3 in the Nodal pathway and Smad1/5/8 in the BMP pathway). The activated Smad proteins bind to the receptor Smad4 and go to the nucleus and activate target genes. In the Nodal pathway the EGF-CFC co receptor is required for Nodal ligand to bind to the type II receptor (A). (C) Binding of the FGF ligand to the FGF receptor results in activation of the FGF signaling pathway. The activated receptor recruits Ras, resulting in activation of Raf. Raf phosphorylates Mek, which activates the Mapk, which enters the nucleus to activate target genes. Figure modified from (Kimelman, 2006).

A role for FGFs in the establishment of the dorso-ventral axis has been shown. BMP genes are initially expressed throughout the blastula but become ventrally restricted where they act to specify ventral cell fates (Schmid et al., 2000). At the same time, FGF activity becomes dorsally restricted. Consistent with this, FGF inhibition, results dorsal expansion of BMP gene expression and a ventralization of the embryo. Together, FGF is acting to set the boundary of BMP expression during blastula stages, suggesting that FGFs are acting upstream of ventral morphogens to establish the dorso-ventral axis (Furthauer et al., 1997). Similarly, blocking FGF with a dominant-negative FGF receptor in *Xenopus*, zebrafish and mouse results in a loss in tail and trunk structures, suggesting a role in ventral-posterior specification (Amaya et al., 1991; Griffin et al., 1995; Yamaguchi et al., 1994).

FGF signals have both direct and indirect effects on gastrulation cell movements. In mouse, FGF receptor 1 mutants die during late gastrulation (Ciruna and Rossant, 2001) and show cell migration, cell fate specification, and patterning defects. In addition, these mutants maintain high levels of *E-cadherin* and while the epithelial cells migrate to the primitive streak, they fail to move away from it (Ciruna et al., 1997; Sun et al., 1999). Indirectly, FGF controls convergent extension movements through regulating *Brachury* (*Xbra)* expression. *Xbra* promotes convergent extension movements by regulating adhesion of cells to fibronectin (Conlon and Smith, 1999; Kwan and Kirschner, 2003). Additionally, there is evidence for a direct chemotactic response of migrating cells to FGF signals (Kubota and Ito, 2000) to coordinate cell movements during gastrulation. In the chick, cells are guided by environmental signals regulated by FGF (Yang et al., 2002). Taken together, FGF signaling plays an important role in regulating cell movements during gastrulation.

FGF signaling is a key player in mesoderm formation and in fact, the first identified mesoderm inducer was FGF (Slack et al., 1987). Inhibition of FGF signaling at the level of the receptors or downstream components of the pathway results in a loss of mesoderm formation. Conversely, gain-of-function experiments show an induction of mesodermal markers (LaBonne et al., 1995; Umbhauer et al., 1995). Through the regulation of T box genes (*spadetail (spt), Brachyury (Xbra), Tbx6*) in *Xenopus* (Strong et al., 2000), mouse (Ciruna and Rossant, 2001; Sun et al., 1999) and zebrafish (Griffin et al., 1998; Zhao et al., 2003) FGFs control the specification and maintenance of the mesoderm. These T box genes serve as important links between mesodermal cell fate and morphogenesis. One role of *spt* is

to regulate convergence movements of paraxial mesoderm during gastrulation (Ho and Kane, 1990).

FGFs also act as neural inducers in lower chordates such as ascidians (Lemaire et al., 2002) and planarians (Cebria et al., 2002), suggesting an evolutionarily conserved role. In mouse, chick, *Xenopus*, and zebrafish, FGFs role in neural induction has been intensively studied and showed conflicting results. Several studies have suggested a role for FGF signaling in neural induction (Alvarez et al., 1998; Bertrand et al., 2003; Hongo et al., 1999; Streit et al., 2000). Specifically, in the chick embryo, FGFs are sufficient to induce preneural markers and inhibiting FGF blocks neural induction by the Hensen's node (Alvarez et al., 1998; Storey et al., 1998; Streit et al., 2000). In *Xenopus* animal cap experiments, FGFs can directly induce neural tissue, although BMP signaling has to be partially attenuated (Kengaku and Okamoto, 1995; Ribisi et al., 2000). Other studies using a dominant-negative FGFR1 showed that neural tissue still forms (Holowacz and Sokol, 1999; Ribisi et al., 2000), suggesting that the FGF signaling mediated through FGFRs other than FGFR1 (Hongo et al., 1999) are important for neural induction.

The mechanism for how FGFs function during neural induction is not fully understood. The recently identified transcription factor *Churchill (chch)* was shown to be involved in mediating FGFs role in neural induction through the regulation of Smad-interacting protein 1 (*Sip1)* (Sheng et al., 2003). *Sip1* binds to and represses Smad1/5 and Smad2/3 transcriptional activation of target genes (Postigo, 2003; Postigo et al., 2003), resulting in the blockage of BMP and Nodal signaling respectively, as well as a direct repressor of *Brachyury* (Verschueren et al., 1999). Additionally, *Sip1* is a direct repressor of *E-cadherin* expression (Comijn et al., 2001), resulting in unusual migration patterns of cells. Through *Sip1*, *chch* was shown to prevent epiblast cells from migrating through the primitive streak and allowing them to remain within the neuroectoderm (Sheng et al., 2003), however, its mechanism of action is not yet known.

Interactions between signaling pathways: While the above signaling pathways all play important roles in germ-layer specification, DV and AP axis formation and gastrulation cell movements, there is significant amount of crosstalk between the various pathways.

In mesoderm formation, FGF has been shown to act as a competence factor for cells to respond to Nodal signals (Cornell and Kimelman, 1994b; LaBonne and Whitman, 1994). In *Xenopus* animal cap experiments, Nodal mediated mesoderm induction is blocked by FGFR1 inhibition (Cornell and Kimelman, 1994a). Induction of dorsal mesoderm, which depends upon Nodal signaling, is inhibited by dominant negative FGFR1 overexpression (Mitchell and Sheets, 2001). Continued FGF signaling during gastrulation is required for maintenance of the mesoderm (Kroll and Amaya, 1996). In fact, Nodal and FGF signaling interact through an autoregulatory loop to maintain mesodermal cell populations (Mathieu et al., 2004). Here, Nodal receptor activation induces activation of the FGF signaling pathway. The two signaling pathways regulate each other to maintain the competence of mesodermal cells.

1.4 Neural induction

Neural induction is the steps when ectodermal cells become specified into neural precursor cells. Later in development, these cells will no longer be able to respond to signals that induce alternative fates, and have thus become committed to a neural fate ultimately differentiating into neurons (Wilson and Edlund, 2001). The neural plate forms out of the dorsal ectoderm, while the ventral ectoderm gives rise to the epidermis. The differentiation of the ectoderm into these two different tissues is a complex process requiring multiple steps and the integration of multiple signaling pathways.

Early experiments into the role of the *Xenopus* organizer showed that transplantation of dorsal mesodermal tissue to the ventral side (prospective belly) of a new embryo resulted in the formation of a twinned embryo (Spemann, 1924) with an almost complete nervous system. Similar experiments have been repeated in zebrafish (Saude et al., 2000). These experiments identified a morphologically distinct group of mesodermal cells on the dorsal side of the embryo known as the shield in teleosts, Hensen's node in birds and mammals, and the organizer in amphibians. This dorsal mesodermal region emits signals into the dorsal ectoderm to differentiate the ectoderm into neural rather than epidermal tissue (Wilson and Edlund, 2001).

These dorsal mesodermal transplant experiments showed that the organizer has the ability to induce neural cells in the surrounding tissue. Molecular analysis of the organizer resulted in the identification of secreted molecules including *chordin* (Sasai et al., 1995), *noggin* (Smith and Harland, 1992), and *follistatin* (Hemmati-Brivanlou et al., 1994) (Figure 1.3). These molecules are all inhibitors of BMP signaling and are highly expressed within the dorsal ectoderm. Conversely, the ventral ectoderm lacks the expression of these molecules, but has a high expression of BMPs, resulting in the induction of epidermal genes. Attenuation of dorsally expressed BMP signaling results in an up regulation of neural genes in the ectoderm. Taken together, a model for neural induction has emerged where neural tissue is first induced during gastrulation when the organizer first develops. The BMP antagonists secreted by the organizer diffuse to the dorsal ectoderm and inhibit BMP signaling, allowing for the induction of neural genes. This model, referred to as the neural default model (Figure 1.5), states that ectodermal cells are fated to become neural cells, but are inhibited from this pathway by BMPs (Wilson et al., 2001).

While the organizer secretes signals to inhibit BMP signaling, is the organizer solely responsible for inducing the entire nervous system? Several observations suggest that other factors are involved. Studies in zebrafish (Saude et al., 2000) and *Xenopus* (Kuroda et al., 2004) have shown that dorsal cells residing outside of the organizer do have neural inductive properties. Furthermore, *chordin* is expressed outside of the organizer itself (Miller-Bertoglio et al., 1997) and zebrafish *dino* mutants (chordin mutants) still generate well patterned neural tissue (Schulte-Merker et al., 1997). Zebrafish mutants lacking an organizer still initiate dorsal *chordin* expression and have well patterned neural tissue (Gritsman et al., 1999). Together these results suggest that not all of the necessary signals required for neural induction are derived from the organizer and furthermore, it is still unclear whether the organizer is specifically required for neural induction. A recent study suggested that non-organizer cells have the ability to induce neural fates (Kuroda et al., 2004). In fact, studies in the chick have shown that neural induction is initiated prior to the start of gastrulation. Here, ectodermal cells are specified during blastula stages prior to the expression of known BMP antagonists (Streit et al., 1998). Furthermore, mice lacking the BMP antagonists Chordin and/or Noggin, and misexpression of BMP antagonists in the chick both result in the formation of neural tissue, suggesting the involvement of other signals.

If the organizer is not the sole source of neural inducing signals, then what other signals are involved? One set of candidate signals are fibroblast growth factors (FGF), which have been shown to play a role in neural induction (Kuroda et al., 2004; Wilson et al., 2001). FGF is required to initiate neural induction in the chick, ascidians, and mouse embryonic stem (ES) cells. When expressed in vivo, FGFs can induce neural identity while inhibition of FGF signaling disrupts neural induction (Bertrand et al., 2003; Hongo et al., 1999). However, FGFs actual role in neural induction has been controversial and species-specific mechanisms may exist. Following FGF inhibition in zebrafish and *Xenopus* embryos show a loss of posterior neural structures but no effect on anterior structures (Amaya et al., 1991; Griffin et al., 1995; Ribisi et al., 2000). Experiments in chick embryos showed a role for FGF in regulating BMP signaling, where blockage of FGF signaling leads to an up-regulation of *bmp* transcription with a loss of neural fates (Streit et al., 2000; Wilson et al., 2000; Wilson et al., 2001). In ascidians, early inhibition of FGF signaling blocks neural induction (Hudson et al., 2003). Taken together, these studies suggest a conserved role for FGF in neural induction. One possible explanation for the contradictory FGF results may be due to the specificity of FGF receptors. A study comparing the neural inducing activities of FGF receptors 1 and 4 suggested that a dominant negative FGFR4 was more effective at inhibiting neural fates (Hongo et al., 1999).

While FGFs exact role in neural induction is not yet known there is experimental evidence for interactions between Smads and FGFs (Massague, 2003; Pera et al., 2003). BMPs bind to and phosphorylate their receptors allowing for the phosphorylation of Smads1/5/8. Once phosphorylated, these Smad proteins act to induce ventral mesoderm as well as to autoregulate BMP gene expression to further propagate the BMP signal. Smad proteins are phosphorylated at two regions. The first, in response from the BMP receptor, phosphorylates the carboxy-terminal region, resulting in epidermal differentiation and mesoderm ventralization. BMP antagonists such as *chordin* and *noggin* inhibit this carboxy-terminal phosphorylated Smad and promote neural gene expression through a decrease in Smad activity. The second phosphorylation region, in the linker region of the protein, becomes phosphorylated in response to Mapk signals (Kretzschmar et al., 1997). Once phosphorylated it has an inhibitory effect on the Smad protein by preventing nuclear localization. FGF mediated phosphorylation of the Smad linker region inhibits Smad

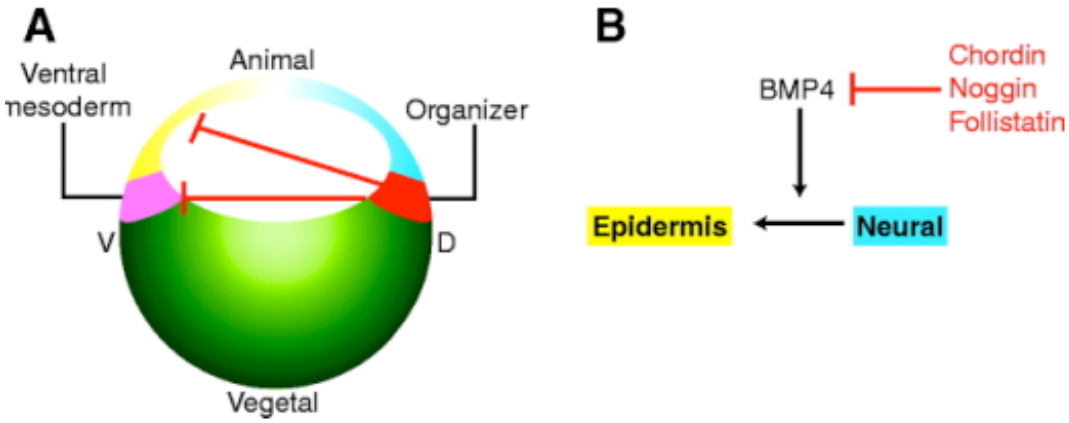

Figure 1.5. Schematic representation of the neural default model in Xenopus. (A) A map of a blastula stage embryo. The organizer is in red, ventral mesoderm is pink, neural tissue is blue, epidermis is yellow, and yolk and endoderm are green. The organizer secretes BMP antagonists (red lines), to inhibit dorsal BMP activity. (B) A genetic diagram of the proposed model. Ectodermal cells are fated to become neural tissue but the presence of BMP proteins prevent a neural fate and induce epidermal fates. Secreted molecules from the organizer such as Chordin, Noggin and Follistatin inhibit BMP activity allowing for ectodermal cells to take on a neural fate. Figure modified from (Stern, 2005).

response to BMP signaling (Pera et al., 2003). It was found that overexpression of wild type Smad1 inhibits neural gene expression while having an increase in epidermal gene expression. Conversely, overexpression of a mutant Smad1 mRNA, which is unable to be phosphorylated by FGF, results in inhibition of neural induction and promotion of epidermal fates. These results showed that FGF activation of Mapk signaling leads to the phosphorylation of specific residues in the Smad1 linker region and inhibits its function. Although, these experiments did not take into account the effect that other endogenous Smads are having, such as Smad5, which is maternally expressed and FGF may be having a similar effect on it. A role of the Smad linker phosphorylation site has not been shown in zebrafish.

FGF signaling may also have a more direct role in neural induction. Recent work in zebrafish (Delaune et al., 2004; Kuroda et al., 2004; Rentzsch et al., 2004) and *Xenopus* (Delaune et al., 2004) have shown that FGF is acting independently of BMP signaling inhibition to promote posterior neural fates. These experiments focused primarily on FGFs role in posterior neural induction and it is not clear if anterior neural is also induced in a similar fashion. However, in these experiments a background in which BMP inhibition was artificially inhibited by using dominant negative forms of Smads was used. This does not rule out the fact that FGF may be inhibiting BMP signaling to induce neural genes. Further support for a direct role for FGF in neural induction has come from recent work in ascidians. Here, BMP inhibition is not involved in neural specification (Darras and Nishida, 2001), rather it was shown that FGF is playing a role as a direct inducer of early neural genes (Bertrand et al., 2003). It was shown that Ets1/2 and GATAa mediate FGFs response and bind to the Otx regulatory element and activate it, resulting in a direct induction of anterior neural gene expression. It is not clear if a similar situation exists in zebrafish or if BMP inhibition is the sole mechanism for induction of neural genes.

Interestingly, mesoderm induction is occurring at a similar time and in close proximity to neural induction, and FGF is an important factor in mesoderm formation (Kimelman and Kirschner, 1987). Since the mesoderm plays an important role in specifying the neural plate, the mechanism of how FGF acts to induce both mesoderm and neural tissue is unknown. One possible mechanism for how these two seemingly different functions are regulated has come from recent work in the chick (Sheng et al., 2003) with the identification

of the *churchill (chch)* gene. *chch* is a transcription factor containing two zinc fingers, induced by FGF. It represses mesodermal genes and sensitizes epiblast cells to further neural inducing signals. Overexpression of *chch* in *Xenopus* embryos results in suppression of the mesodermal marker *brachyury* (Sheng et al., 2003). Morpholino knockdown of *chch* in the chick epiblast results in inappropriate migration of epiblast cells through the primitive streak. These cells emerge from the primitive streak and gave rise to paraxial mesoderm (Sheng et al., 2003). This suggests that *chch* is required to limit ingression of the epiblast allowing those cells to become neural tissue. The effect of *chch* in the assays in the frog and chick is the same (to limit mesoderm) but the mechanisms of action in these two experiments likely differ. Cell movements are not thought to be required for mesoderm induction in the animal cap assay. The chick experiments do not address the question of whether the migration of *chch*-inhibited epiblast cells causes them to be exposed to mesoderm-inducing signals or whether they migrate because they have already acquired mesodermal properties.

In addition, the chick experiments implicate Smad-interacting protein-1 (*Sip1*) as a direct target of *chch* and suggest that Sip1 is the major *chch* effector involved in blocking ingression of the epiblast. *Sip1* is also a zinc finger protein whose overexpression can induce neural markers in animal caps and cause a hyperneuralized phenotype (Eisaki et al., 2000), it is also a known direct repressor of *brachyury* expression. *Sip1* was also identified in a screen for proteins that associate with Smad1 (Verschueren et al., 1999). This association occurs only when Smad1 is activated by BMP receptor mediated phosphorylation (Postigo, 2003; Verschueren et al., 1999), suggesting that *Sip1* functions as a regulator of BMP signaling. Furthermore, *Xenopus Sip1* has been shown to directly repress epidermal gene expression, suggesting that *Sip1* is involved in inhibiting BMP signaling and inducing neural cell fate (Comijn et al., 2001; Nitta et al., 2004; van Grunsven et al., 2000). *chch* functions via *Sip1* to induce neural genes and inhibit mesodermal genes in the neural plate and is induced by FGF. Therefore, *chch* may function to separate the two functions of FGF, mesoderm induction and neural induction. *chch* and *Sip1* have not yet been characterized in the zebrafish.

Many questions about the mechanism of how the neural domain is established remain to be answered. For my thesis work presented here, the role of FGF signaling early neural

development in zebrafish was examined. I have shown that the specification of neural tissue in zebrafish requires FGF signals to repress early BMP gene transcription and to regulate the activities of Chordin and other mesodermal factors at later times in development. The mechanism of how FGF signals are regulated between patterning of neural and mesodermal tissues was also examined. Here, the FGF regulated gene, *churchill*, is shown to regulate its activity between the two functions. *churchill* functions to limit the transcriptional response to Nodal signals and regulates cell movements during early development. Taken together, these results show that FGF signaling is required for both neural and mesodermal gene expression and that *churchill* mediates these FGF function.

Chapter 2: Chordin, FGF signaling, and mesodermal factors cooperate in zebrafish neural induction

This chapter has been previously published in Developmental Biology, 279(2005) 1-19.

2.1 Introduction:

During embryogenesis, the neural plate, which will give rise to the entire central nervous system encompassing the brain and spinal cord is specified within the ectoderm. The longstanding model for neural induction and initial polarization of the neural plate is the activator-transformer model first proposed by Nieuwkoop (Nieuwkoop, 1952). In this model, an activator signal distinguishes neural ectoderm from non-neural ectoderm (epidermis). Initially, the neural ectoderm is anterior in character and is subsequently patterned by a transformation step to generate posterior fates. This model predicts that neural and non-neural ectoderm are in equilibrium, therefore, promotion of neural fates should come at the expense of epidermal fates. Conversely, impeding neural induction should expand the epidermal domain.

In the classic experiments, Spemann and Mangold observed that transplantation of dorsal mesoderm (termed the organizer) to a ventral location induced a complete secondary axis including a well patterned neural tube (Spemann, 1924). Elegant experiments in *Xenopus* laevis identified molecules expressed in the dorsal mesoderm that have potent neural inductive activity. Prominent among these molecules are *chordin* and *noggin* (Sasai et al., 1995; Smith and Harland, 1992). In vertebrates, neural induction occurs in a dorsal sector of the embryo where BMP (bone morphogenetic protein) signaling has been repressed (Hemmati-Brivanlou and Melton, 1997). Chordin and Noggin inhibit BMP signaling by binding to extracellular BMP ligands and interfering with receptor activation (Fainsod et al., 1997; Piccolo et al., 1996; Zimmerman et al., 1996).

The activities of the organizer and extracellular BMP antagonists are not entirely linked. In zebrafish, dorsal cells with neural inductive activity reside outside the morphological boundaries of the organizer (Grinblat et al., 1998; Saude et al., 2000) and

chordin expression also stretches beyond the organizer (Miller-Bertoglio et al., 1997). In the chick, the node is able to act as a neural inducer prior to the expression of known BMP antagonists (Streit et al., 1998). While experiments to knockdown Chordin function in *Xenopus* also support the notion that Chordin is an essential component of the neuralizing activity of the organizer (Oelgeschlager et al., 2003) recent experiments also suggest that Chordin is required outside of the organizer for specification of some anterior neural fates (Kuroda et al., 2004).

Despite the demonstration that both the organizer and extracellular BMP antagonists are sufficient to induce neural tissue in a variety of assays, genetic evidence suggests that neural induction occurs in the absence of the organizer or extracellular BMP antagonists. Mouse and zebrafish mutants that lack the organizer still undergo neuralization (Feldman et al., 1998; Gritsman et al., 1999; Klingensmith et al., 1999). Zebrafish mutants that lack the organizer still maintain dorsal expression of *chordin* (Gritsman et al., 1999; Sirotkin et al., 2000a). In these mutants, specification of neural tissue may result from extracellular antagonism of BMP signaling by Chordin. The Chordin locus is disrupted in zebrafish *dino* mutants, which have reductions in anterior neural tissues. Likewise, mice that are double mutant for *chordin* and *noggin* have anterior neural truncations (Bachiller et al., 2000; Schulte-Merker et al., 1997). Analysis of these mutants suggests that antagonism of BMP signaling by Chordin and related molecules are one key mechanism of neural induction but that additional signaling events play important roles.

The fact that BMP antagonism is a key component of neural induction has led to the formation of the neural default model (Figure 1.5). In this model, ectodermal cells are naturally fated to take on neural fates, but in the presence of BMP signals, ectodermal cells will take on epidermal fates (Stern, 2006). Thus, BMP signaling needs to be inhibited in ectodermal cells in order for neural genes to be expressed. These BMP inhibitory signals, such as *chordin*, and *noggin*, are expressed from the dorsal organizer and act within the dorsal ectodermal region to inhibit BMP signals, resulting in neural gene expression. Since neural induction still occurs even in the absence of an organizer and its expressed genes, other signals must be required for neural induction to occur.

One additional class of molecules that have been implicated in neural induction is the Fibroblast growth factors (FGFs). Their role in neural induction has been controversial and

experiments in different model systems have indicated that there may be species-specific mechanisms of neural induction. Manipulations of chick embryos suggest a role for FGF in neural induction (Streit et al., 2000; Wilson and Edlund, 2001; Wilson et al., 2000) and that FGFs may attenuate BMP signaling by repressing the transcription of BMP4 and BMP7 (Wilson et al., 2000).

However, overexpressing a dominant-negative FGF receptor 1 (XFD) or an inhibitory *Ras* construct in zebrafish and frog embryos, doesn't prevent formation of anterior neural structures (Amaya et al., 1991; Griffin et al., 1995; Ribisi et al., 2000). These embryos lack all posterior tissue, including spinal cord, but contain hindbrain and normal anterior structures. Furthermore, isolated XFD-expressing cells are capable of becoming spinal cord (Kroll and Amaya, 1996; Ribisi et al., 2000). Together, these results suggest that FGF signaling is not required for neural induction. However, Hongo et al. (1999) demonstrated that in an *in vitro* culture system blocking FGF signaling with Δ-FGFR-4 or to a lesser extent XFD, inhibits neural induction by the organizer and blocks autonomous neuralization of cultured disassociated ectodermal cells. In those experiments, whole embryos injected with Δ-FGFR-4 mRNA still generated anterior neural tissue at late stages. One mechanism by which FGF may act as a neural inducer was suggested by the observation that BMP signaling can be quashed by FGF-mediated phosphorylation of the Smad1 linker region at consensus MAP-ERK kinase phosphorylation sites (Pera et al., 2003).

The work here shows that in zebrafish, neural tissue is induced as a result of the combined activities of FGF signaling, Chordin and Nodal downstream targets. Inhibition of FGF signaling in wild-type embryos results in early deficits in neural specification and an expansion of non-neural ectoderm. However, the anterior neural domain later recovers in a Nodal-dependent fashion following FGF inhibition. These results demonstrate that FGF acts to diminish BMP transcript levels prior to the start of gastrulation. Furthermore, while FGF induces expression of *chordin* transcripts, it also represses BMP transcript levels by a translation independent mechanism. Together, these findings suggest that FGF acts at multiple levels to repress BMP signaling and define the neural territory.

2.2 Results:

2.2.1 Neural tissue develops in the absence of Chordin and mesoderm:

Zebrafish maternal-zygotic *one-eyed pinhead* (MZ*oep*) mutants are defective in Nodal signaling and lack all trunk mesendoderm including the organizer, yet generate a broad, well patterned neural plate (Gritsman et al., 1999; Sirotkin et al., 2000a). While most organizer markers are not expressed in Nodal signaling mutants, expression of *chordin*, a potent neural inducer, is initiated in these embryos (Gritsman et al., 1999; Sirotkin et al., 2000a). In *Xenopus*, it has been suggested that expression of *chordin* at blastula stages within the dorsal animal cap is required for mesoderm independent specification of anterior neural fates (Kuroda et al., 2004). Since the zebrafish *chordin* locus is disrupted in *dino* mutants (Schulte-Merker et al., 1997), neural specification was determined in the zebrafish Nodal signaling mutants is mediated by *chordin* by generating MZ*oep;dino* double mutants (Figure 2.1).

MZ*oep;dino* double mutants have reduced neural tissue compared to MZ*oep* single mutants at 24 hrs (Figure 2.1 A-D). The double mutants also have fewer, broader tail somites than MZ*oep* single mutants. A similar posterior expansion is also observed in *dino* single mutants (Hammerschmidt et al., 1996; Schulte-Merker et al., 1997) and is a predicted result of excess BMP signaling. The expression domains of anterior markers (*otx2* and *opl*) and a posterior neural markers (*hoxb1b*) are dramatically reduced during gastrulation in the double mutant (Figure 2.1 E-J). At the same stages, *gata2* expression, which marks presumptive epidermis, is expanded in the MZ*oep;dino* double mutants (Figure 2.1 K, L). During early somitogenesis, pax2.1 (midbrain) and krox20 (r3 and r5) are both correctly expressed in the double mutant, albeit in narrow domains (Figure 2.1 M-P). These results demonstrate that neural tissue is induced in MZ*oep;dino* double mutants and that the neural tissue undergoes correct anterior-posterior patterning. Since a small amount of neural tissue is present in MZ*oep;dino* double mutants, it can be concluded that Chordin is not the sole signal responsible for specification of neural tissue in MZ*oep* mutants.

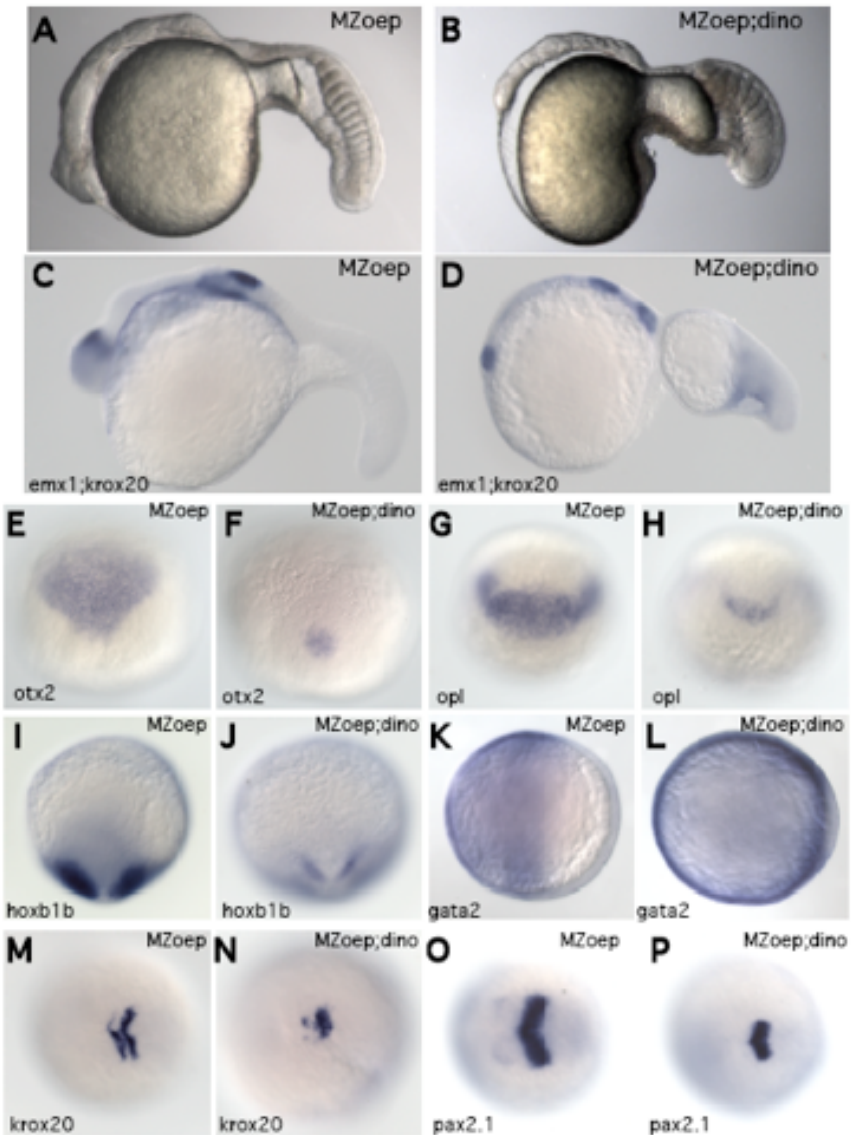

Figure 2.1. Neural tissue is maintained in MZ*oep;dino* double mutants. Lateral views of living MZ*oep* and MZ*oep;dino* double mutants (A,B) at 22hr. The double mutant has reduced neural tissue and large tail somites compared to MZ*oep* single mutants. Analysis of the expression patterns of neural and presumptive epidermal markers in MZ*oep* and MZ*oep;dino* double mutants by whole mount RNA *in situ* hybridization. The presence of neural tissue at 22 hrs is confirmed by the expression of *emx1* and *krox20* (C, D). The expression domains of the anterior neural markers *otx2* and *opl* and the posterior neural marker, *hoxb1b*, are reduced in MZ*oep;dino* double mutants (F, H, J) compared to MZ*oep* mutants (E, G, I). The *gata2* expression domain is expanded dorsally in MZ*oep;dino* double mutants (K, L). During early somitogenesis, the neural plate is narrow in the double mutant as revealed by *krox20* and *pax2.1* expression (M-P). (C, D) are lateral views; (E-H) are dorsal views at 70% epiboly (mid-gastrula); (I, J) are dorsal views at late gastrula (90% epiboly); (K, L) are animal pole views at 70% epiboly (mid-gastrula); (M-P) are dorsal views at the 3-somite stage. Genotypes of all embryos were determined following photography by PCR based analysis. (Data produced by Jack Niemiec)

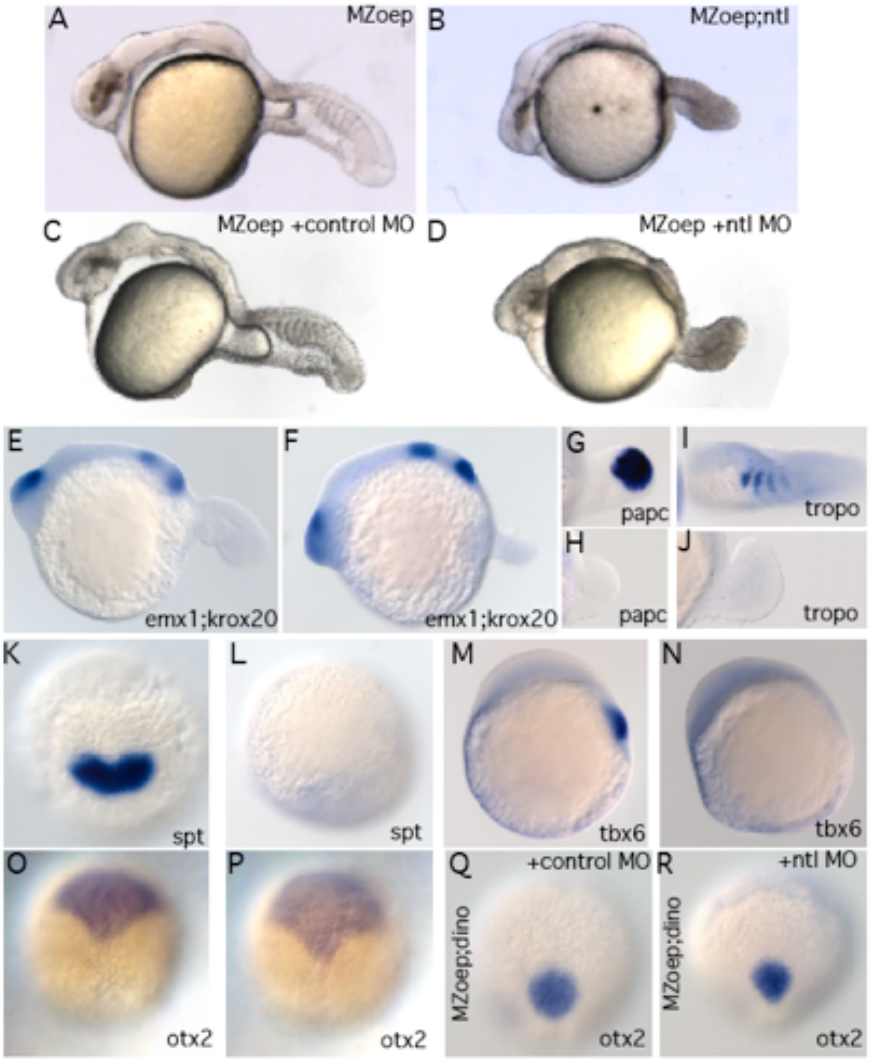

Figure 2.2. Mesoderm is not required for neural induction. Lateral views of live MZ*oep* and MZ*oep;ntl* double mutant embryos (A,B). The double mutant lacks tail somites but forms anterior neural tissue. The double mutant phenotype can be phenocopied by microinjection of *ntl* morpholinos into MZ*oep* mutants (C, D). Analysis of the expression patterns of neural and mesodermal markers in MZ*oep* and MZ*oep;ntl* double mutants by whole mount RNA *in situ* hybridization. At 24 hrs, expression of *emx1* and *krox20* is in indistinguishable in MZ*oep* (E) and MZ*oep;ntl* double mutant embryos (F). While MZ*oep* mutants express markers of tail mesoderm including *papc*, *α-tropomyosin*, *spt* and *tbx6* (G, I, K, M), these markers are all absent in MZ*oep;ntl* double mutant embryos (H, J, L, N). Early expression of *otx2* during gastrulation is unaffected in MZ*oep;ntl* double mutant embryos (P) compared to MZ*oep* single mutants (O). The small *otx2* domain in MZ*oep;dino* embryos is not altered by treatment with *ntl* morpholinos (Q, R). (A-F) 24hr embryos; (G, H) lateral views of tails of 23 hr or (I, J) 24 hr embryos; (K, L) dorsal views of 2-sominte embryos, anterior is toward the top; (M, N) lateral views of 2-somite embryos; (O-R) dorsal views of mid-gastrula embryos (70% epiboly). Genotypes of all embryos were determined following photography by PCR based analysis. (Data produced by Jack Niemiec)

What signals in MZ*oep;dino* might account for the remaining neural tissue? Mesoderm is often considered as a source of factors that neuralize the ectoderm. Because of the abnormal gastrulation movements in Nodal mutants, the location where prospective anterior neural tissue is specified, is vegetally displaced by 90º compared to wild-type embryos (Gritsman et al., 1999). It is possible that in these mutants the dorsal ectoderm is exposed to signals from ventral (tail) mesoderm that may promote specification of the anterior neural domain. *No-tail (ntl)* is the zebrafish homologue of Brachyury and is required for specification of tail mesoderm (Halpern et al., 1993; Schulte-Merker et al., 1994). To determine whether the remaining tail mesoderm is the source of neuralizing signals in the absence of dorsal/trunk mesoderm, MZ*oep;ntl* double mutants were generated (Figure 2.2).

From the earliest stages MZ*oep* mutants show deficits in markers of trunk mesoderm but posterior mesoderm is specified and tail somites form (Gritsman et al., 1999). In MZ*oep;ntl* double mutant embryos, no tail mesoderm is generated as evidenced by the absence of posterior mesodermal markers during early somitogenesis including *spadetail*, and *tbx6* and later tail markers including *papc* and *α-tropomyosin*, (Figure 2.2 G-N) suggesting that these embryos lack all mesoderm.

During gastrulation, expression of *otx2* in the anterior neural plate in MZ*oep;ntl* double mutants embryos is comparable to MZ*oep* single mutants (Figure 2.2 O, P). Likewise, at 24 hours, the *emx* and *krox20* expression domains are similar to the domains in MZ*oep* embryos (Figure 2.2 E, F). Neural induction and patterning appears to be unaffected by the elimination of the remaining tail mesoderm in Nodal mutant embryos.

To determine whether Chordin masks a weak neural inducing activity of factors originating in tail mesoderm, *ntl* function was eliminated in MZ*oep;dino* double mutants using antisense morpholinos directed against the *ntl* translation start site (Nasevicius and Ekker, 2000). Microinjection of the morpholinos into MZ*oep* embryos phenocopies MZ*oep;ntl* double mutants (Figure 2.2 C, D). Treatment of MZ*oep;dino* double mutant embryos with *ntl* morpholinos does not alter expression of *otx2* during gastrulation (Figure 2.2 Q, R). These results suggest that tail mesoderm does not play a role in specification of the neural plate in MZ*oep* mutants.

2.2.2 FGF signaling is required for neural induction in zebrafish:

While neural tissue is formed in the absence of mesoderm, signals that induce neural tissue may originate from the marginal cells that are precursors to the mesoderm and endoderm in wild-type embryos. In Nodal mutants, these cells ultimately form neural tissue (Feldman et al., 2000). However, prior to the onset of gastrulation, these cells express markers characteristic of mesendodermal precursors including *wnt11*, *tbx6* and *spt* (Gritsman et al., 1999; Mathieu et al., 2004). FGF signaling is also active in mesendodermal precursors and has been proposed to act as a neural inducer in some species. It is possible that the activity of FGF in neural induction might be more apparent in the absence of dorsal mesoderm. Therefore, it was determined whether FGF signaling is required to generate the neural tissue that is observed in MZ*oep* mutants.

FGF signaling was blocked by overexpressing the dominant negative FGF receptor XFD (Amaya et al., 1991) in MZ*oep* mutant embryos. XFD has been used to block FGF signaling in both *Xenopus* and zebrafish embryos (Amaya et al., 1991; Griffin et al., 1995; Kroll and Amaya, 1996). The primary deficits reported in these experiments were the elimination of trunk and tail mesoderm. Deficits were not observed in formation of anterior neural tissue. However, microinjection of XFD into MZ*oep* mutants severely reduced the amount of neural tissue present at 24 hrs compared to control injected MZ*oep* mutant embryos (Figure 2.3 C, D). Microinjection of XFD into wild-type embryos resulted in elimination of trunk and tail mesoderm. However, as in previous experiments anterior neural tissue appeared intact at 24 hrs (Figure 2.3 A, B). These experiments demonstrate that XFD treatment has markedly different effects on wild type and MZ*oep* mutant embryos.

If FGF signaling is required for neural induction, impeding FGF signaling will inhibit expression of neural markers during gastrulation and enhance expression of markers of presumptive epidermis. At mid-gastrula stages, the expression of the anterior neural markers *otx2* (Figure 2.3 E, F), *opl* (Figure 2.3 I, J) and *cyp26* (data not shown) are all reduced in MZ*oep* mutants after XFD treatment when assayed by RNA *in situ* hybridization. During gastrulation, the *gata2* (Figure 2.2 M, N) and *gata3* (data not shown) expression domains in the presumptive epidermis are greatly expanded by XFD treatment.

The expression of neural and non-neural ectoderm markers was also examined in mid-gastrula stage MZ*oep* embryos using real-time PCR. Consistent with the RNA *in situ* hybridization results, XFD treated MZ*oep* embryos show dramatic decreases in the expression levels of the neural markers compared to controls. In control injected embryos, the expression levels of *otx2* and *hoxb1b* were > 4 times higher than embryos injected with XFD (Figure 2.3 Q). Conversely, XFD treated embryos expressed *gata2* and *gata3* at levels ~2.5 times greater than control injected embryos (Figure 2.3 Q). These results show that blocking FGF signaling with XFD in MZ*oep* mutants promotes expression of markers of presumptive epidermis at the expense of neural markers. Therefore, FGF signaling mediates specification of the neural domain in MZ*oep* mutants.

Since impeding FGF signaling severely reduces anterior neural tissue in MZ*oep* mutants during gastrulation, why XFD treated wild-type embryos generate overtly wild-type anterior neural structures by 24 hrs? One possibility is that the deficits produced by inhibition of FGF signaling in MZ*oep* mutants are not apparent in wild-type embryos due to redundant activity of the organizer (dorsal mesoderm). To test this hypothesis, ectodermal markers in wild-type gastrula stage embryos following inhibition of FGF signaling was assayed. These treatments produced clear deficits in neural specification.

Expression of anterior neural markers including *otx2* (Figure 2.3 G, H), *opl (K, L)* and *cyp26* (data not shown) during gastrulation was assayed using RNA *in situ* hybridization. The expression domains of these markers were greatly reduced and shifted toward the margin. At the same stages, the expression domains of *gata2* (Figure 2.3 O, P) and *gata3* (data not shown) in the presumptive epidermis were expanded. Real-time PCR was used to measure the effects of inhibiting FGF signaling with XFD on neural induction in wild-type embryos at mid-gastrula stages (Figure 2.3 R). Control injected embryos expressed the neural markers *otx2* and *hoxb1b* at levels nearly 4 times higher than XFD injected embryos. Conversely, XFD treated embryos expressed the markers of presumptive epidermis *gata2* and *gata3* at about twice the levels of control injected embryos.

In addition to using XFD to block FGF signaling, an additional construct to block FGF signaling, Δ-FGFR-4 (Hongo et al., 1999), was used. XFD is a dominant negative FGF type 1 receptor and Δ-FGFR-4 is a dominant negative type 4 receptor. Since FGF receptors form heterodimers each of these reagents may block signaling through multiple receptors.

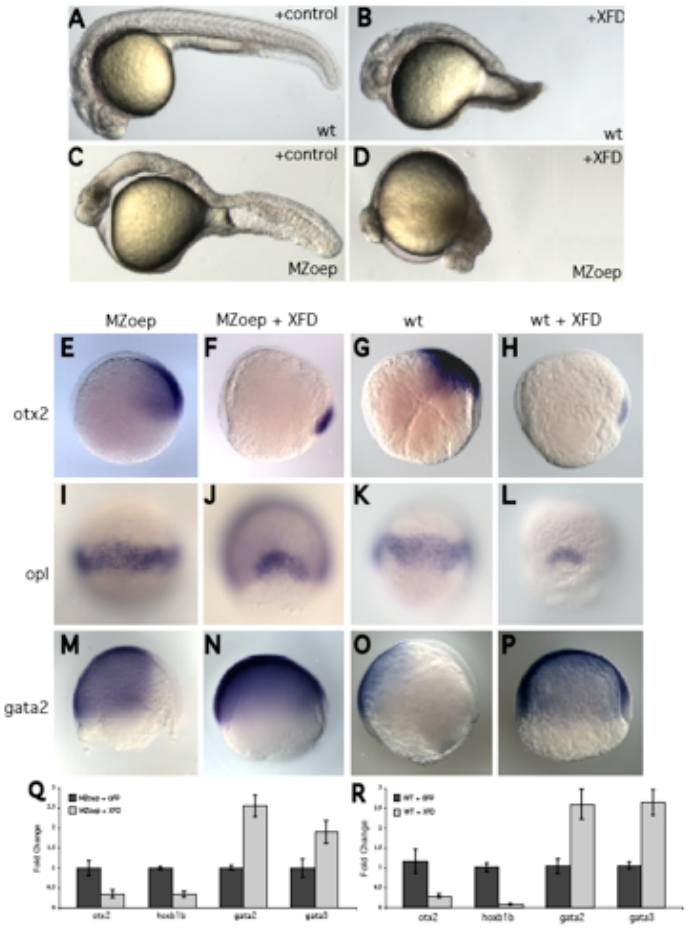

Figure 2.3. XFD blocks neural induction in MZ*oep* mutants and wild-type embryos. Analysis of the expression patterns of ectodermal markers in control and XFD injected MZ*oep* mutant embryos. Lateral views of 24 hr live control injected wild-type (A) and MZ*oep* mutant (C) embryos and XFD injected wild-type (B) and MZ*oep* (D) embryos. XFD overexpression results in posterior defects in wild-type embryos but anterior neural deficits are apparent in XFD injected MZ*oep* mutant embryos. Whole mount RNA *in situ* hybridization anterior neural and ectodermal markers in MZ*oep* and wild-type control (E, G, I, K, M, O) and XFD (F, H, J, L, N, P) injected MZ*oep* mutant embryos and wild-type embryos at mid-gastrula (70% epiboly). The expression domains of the anterior neural markers *otx2* (E, F, G, H) and *opl* (I, J, K, L) are shifted toward the margin and dramatically reduced in XFD injected embryos. The expression domains of *gata2* (M, N, O, P) in ventral ectoderm in XFD treated embryos are expanded compared to control injected embryos. For all microinjection experiments 125 pg of XFD mRNA was injected. The consequence of XFD treatment on transcript levels of markers of neural tissue and presumptive epidermis in MZ*oep* mutants and wild-type embryos was monitored by real-time PCR (Q, R). The levels of neural markers *otx2* and *hoxb1b* are decreased in embryos microinjected with of 125 pg XFD mRNA, while the levels of presumptive epidermal markers *gata2* and *gata3* are increased. The fold change (y-axis) of these markers is set relative to control (GFP) injected embryos. Embryos were collected at mid-gastrulation (70% epiboly). (A-P produced by Jack Niemiec)

and an expansion of markers of presumptive epidermis at mid-gastrula stages (data not shown). Co-injection of XFD and Δ-FGFR-4 produces effects on the neural plate similar to either construct alone (data not shown). This suggests that both constructs block similar signaling events required for generation of the neural plate.

These results show that inhibiting FGF signaling in wild-type embryos inhibits the expression of neural markers and enhances expression of markers of the presumptive epidermis during gastrulation. Since expression levels of these markers is indicative of cell fate choice within the ectoderm, it can be concluded that in zebrafish FGF signaling mediates ectodermal cell fate decisions and is required for neural induction.

2.2.3 Recovery of anterior neural tissue following inhibition of FGF signaling requires Nodal signaling:

Since both wild type and MZ*oep* mutant show anterior neural deficits during gastrulation following inhibition of FGF signaling, but only MZ*oep* mutants show anterior neural defects at 24 hrs (Figure 2.3 A-D), wild-type embryos must be able to generate neural tissue after mid-gastrula stages following inhibition of FGF signaling, but MZ*oep* embryos cannot. To determine the time at which the neural tissue recovers in wild-type embryos, RNA *in situ* hybridization using an *otx2* antisense probe at various time points during late-gastrula stages and early somitogenesis was performed. By the 6-somite stage, expression of *otx2* is comparable in control and XFD injected wild-type embryos (Figure 2.4 A, B) In contrast, MZ*oep* embryos injected with XFD have diminished expression of *otx2* at the 6-somite stage (Figure 2.4 C, D). *otx2* expression was also measured by real-time PCR in both wild-type and MZ*oep* XFD injected embryos at the 6-somite stage (Figure 2.4 I). In agreement with the *in situ* hybridization data, *otx2* expression levels in wild-type embryos recover to control levels following XFD treatment, while MZ*oep* embryos fail to recover. These results suggest that the recovery of neural tissue in wild-type embryos with compromised FGF signaling depends on Nodal signaling.

2.2.4 Synergy between FGF signaling and Chordin in Neural specification:

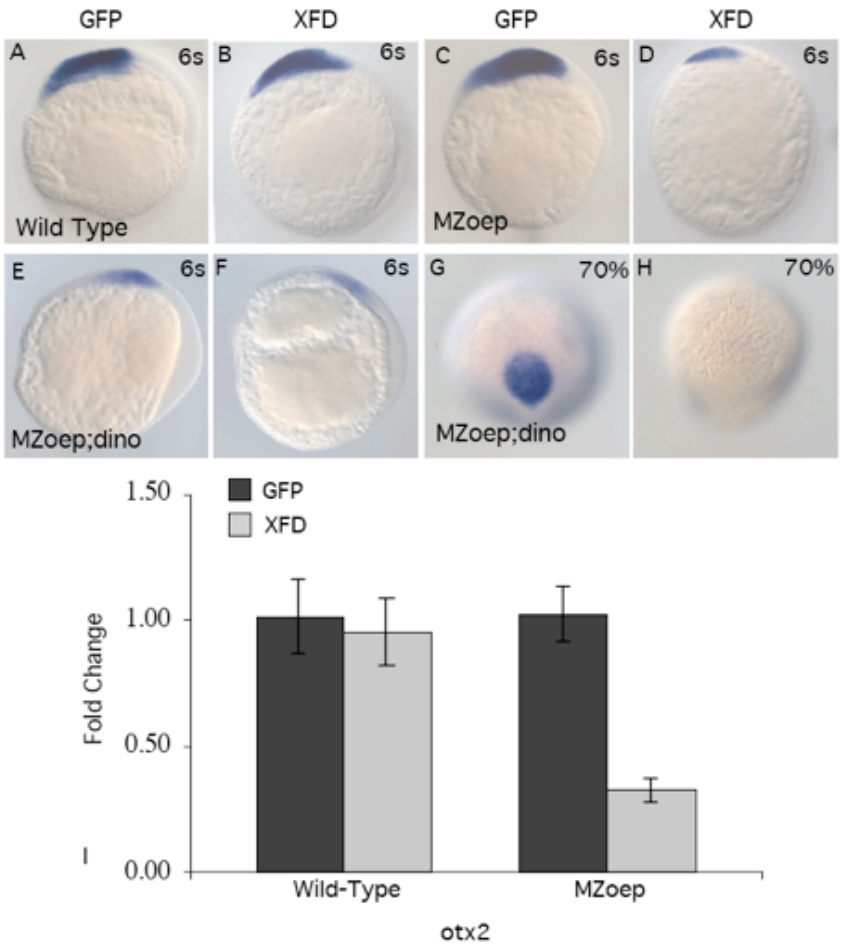

Figure 2.4. Recovery of anterior neural tissue following FGF inhibition depends on Nodal signaling. (A-H) otx2 *in situ* hybridization of wild type, MZ*oep* and MZ*oep; dino* embryos microinjected with 125 pg XFD or GFP mRNA. Expression of *otx2* is comparable at the 6-somite stage in wild-type embryo microinjected with GFP or XFD mRNA (A, B). While XFD injected MZ*oep* embryos have a reduced *otx2* domain (C, D). The *otx2* domain is comparable in XFD and GFP injected MZ*oep*;*dino* mutant embryos embryos at the 6-somite stage (E, F), while *otx2* expression is eliminated in XFD injected MZ*oep; dino* embryos at 70% epiboly (mid-gastrula) (G, H). Stages of embryos are indicated. (A-F) are lateral views, (G, H) are dorsal views. (I) Real-time PCR analysis of *otx2* transcript levels in wild type and MZoep XFD injected embryos at the 6-somite stage. The fold change (y-axis) of these markers is set relative to control (GFP) injected embryos. XFD injected MZoep embryos show a decrease in *otx2* expression while XFD injected wild-type embryos show no change in *otx2* expression compared to controls.

To determine whether there is redundancy in the activities of FGF signaling, Chordin and additional mesodermal factors in neural induction, XFD was used in MZ*oep;dino* double mutants. At mid-gastrulation *otx2* is not expressed in XFD treated MZ*oep;dino* double mutants embryos (Figure 2.4 G, H). However, by the 6-somite stage, *otx2* is expressed at low levels (Figure 2.4 E, F). These results conclude that the expression of neural markers at mid-gastrula stages requires FGF signaling, Chordin and downstream targets of Nodal signaling (mesoderm). Subsequent expression of neural markers may depend on additional late acting factors or may be the result of an inability of microinjected XFD RNA to completely repress FGF signaling at later stages.

2.2.5 FGF signaling represses transcription of BMPs:

Since FGF activity has been shown to repress BMP transcript levels in the chick, the effects of blocking FGF signaling on expression of neural markers could be traced to a direct impact on BMP transcript levels. Three zebrafish BMP family members are expressed during the late blastula and early gastrula periods, *bmp2*, *bmp4*, and *bmp7* (Kishimoto et al., 1997; Schmid et al., 2000). All of these molecules have been shown to regulate epidermal cell fate choices within the ectoderm. Overwhelming evidence suggests that inhibition of BMP signaling promotes expression of neural makers and represses epidermal fates (Munoz-Sanjuan and Brivanlou, 2002; Stern, 2002).

To determine the role of FGF signaling in regulating BMP transcription, the effects of inhibiting FGF signaling on the expression of BMP ligands was analyzed. Microinjection of XFD or Δ-FGFR-4 at the 1-4 cell stage resulted in increased levels of *bmp2*, *bmp4*, and *bmp7* transcripts during late-blastula and early-gastrulation stages as assayed by real-time PCR (Figure 2.5). During the late-blastula period XFD and Δ-FGFR-4 injected embryos show almost twice the levels of *bmp2* transcripts, and modest increases in *bmp4* and *bmp7* transcript levels, as compared to control injected embryos (Figure 2.5 A, C). By early-gastrulation, the effects of both treatments on *bmp4* and *bmp7* transcription are more evident, although not as substantial as the effect on *bmp2* transcript levels (Figure 2.5 B, D).

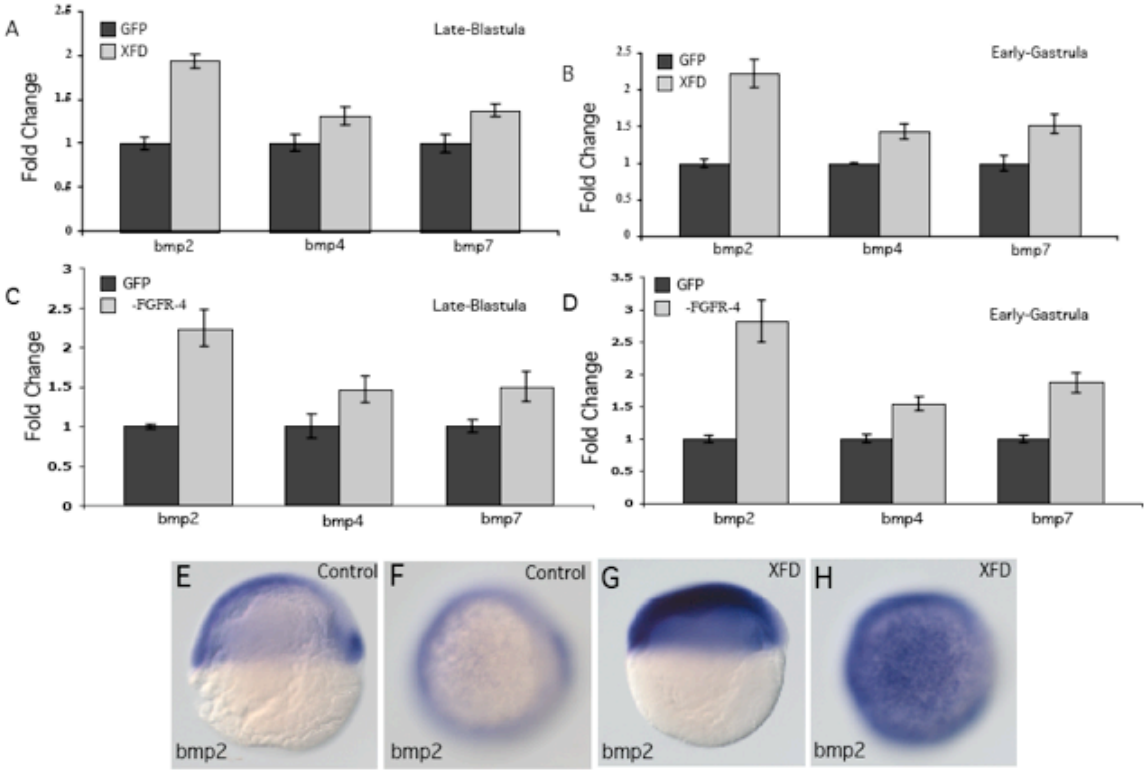

Figure 2.5. FGF signaling represses BMP transcription. Real-time PCR analysis of XFD (A, B) and Δ-FGFR-4 (C, D) microinjected wild-type embryos during late blastula and early gastrula stages. The fold change (y-axis) of the markers *bmp2*, *bmp4*, and *bmp7* is set relative to control (GFP) injected embryos. XFD and Δ-FGFR-4 injected embryos show an increase BMP transcript levels during late blastula stages. (E-H) RNA *in situ* hybridization of *bmp2* expression in control (E, F) and XFD injected wild-type embryos (G, H). In XFD injected embryos the *bmp2* expression domain extends into the dorsal ectoderm. (E, G) are lateral views of shield stage embryos and (F, H) are animal pole views of the same embryos.

To determine whether the increases in *bmp* transcript levels correlate with an expansion of *bmp* transcripts into the dorsal BMP-free zone that gives rise to the neural plate, *bmp* expression after XFD microinjection by whole-mount RNA in situ hybridization (Figure 2.5 E-H) was examined. In XFD treated embryos, b*mp2* (Figure 2.5 E-H) and *bmp4* (data not shown) transcripts extend farther dorsal than in control-injected embryos. Taken together, both the RNA *in-situ* hybridization and real-time PCR data show that inhibition of FGF signaling enhances BMP transcript levels.

2.2.6 FGF signaling regulates blastula stage BMP transcript levels:

The above results demonstrate that microinjection of mRNAs that block FGF signaling into 1-4 cell embryos results in late blastula and early gastrula stage increases in BMP transcript levels. To more precisely determine when FGF signaling is required, reagents that allowed activation or repression of FGF signaling at specific stages were utilized. An inducible FGF type I receptor was used to control for the activation of FGF signaling (iFGFR-1) (Pownall et al., 2003; Welm et al., 2002). This construct contains two mutant FKBP12 dimerization domains fused to the carboxy terminus of the FGFR1 receptor. A small synthetic molecule, AP20187, induces dimerization of the FKBP12 domains and FGF receptor activation. To block FGF signaling at specific stages of development, a pharmacological inhibitor of FGF, SU5402 (Mohammadi et al., 1996) was used. Both methods allowed for the activation or inhibition of FGF signaling at controlled time points throughout development.

To determine the effect of activation of FGF signaling on BMP transcript levels FGF signaling was activated with the iFGFR-1. FGF receptor activation decreases early-gastrula stage expression of BMP ligands (Figure 2.6). Embryos were injected with iFGFR-1 and treated with AP20187 or control media just prior to the mid-blastula transition (512-cell stage). These embryos were allowed to develop to early and mid-gastrula stages. At shield stage (early gastrula), embryos were collected and *bmp* transcript levels were monitored using real-time PCR. Activation of FGF signaling at 512-cell stage reduced the levels of all three *bmp* transcripts at shield stage to about 50% wild-type levels (Figure 2.6 A). By late-gastrulation, this treatment resulted in increases in the transcript levels of the neural markers

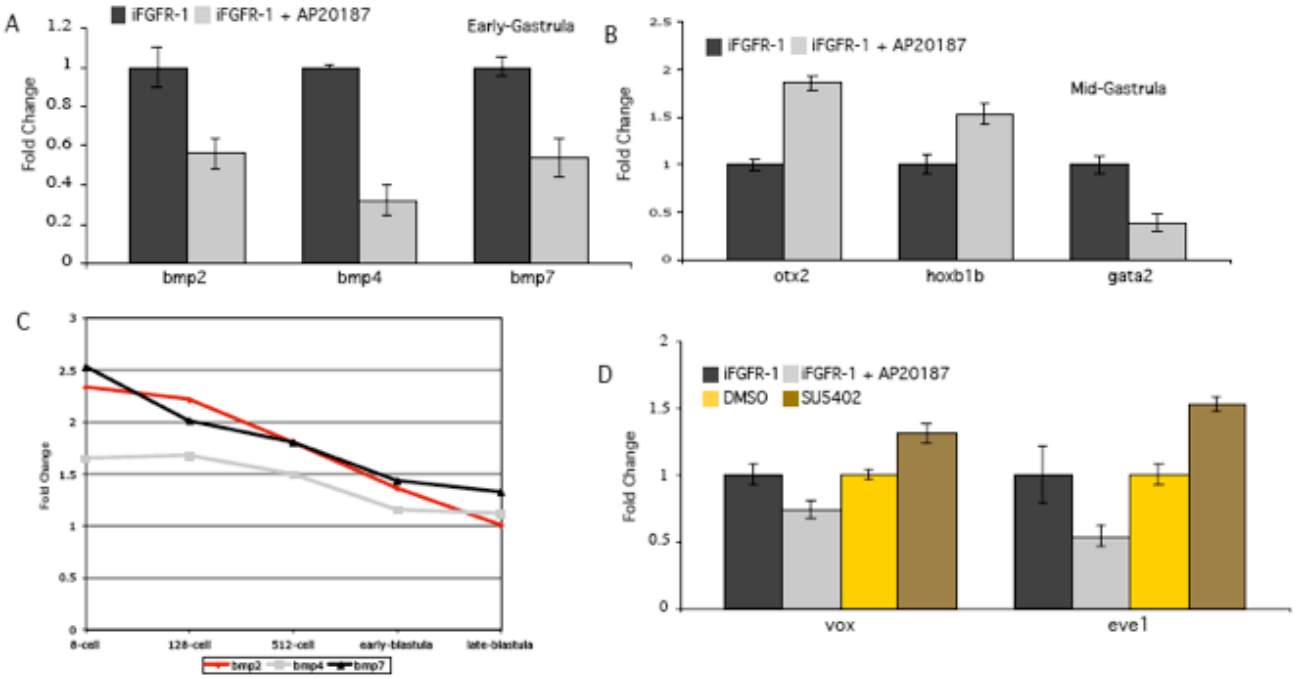

Figure 2.6. FGF signaling is required during the late blastula period to regulate BMP transcription. Embryos were injected with iFGFR-1 and activated with AP20187 at the 512-cell stage. Embryos were collected at early and mid gastrula stages for real-time PCR. Embryos at early gastrulation (shield stage) (A) were tested for their fold change (y-axis) of *bmp2*, *bmp4*, and *bmp7* and for their expression of *otx2, hoxb1b*, and *gata2* (B) at mid-gastrulation (70% epiboly). Activating FGF signaling at the 512-cell stage results in an early decrease in *bmp2, bmp4*, and *bmp7* expression at shield stage. At mid-gastrulation, these embryos have increases in *otx2* and *hoxb1b* transcript levels and a decrease in *gata2* levels. (C) FGF signaling was inhibited with the pharmacological drug SU5402 at 8 cell, 128 cell, 512 cell, early blastula and late blastula and collected at shield stage (early gastrula) for real-time PCR analysis. Graphed is the fold change (y-axis) for *bmp2, bmp4* and *bmp7* levels relative to control treated embryos. These results show that the effectiveness of the SU5402 treatment in blocking repression of BMP transcript levels diminishes between the 512-cell and early blastula (sphere stages). (D) FGF signaling was either inhibited or activated with SU5402 or AP20187 at the 512-cell stage. Embryos were collected at the shield stage (early gastrula) for their fold change (y-axis) of *vox* and *eve1*. Activating FGF signaling results in a 25% and 50% reduction in transcript levels for *vox* and *eve1*, while inhibiting FGF results in a 30% and 50% increase in *vox* and *eve1* transcript levels. These results show that inhibiting or activating FGF at the 512-cell stage results in loss of BMP target expression.

otx2 and *hoxb1b* and a corresponding decrease in the transcript levels of the presumptive epidermal marker, *gata2* (Figure 2.6 B). These results demonstrate that activation of FGF signaling during the late blastula and early gastrula stages reduces levels of *bmp* transcripts and enhances expression of early neural markers at the expense of presumptive epidermal markers.

To determine the stages when FGF signaling is required to repress BMP transcript levels, embryos were treated with the FGF inhibitor, SU5402, at 8 cell, 128 cell, 512 cell, sphere, and 30% epiboly stages and collected at shield stage (early gastrula). The relative *bmp* expression levels were monitored by real-time PCR. Like XFD and Δ-FGFR-4, early SU5402 FGF inhibition results in an increase in *bmp2*, *bmp4*, and *bmp7* expression at late blastula and early gastrula stages (Figure 2.6 C). Inhibiting FGF signaling prior to the mid-blastula transition (8, 128 or 512 cell stages) results in an increase in *bmp2, bmp4* and *bmp7* transcript levels at shield stage (early gastrula). However, by sphere stage (late blastula) the ability of SU5402 to increase BMP transcript levels at shield stage decreases substantially (Figure 2.6 C). These results demonstrate that FGF signaling acts between the 512-cell stage and sphere stage to repress BMP transcript levels and suggests that the FGF ligands responsible for this activity are likely to be encoded by early zygotic genes.

To determine whether FGF also regulates early expression of BMP target genes, the epidermal markers *vox* and *eve1* (Joly et al., 1993; Melby et al., 2000) expression levels after manipulating FGF signaling were monitored. FGF signaling was inhibited or activated using the SU5402 or iFGFR-1/AP20187 methods at the 512-cell stage. Samples were then collected at shield stage for real time PCR for *vox* and *eve1*. Inhibiting FGF results in about a 30% increase in *vox* and a 50% increase in *eve1* expression (Figure 2.6 D). Conversely, activating FGF signaling results in 25% and 50% reduction in *vox* and *eve1* respectively. These results suggest that prior to early gastrula stages FGF acts to diminish output of the BMP pathway.

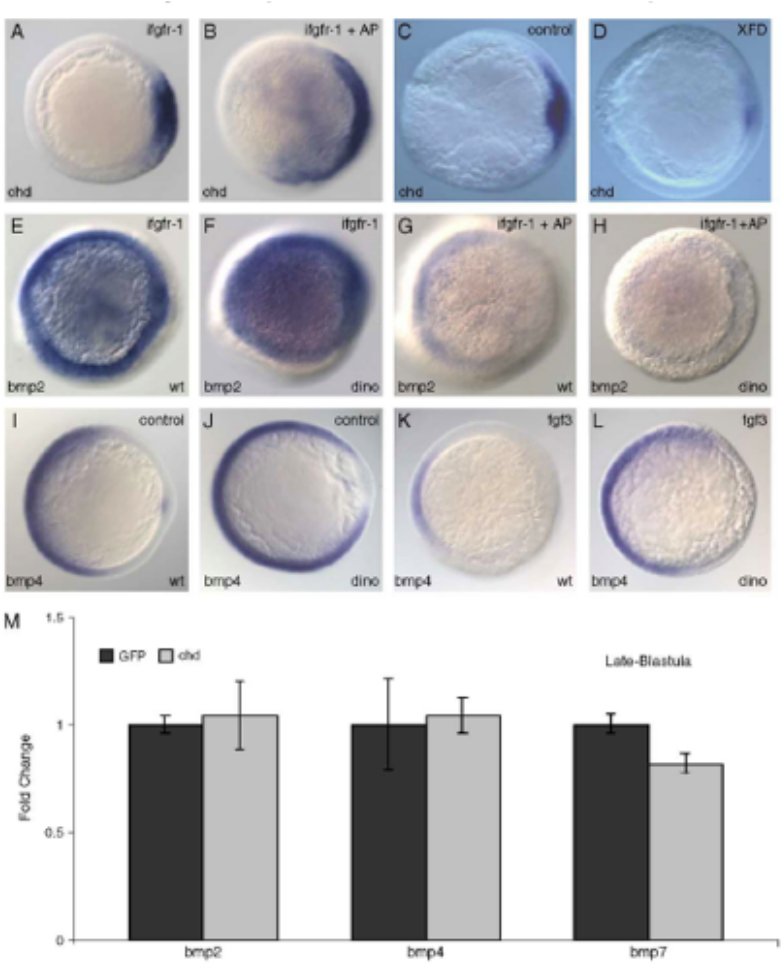

Figure 2.7. FGF regulates chordin expression but does not require Chordin to repress BMP transcript levels. Addition of AP20187 to iFGFR-1 injected embryos induces *chordin* expression (B) throughout the embryo while in the absence of AP20187 iFGFR-1 embryos maintain wild-type levels of *chordin* (A) at shield stage (early gastrula). Microinjection of 125 pg XFD mRNA has the opposite effect and dramatically reduces *chordin* expression at shield stage (D) compared to control injected embryos (C). Whole mount RNA *in situ* hybridization of embryos from a dino heterozygote intercross (E-L). *bmp2* expression at shield stage in iFGFR-1 injected embryos (E-H) exposed to AP20187 (G, H) or embryo water (E, F). The dino mutation does not suppress the activity of iFGFR-1 to repress bmp transcript levels. Genotypes of embryos are indicated. (I-L) *bmp4* expression at shield stage in control (I, J) or embryos injected with 50 pg fgf3 mRNA injected embryos (K, L). All views are animal pole. Genotypes of embryos were determined by PCR based genotyping following photography. To determine if *chordin* has an effect on BMP gene transcription, real-time PCR was performed on embryos injected with 100 pg chordin and collected at the blastula stage (M). Graphed is the fold change (y-axis) for *bmp2, bmp4* and *bmp7* levels relative to control injected embryos. These results show that chordin overexpression does not have an effect on BMP transcript levels at the blastula stage.

2.2.7 Early FGF regulation of BMP transcription is independent of Chordin:

Repression of BMP transcript levels might be caused by disruption of BMP autoregulation since BMP signaling induces transcription of BMP ligands in an autoregulatory loop (Hild et al., 1999; Jones et al., 1992). Alternatively, FGF signaling might act to repress the initial transcription of BMPs. Either mechanism could account for the effects of FGF on ectodermal cell fate choices.

One mechanism of action of FGF to regulate *bmp* expression could be via controlling the expression of the BMP-antagonist Chordin. Chordin inhibits autoregulation of BMP expression by blocking BMP signaling. Activation of the FGF pathway with iFGFR-1 or FGF3 mRNA induces *chordin* expression (Figure 2.7 B and data not shown and (Koshida et al., 2002). More importantly, suppressing FGF signaling with XFD sharply reduces expression of *chordin* at the start of gastrulation (Figure 2.7 C, D) and throughout the gastrula period (data not shown). These results demonstrate that FGF signaling is essential for *chordin* expression.

It has been suggested that the activity of FGF3 in regulating neural marker expression in late gastrula embryos is abolished in *dino* mutants (Koshida et al., 2002). To determine whether FGF acts via Chordin to repress *bmp* transcript levels, iFGFR-1 mRNA (Figure 2.7 E-H) or fgf3 mRNA (Figure 2.7 I-L) was injected into embryos from *dino* heterozygote intercrosses. Embryos were subjected to RNA *in situ* hybridization with *bmp4* or *bmp2* probes. As in earlier experiments, activation of FGF signaling with either reagent resulted in decreases in *bmp* transcript levels in wild-type embryos. Activation of FGF signaling in *dino* mutants also resulted in decreases in *bmp* transcript levels (Figure 2.7 G, H and K, L). Furthermore, overexpression of *chordin* does not impact blastula stage expression of BMPs (Figure 2.7 M). These results suggest that while induction of *chordin* transcription is one means by which FGF can repress BMP signaling and BMP transcript levels by autoregulation, this mechanism does not account for the late blastula stage clearing of BMP transcripts from the dorsal ectoderm.

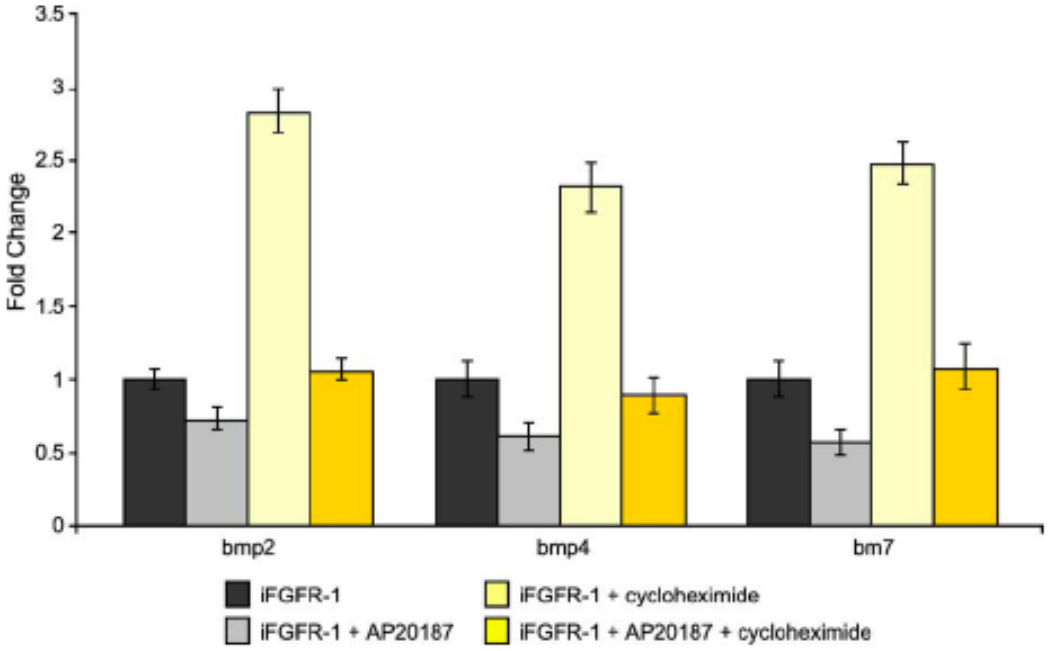

Figure 2.8. FGF signaling does not require protein synthesis to inhibit BMP signaling. Embryos were injected with iFGFR-1 and treated with AP20187, cycloheximide or both at the 512 cell stage. Embryos were collected after one hour for real-time PCR analysis. The fold change (y-axis) of the BMP markers *bmp2, bmp4* and *bmp7* is graphed relative to the control (iFGFR-1). These results show that protein synthesis is not required for FGF signaling to inhibit BMP transcript levels.

2.2.8 FGF does not require protein synthesis to inhibit BMP signaling during the late blastula period:

To further address the means by which activation of FGF signaling represses *bmp* transcript levels, I investigated whether FGF mediated repression requires protein synthesis. FGF signaling was activated just prior to the MBT using the iFGFR-1 construct and placed embryos in cycloheximide to block translation. Samples were placed in AP20187, cycloheximide, or both reagents, and collected embryos after one hour. BMP transcript levels were then examined by real-time PCR (Figure 2.8). Treatment of embryos with cycloheximide resulted in greater than 2 fold increase in levels of each of the *bmp* transcripts compared to control embryos. But when FGF signaling was activated in the presence of cycloheximide, the expression levels of *bmp2*, *bmp4* and *bmp7* returned to near baseline levels. Activation of FGF signaling with AP20187 in the absence of cycloheximide results in a 30-50% decrease in *bmp2*, *bmp4* and *bmp7* transcript levels. These results demonstrate that FGF signaling does not require protein synthesis to repress BMP transcript levels during the late blastula period.

2.3 Discussion:

The vertebrate ectoderm is partitioned into neural and non-neural territories as a result of inhibition of BMP signaling. The mechanisms by which the BMP-free zone is established are complex and investigators working on various model organisms have focused on different mechanisms. The results presented here investigated the interplay between Chordin, the Nodal pathway, which is required for induction of mesoderm, and the FGF pathway and demonstrate that all three contribute to the establishment of the neural territory.

2.3.1 The early neural domain is established by the combined actions of Chordin and the Nodal and FGF signaling pathways:

As a means of identifying endogenous neural inductive signals, I sought to determine the signals that generate neural tissue in Nodal signaling mutants. These embryos lack trunk mesendoderm and markers of dorsal mesoderm except *chordin*, yet have well patterned neural tissue despite undergoing abnormal morphogenesis. Since Chordin is a potent neural inducer, the role of Chordin in neural induction in the absence of dorsal mesoderm was examined by generating MZ*oep;dino* double mutants. Neural markers are still expressed in these double mutants, although in restricted territories (Figure 2.1). This result suggests that, although Chordin plays a substantial role in specification of neural tissue in MZ*oep* mutants (and in wild-type embryos), additional factors must be involved.

Recent experiments in *Xenopus* have suggested that Chordin is required for neural induction in the absence of mesoderm (Kuroda et al., 2004). Here an early population of dorsal ectodermal cells that express *chordin* and *noggin* and give rise to parts of the CNS was identified. MZ*oep;dino* double mutants also lack Noggin since its expression also depends on Nodal signaling (Sirotkin et al., 2000b) (and data not shown). These findings may reflect species specific mechanisms or be due to differences in the combined effects of CerS and *chd* morpholinos compared to MZ*oep;dino* double mutants. However, it is plausible that the neural tissue observed in the absence of mesoderm and Chordin is a result of autonomous signals from the ectoderm as observed in the Kuroda study.

Since mesoderm is thought to be a key source of neural inductive signals, the ventral mesoderm (tail), which is maintained in the absence of Nodal signaling as a possible source of neural inducing signals was analyzed. Unlike in wild-type embryos, cells that are fated to become tail mesoderm are positioned adjacent to the dorsal ectoderm in MZ*oep* mutants (Carmany-Rampey and Schier, 2001). MZ*oep* single mutants lack mesodermal markers during gastrulation but do ultimately form tail somites (Gritsman et al., 1999). No mesoderm is specified in MZ*oep;ntl* double mutants as demonstrated by the absence of mesodermal markers during somitogenesis (Figure 2.2). Neural specification is unaffected in these mutants as evidenced by maintenance of *otx2* expression in a domain comparable to MZ*oep* single mutants (Figure 2.2 O, P). Since these embryos still express *chordin*, it was determined whether tail mesoderm and Chordin have redundant roles in neural specification by eliminating the remaining ventral mesoderm in MZ*oep;dino* double mutants using *ntl* morpholinos. This treatment did not alter the *otx2* expression domain of MZ*oep;dino* double

mutant embryos (Figure 2.2 Q, R). From these experiments it can be concluded that factors in addition to Chordin and molecules found in the mesoderm are required for the specification of anterior neural tissue.

However, despite the failure of mutant marginal cells to become differentiated mesoderm, it is likely that these cells retain some signaling capabilities characteristic of mesoderm. In fact, the expression of *krox20* demonstrates that the signals that posteriorize the neural plate to form the hindbrain are still present in these mutant embryos. These posteriorizing signals are thought to originate from somite precursors (Stern et al., 1991; Woo and Fraser, 1997). The maintenance of this signaling activity implies that the mutant marginal cells retain some activities characteristic of mesendodermal precursors.

An FGF mediated signal may account for such an activity in mesendodermal precursors. Studies in the chick have implicated an early role for FGF signaling in defining the neural territory (Wilson and Edlund, 2001; Wilson et al., 2000). However, experiments on the role of FGF in neural induction in amphibians and zebrafish have produced conflicting conclusions (Hongo et al., 1999; Kroll and Amaya, 1996; Pera et al., 2003; Ribisi et al., 2000). While recent experiments have suggested that FGFs act as neural inducers, one to two day frog or fish embryos that have been treated with XFD (Amaya et al., 1991; Griffin et al., 1995) or Δ-FGFR-4 (Hongo et al., 1999)(and unpublished result) often still have eyes and well patterned anterior neural tissue. Therefore, the effects of FGF on neural cell fate choice in zebrafish was carefully examined.

The effects of blocking FGF signaling in Nodal mutants and wild-type embryos clearly demonstrate that FGF signaling is required for proper neural and epidermal cell fate choice within the ectoderm. Inhibiting FGF signaling in both Nodal mutants and wild-type embryos led to a decrease in the domains of neural markers during gastrulation (Figure 2.3). In both wild type and MZ*oep* mutant embryos with compromised FGF signaling, the early neural domain was reduced and shifted closer to the margin. The position of the neural domain suggests that it may be generated in response to signals from the margin.

The analysis of transcript levels using real-time PCR revealed a decrease in expression levels of neural markers and corresponding increases in expression levels of markers of ventral ectoderm. Since the size of the expression domains of markers and their expression levels are likely to correlate to cell numbers, blocking FGF signaling increases the

number of ectodermal cells adopting non-neural fates and decreases the number of cells adopting neural fates.

FGF has also been implicated as an important posteriorizing signal. If the sole role of FGF were in posteriorization of the neural plate, the manipulations done here would have resulted in an increase in the expression of anterior neural markers, without an alteration of the expression of markers of non-neural ectoderm. Previous experiments using XFD in zebrafish have led to the conclusion that following XFD treatment *hoxb1b* expression is sharply reduced while *otx2* expression is expanded toward the margin (Kudoh et al., 2002). Additionally, a repression of *hoxb1b* expression and a vegetal shift of *otx2* expression was observed along with a clear decrease in the size of the *otx2* domain and decreases in *otx2* transcript levels. The reason for the differences in results is not fully understood, the analysis done here was performed at an earlier stage (mid- gastrula) while the other observations were made near the end of gastrulation and *otx2* levels may have begun to recover.

Both XFD and Δ-FGFR-4 (data not shown) produced defects in anterior neural tissues and no significant differences between these reagents were observed. Since the specificity of these dominant negative constructs is unknown it is not known which FGF receptors are being blocked. However, it is plausible that both FGFR-1 and FGFR-4 play a role in mediating neural induction by FGF.

2.3.2 Recovery of neural tissue in embryos with impaired FGF signaling:

These results demonstrate that XFD blocks neural induction at mid-gastrula stages, but that *otx2* expression recovers to wild-type levels by the 6-somite stage (Figure 2.4). This recovery depends on mesoderm (Nodal signaling) as *otx2* expression remains reduced in XFD injected MZ*oep* mutants at the 6-somite stage and deficits in anterior neural tissue are apparent in these embryos at 24 hrs (Figure 2.3 D). Despite the clear deficits in neural marker expression during gastrulation following inhibition of FGF signaling in wild-type embryos, neural tissue recovers to produce brains of overtly normal size and structure.

These experiments suggest that the ectoderm may remain competent to respond to neural inducing signals throughout gastrulation. Surprisingly, even though neural marker expression is delayed in the dorsal ectoderm after inhibition of FGF signaling, largely normal

morphogenesis and patterning ensue. The origin of the *otx2* expressing cells that observed at the 6-somite stage may have arisen from a late acting signal that acts on the *gata2/3* positive cells that populate the dorsal ectoderm in embryos with compromised FGF signaling. It is also possible that inductive signals act on a cell population that exists within the ectoderm that expresses neither neural or epidermal markers. Alternatively, the smaller population of anterior neural cells in embryos with impaired FGF signaling may be subjected to fewer limitations on proliferation than cells in the wild-type neural domain.

Redundant activities between FGF and downstream Nodal target genes in neural induction also may occur. Virtually all mesendodermal genes require Nodal signaling and the effect of Nodal is likely to be indirect. FGF has been shown to act downstream of Nodal in mesoderm induction in zebrafish embryos (Mathieu et al., 2004) and the possibility that the Nodal target mediating the recovery is actually a late acting FGF not inhibited by these treatments.

It is also plausible that the recovery of *otx2* expression in MZ*oep* embryos with compromised FGF signaling stems from the abnormal cellular topography created by the failure of mutant marginal cells to involute (Carmany-Rampey and Schier, 2001). Marginal cells in MZ*oep* mutants may remain in contact with the ectoderm for a longer period than in wild-type embryos. This additional time may allow inductive interactions that do not occur in wild-type embryos.

Since blocking FGF signaling in *MZoep;dino* double mutants completely abolishes *otx2* expression at mid-gastrulation (Figure 2.4 H), the early neural domain is established by the activities of Chordin, FGF and Nodal targets acting in concert. The analysis of these mutants also implies that FGF signaling is sufficient to induce some neural markers in the absence of organizer activity and Chordin. This result contrasts with conclusions from the chick that suggest that FGF is not sufficient for neural induction (Streit et al., 2000; Wilson et al., 2000). Further experiments will be necessary to determine whether this difference reflects subtleties in the assay conditions or fundamental species-specific mechanisms.

2.3.3 FGF signaling represses BMP activity on multiple levels:

Repression of BMP signaling is thought to be a critical step in establishing the neural domain. These results demonstrate that FGF signaling in the zebrafish blastula is required to suppress expression of BMP ligands. Activation of FGF signaling represses BMP expression (Figures 2.6-2.8) and impeding FGF signaling with XFD, Δ-FGFR-4 or SU5402 (Figures 2.5, 2.6) results in increased expression levels of *bmp* 2, 4 and 7. These results extend and support recent findings in zebrafish that modulation of FGF activity regulates expression of BMP ligands (Furthauer et al., 2004).

Since the ability of SU5402 to derepress BMP transcript levels diminishes between the 512-cell and sphere stages, the endogenous FGF signaling events must occur around the time of the mid-blastula transition. Therefore, it is likely that the FGF pathway is activated by an early zygotic gene product. These results are consistent with the findings of Wilson et al (2000) that demonstrated a role for FGF signaling in repressing BMP transcription in the chick. Together, these data suggest that repression of BMP transcription by FGF signaling may be a common, early step in defining the neural territory in vertebrates.

Transcription of BMPs is also a readout of BMP signaling since BMPs autoregulate their own transcription (Hild et al., 1999; Jones et al., 1992). However, two lines of evidence indicate that the early effect on BMP transcript levels is not due to blocking BMP autoregulation: First, FGF can repress BMP transcript levels in the absence of protein synthesis at early stages (Figure 2.8) and second, Chordin overexpression cannot alter levels of BMP transcripts at these stages (Figure 2.7 M). Therefore, FGF must be acting to repress early zygotic transcription of BMP ligands. In early gastrula embryos, a decrease in transcript levels of the BMP target genes, *vox* and *eve1,* in response to upregulated FGF signaling was observed. Conversely, increased levels in response to inhibition of FGF activity (Figure 2.6 D). This effect could be caused by diminished levels of BMP ligands or by another means of blocking BMP signaling.

It was also observed that FGF signaling is required for the expression of *chordin* (Figure 2.7). However, the finding that BMP transcription can still be repressed in *dino* mutants (which lack Chordin) by activation of FGF signaling (Figure 2.7) provides further evidence that FGF must act via additional mechanisms.

Nevertheless, regulation of *chordin* expression by FGF is likely to be an important mechanism by which presumptive neural tissue is protected from the anti-neuralizing effects

of BMPs. Additionally, there are other mechanisms of regulation of BMP signaling by FGF signaling. The human Smad1 protein contains four consensus ERK-MAP kinase phosphorylation sites (Kretzschmar et al., 1997). These sites have been shown to negatively regulate Smad1 in response to a receptor tyrosine kinase activity (Kretzschmar et al., 1997; Pera et al., 2003). The role of these sites in blocking BMP autoregulation has not yet been elucidated, although the sites are clearly important in modulating BMP signal transduction.

Responses to FGF signaling during early cell fate choice in the chick are mediated by Sip1 (Smad interacting protein1)(Sheng et al., 2003). This mechanism could also be important to the down-regulation of BMP transcripts by FGF in zebrafish by suppressing early TGF-β signals that may be required for BMP expression. Indeed, in zebrafish, experimental evidence suggests that some BMP expression may be regulated by a maternal GDF6 related molecule, Radar (Sidi et al., 2003). FGF could down-regulate BMP expression by acting via Sip1 to block induction of transcription by Radar. It will be important to determine the early mechanisms by which BMP transcription is repressed by FGF.

BMP transcription is increased when protein synthesis is blocked after the MBT in the absence of additional treatments (Figure 2.8). This suggests translation of an early zygotic gene is likely required to suppress BMP transcription. Zygotic transcriptional regulators including the *iroquois* homeobox genes and *bozozok* have been shown to repress BMP transcription and might mediate this activity (Fekany-Lee et al., 2000; Gomez-Skarmeta et al., 2001; Leung et al., 2003). Phosphorylation of Irx2 in response to FGF8 has been shown to be involved in cerebellum formation in the chick (Matsumoto et al., 2004) and it is plausible that early acting *iroquois* genes may also be regulated by FGF signaling.

The effects of FGF on the initial specification of neural tissue may not be limited to regulation of BMP signaling. Bertrand et al, have elegantly demonstrated that in ascidians, FGF 9/16/20 directly regulates Otx expression via Ets1/2 and GATAa (Bertrand et al., 2003). A BMP independent function of FGF has also been suggested in the chick (Wilson et al., 2001). Recently, experiments in zebrafish have demonstrated that FGF is involved in specification of presumptive spinal cord in a ventral domain of the embryo where high BMP activity is present (Kudoh et al., 2004). This finding strongly implies that FGF has activities in neural specification that are independent of regulation of BMP signaling. While the

Kudoh study focused on posterior neural specification FGF may also have similar functions in anterior neural specification.

FGF also plays a direct role in mesoderm formation (Kimelman and Kirschner, 1987) in addition to its roles in neural induction. How these seemingly distinct activities are regulated is an important question. Some insight comes from recent work in the chick that implicates the zinc finger protein, Churchill, as a switch that modulates the activity of FGF on the mesoderm (Sheng et al., 2003). It has not yet been determined if Churchill has a similar function in zebrafish.

Taken together, this work along with the work of others, suggest a model where FGF acts at multiple levels to suppress BMP signaling. FGF is likely to have additional direct effects on neural specification. Nodal also regulates *chordin* expression and through induction of the mesoderm has additional influences on the neural domain. The clearing of BMP transcripts from the dorsal ectoderm during late blastula stages is mediated by FGF. The endogenous FGF ligand that functions in this context is unknown as is the means by which its activity is regulated. These results support a unifying mechanism for neural induction in vertebrates where FGF acts during the late blastula period to establish a presumptive neural precursor population that is devoid of BMP transcripts. Later signals from the organizer and Chordin serve to protect those precursors from the effects of BMP signaling and to reinforce the neural character of the dorsal ectoderm.

2.4 Materials and Methods:

2.4.1 Zebrafish stocks and embryo maintenance:

Adult zebrafish stocks were maintained at 28.5°C. Embryos were produced by natural matings of appropriate adult fish, collected and stored at 28.5°C in embryo medium until desired stage according to Kimmel et al. The following mutant alleles were used in this study: *dino*^{tt250}, *ntl*^{b160}, Mz*oep*^{tz57}, as well as TL wild-type fish.

2.4.2 Pharmacologic treatments:

FGF signaling was pharmacogically inhibited by placing whole embryos of the appropriate stage into 60 μM SU5402 (Calbiochem, La Jolla, CA.). The inducible FGF receptor 1 (iFGFR-1) construct was activated at the appropriate stage with 1.25μM AP20187 (ARIAD Pharmaceuticals, www.ariad.com/regulationkits). Embryos were left in AP20187 and allowed to develop to the appropriate stage. The iFGFR-1 construct did not have an effect unless embryos were placed into AP20187. Protein synthesis was inhibited by placing embryos into 1μM cycloheximide (Sigma-Aldrich, St. Louis, MO) for one hour.

2.4.3 mRNA synthesis and microinjections of mRNAs and morpholinos:

Sense mRNA was made using the mMESSAGE mMACHINE kit (Ambion) RNA synthesis kit. The XFD, Δ-FGFR-4, *fgf3* and *chordin* (Amaya et al., 1991; Hongo et al., 1999; Kiefer et al., 1996; Miller-Bertoglio et al., 1997) constructs have been previously described. *ntl* morpholinos were by Gene Tools (Philomath, OR) and have been previously described (Nasevicius and Ekker, 2000). Prior to microinjections, embryos were dechorionated in 2mg/ml pronase (Sigma-Aldrich, St. Louis, MO). One- to-four cell embryos were injected with 0.5nl RNA diluted in 0.2 M KCl and phenol red. At the appropriate stage, embryos were fixed in 4% paraformaldehyde for *in situ* hybridization or placed in TRIzol reagent (Invitrogen) for RNA extraction.

2.4.4 Whole-mount *in-situ* hybridization, photography, and genotyping:

Embryos were fixed in 4% paraformaldehyde in phosphate-buffered saline (PBS) overnight at 4°C then stored in 100% methanol for storage at -20°C. *In situ* hybridizations were done as previously described (Thisse et al., 1993). Constructs used to synthesize the following probes have been described previously: *bmp2, bmp4, cyp26, emx1, gata2, gata3, hoxb1b, krox20, otx2, opl, pax2.1, papc, spt,* and *tbx6* (Detrich et al., 1995; Griffin et al., 1998; Grinblat and Sive, 2001; Hug et al., 1997; Krauss et al., 1991; Kudoh et al., 2002; Mori et al., 1994; Morita et al., 1995; Neave et al., 1995; Nikaido et al., 1997; Oxtoby and Jowett, 1993;

Yamamoto et al., 1998). After *in situ* hybridization, embryos were washed in benzyl benzoate: benzyl alcohol (2:1), mounted in Canada balsam: methyl salicylate (40:1) and photographed using an Zeiss Axiocam mounted on a Zeiss Axioplan microscope. Genomic DNA for genotyping was extracted by using the Qiagen DNeasy tissue kit. Primers and restriction enzymes used to genotype *dino*^{tt250}and *ntl*^{b160} were:

F dino 5'-ATTGTCTCAATCAGGTTGCTCC-3',

R dino 5'-CGGGTTGGTTTTATTTGTAA-3' (Msp1 restriction site polymorphism)

F:ntl 5'-GAAGTGACCACAAGGAAGTCC-3'

R:ntl 5'-ACGAACCCGAGGAGTGAACAG-3' (Alu1 restriction site polymorphism)

2.4.5 Analysis of gene expression by real-time PCR:

Total RNA was prepared from pools of 10 embryos using TRIzol Reagent (Invitrogen). For each experiment, three pools of experimental samples, and two pools of control samples were run. cDNA was synthesized from 0.5µg RNA using the SuperScript First Strand Synthesis Kit (Invitrogen) in a volume of 10µl. After the RT reaction, the volume of each cDNA sample was brought up to 100µl in dH20. Real-time PCR was carried out using an ABI Prism 7700 sequence detection system (Applied Biosystems). The real-time PCR reactions were set up using 5µl cDNA, 7.5µl 2x SYBR Green I mastermix (Eurogenetec, Philadelphia, PA.), and forward and reverse primers (100nM final concentration each) in a final volume of 15µl. All reactions were run with a melting temperature of 55°C. The sequences for the primer pairs are (forward primer/reverse primer):

β-actin, GATTCGCTGGAGATGATG/GTCTTTCTGTCCCATACCAA;

bmp2, TGGTGCAGGACTCTCACAC/TGGAGCACCTCTACAAGGAG;

bmp4, CAAACACCACACCAAAAGTG/TCTGCGGTGGATATGAGTTC;

bmp7, TGCAGCTCTTAGTGGAGACC/AAACGGCTGCTTATTCTGAG;

otx2, CCACTTTCTACCTCCTCCTC/TAGGAAGTGGAACCAGCATA;

hoxb1b, TTAAACAAGCGCCAACCTTT/GTGGTGAAATTGGTGCGTAT;

gata2, GCTGAATGTGTGAACTGTGGA/TGGCTTGATAAGGGGTCTGT;

gata3, CCTGCGGACTTTACCACAAG/ACAGTTTGCGCATGAGGTC;

vox, CTCATCTCCAAGCTTTTCAG/GAATTTGGTTCTGATTCTGC;

eve1, GGGTAGTCTCTCTGGGTTTT/GAATAGAGAGCTGGTTGTGG.

Each sample was run in duplicate along with a negative (water) control. In order to compare expression levels between control and experimentally treated embryos, a dilution series of non-injected cDNA control were included for each primer set in each run. The dilution series was serially diluted in the following conditions: 1:0 cDNA: H_20; 1:10 cDNA: H_20; 1:100 cDNA: H_20; and 1:1000 cDNA: H_20. This dilution series allowed a standard curve to be made for each primer set in each reaction.

For the analysis of the real-time PCR reactions, the duplicate Ct values for each sample was averaged together and the relative amount of RNA was determined by interpolating the samples Ct value to the standard curve. The relative amount of RNA was normalized to the relative amounts of the endogenous control (β-actin). The fold change was determined by comparing the normalized value of the experimental samples to the normalized value of the control samples. Data shown is the average of two independent experiments.

Chapter 3: Expression and regulation of the zinc finger transcription factor Churchill during zebrafish development

This chapter has been published in Gene Expression Patterns, 7 (2007) 645-650.

3.1 Introduction

Churchill (*chch*) is a small, highly conserved zinc finger transcription factor identified in a differential screen to isolate genes induced by Hensen's node (Sheng et al., 2003). *chch* was proposed to function as a switch between the functions of FGF in neural and mesoderm induction (Sheng et al., 2003). Morpholino knockdown of *chch* in the chick epiblast results in inappropriate migration of cells through the primitive streak (Sheng et al., 2003). This demonstrates that *chch* represses the movement of epiblast cells and allows them to remain in the prospective neural plate where they subsequently give rise to neural tissue (Sheng et al., 2003). Overexpression of *chch* in Xenopus results in suppression of the mesodermal marker *brachyury (Xbra)* in embryos and animal cap assays (Sheng et al., 2003; Snir et al., 2006). FGF4 or FGF8 are sufficient to induce *chch* expression in the chick. In Xenopus, *chch* expression is regulated by XLPOU91 which mediates FGF responsiveness (Snir et al., 2006).

chch acts primarily via induction of Smad interacting protein 1 (Sip1) (Sheng et al., 2003; Snir et al., 2006). Sip1 is a direct regulator of *Xbra* (Verschueren et al., 1999) and E-cadherin (Comijn et al., 2001) and binds activated forms Smad1/5 and Smad2/3 to repress their transcriptional activity (Postigo, 2003; Postigo et al., 2003). These functions may mediate the activity of *chch* as a regulator of cell movement and germ layer specification.

chch expression has only been described in the chick and in a cnidarian. In the chick, *chch* expression begins at stage 4 and is restricted to the prospective neural plate and the neural plate (Sheng et al., 2003). In the cnidarian, Nematostella vectensis, a *chch* homologue is expressed in the pharyngeal endoderm, in a structure that expresses several factors found in the Spemann organizer (Matus et al., 2007). *chch* expression has not been described in other species.

Here, the pattern of expression of the zebrafish *chch* gene was examined. Unlike in the chick, a broad expression pattern that is not restricted to the neural plate is observed. Furthermore, *chch* is zygotically expressed prior to the mid-blastula transition. During blastula and gastrula stages *chch* expression is widespread but becomes restricted to ventral epidermis during somitogenesis. At 30 hpf *chch* is expressed in anterior neural tissue and ventral epidermis. By 48hrs, expression is weak and specific domains are not detected until 4 dpf, when *chch* transcripts are enriched in the pharynx and gut. Finally, similar as in the chick, FGF signaling is required for *chch* expression is shown, but additional factors in regulating *chch* expression.

3.2 Results:

3.2.1 Zebrafish *chch* is expressed prior to the MBT.

A zebrafish *chch* homologue was identified by searching the zebrafish genome database (Sanger, www.ensembl.org/Danio_rerio) using the chick protein sequence as a source sequence. A single *chch* cDNA was identified (Genbank accession # BC085457). This sequence contains the entire coding sequence (339bp) as well as 5'- and 3'- UTR regions (82bp and 515bp respectively). The *chch* genomic structure contains 4 exons. The predicted amino acid sequence is 112 amino acids long and shares about 85% identity and about 70% similarity with the chick *chch* protein (as reported by Sheng et al. 2003).

The temporal and spatial expression of zebrafish *chch* was examined by RT-PCR and whole mount RNA *in situ* hybridization. *chch* transcripts were detected by RT-PCR throughout the first 48hrs of development (Figure 3.1). The *chch* expression pattern was examined by RNA *in situ* hybridization using two non-overlapping probes (one containing the 5'-UTR and the coding sequence, and a second containing only the 3'-UTR). Both probes gave similar results and only one is shown (Figure 3.2 A-L). During early cleavage stages, *chch* transcripts are detected throughout the cytoplasm of each cell, but also in a punctate

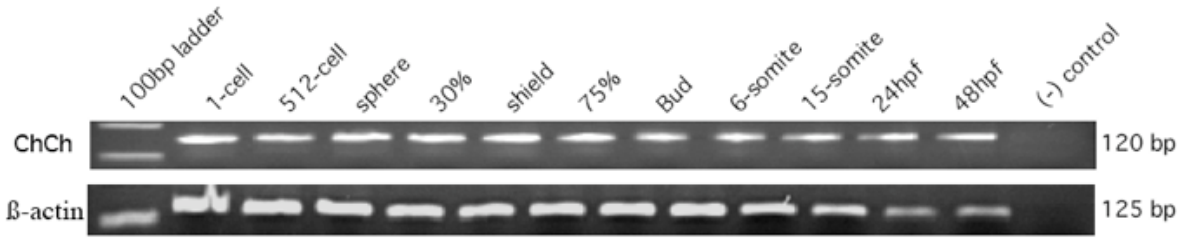

Figure 3.1. RT-PCR analysis of *chch* expression. RT-PCR of mRNA from staged wild-type embryos with *chch* specific primers reveals that *chch* transcripts are present during the first 48hrs of development at all stages analyzed. ß-actin was run as a PCR control

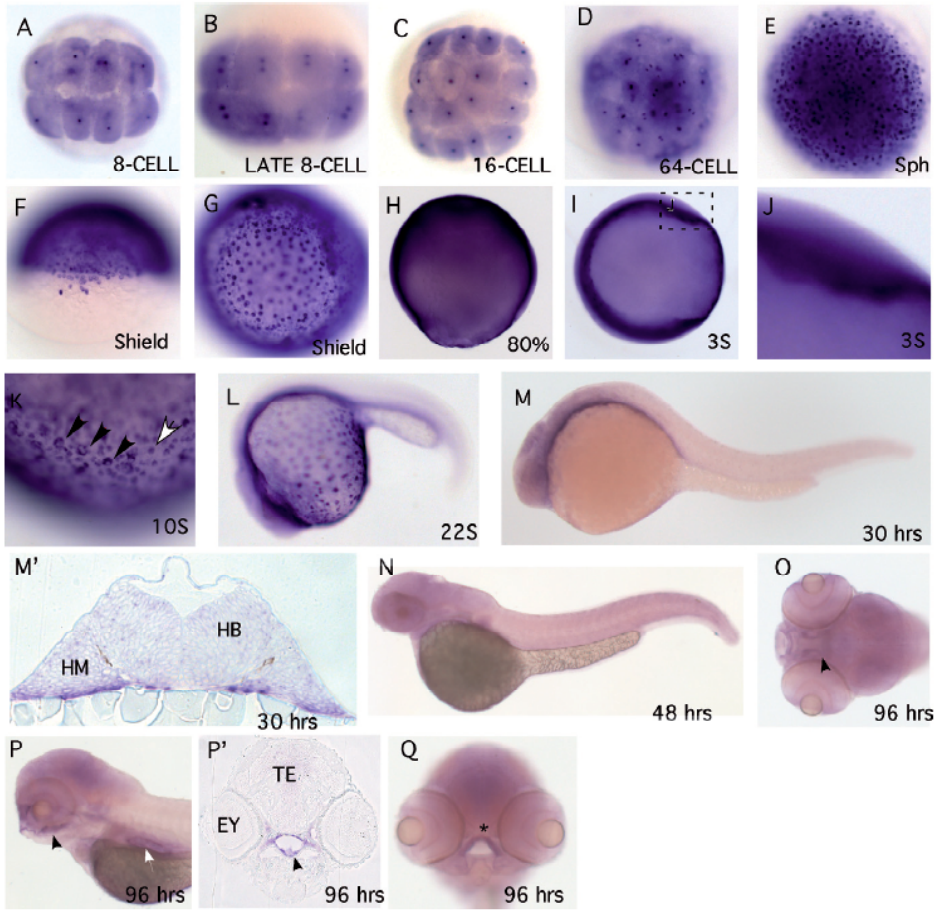

Figure 3.2. Whole mount RNA *in situ* hybridization analysis of *chch* expression in zebrafish. The *chch* expression pattern was examined in zebrafish by RNA *in situ* hybridization. *In situ* hybridization probes to the 5'-UTR and coding region or just the 3'-UTR were used; both gave similar results and only one is shown. During cleavage stages, *chch* transcripts are detected in the cytoplasm of all cells. Concentrated stain is also detected in the nucleus of each cell (A-D). At sphere and shield stages, *chch* is widely expressed and some cells express higher levels of transcript including a subset of forerunner cells (E-G). At 80% *chch* is ubiquitously expressed throughout the embryo but the punctate stain is less apparent (H). From the three-somite stage through the 22-somite stage *chch* transcripts are weakly detected throughout the embryo with highest levels in the ventral most regions of the embryo close to the yolk (I-L) and in a punctate pattern on the surface of the yolk (focus on the surface of the yolk) (K). In panel K, the black arrowheads mark presumptive mucous cells and the white arrowhead is a presumptive keratinocyte. At 30 hpf *chch* transcripts are enriched in anterior neural tissue and ventral cells adjacent to the yolk (M) and (M'). The section in M' is at the level of the hindbrain. At 48 hpf *chch* expression is weak and indistinct (N). At 96 hpf chch transcripts are detected in the pharynx (black arrowhead), gut (white arrowhead) and ethmoid plate (asterisk) (O-Q, section in P'). A-E, G are animal pole views. F and O are dorsal views; H-N and P are lateral views and Q is a frontal view. Abbreviations used are: hindbrain (HB), head mesoderm (HM), eye (Ey) and tectum (TE). (A-M, N-O, Q performed by Laurie Mentzer; and M' and P' performed by Kieth Gates)

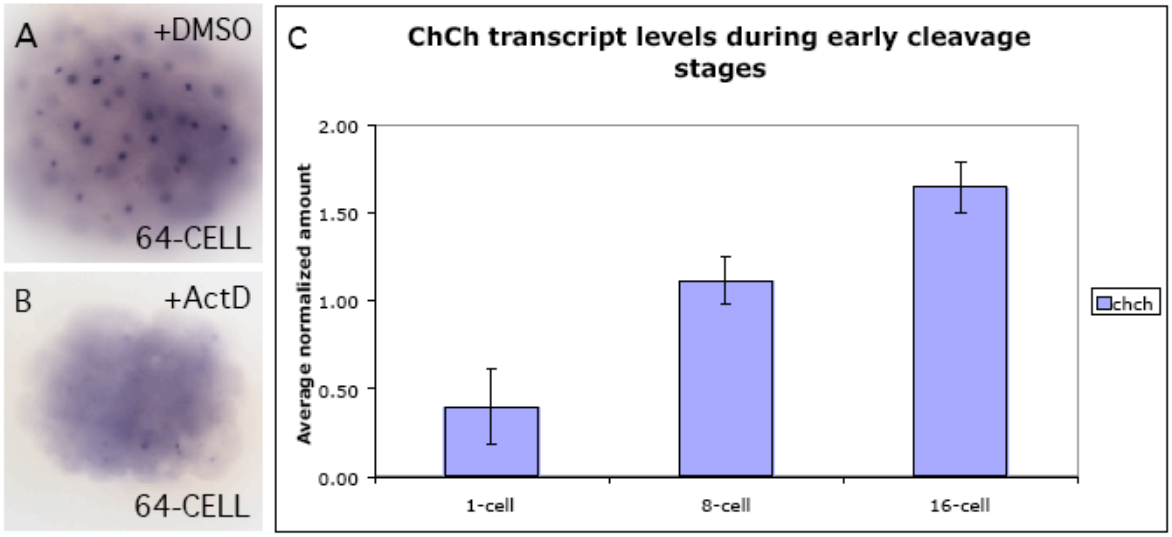

Figure 3.3. *chch* is zygotically expressed prior to the mid-blastula transition. To determine if the early nuclear stain observed represents new zygotic transcripts, embryos were microinjected with the transcription inhibitor Actinomycin D (B) or DMSO (A). Embryos were collected at the 64-cell stage and examined for *chch* expression by RNA *in situ* hybridization. Following Actinomycin D treatment, the nuclear stain is lost. As a further test to confirm early zygotic transcription of *chch*, real-time PCR was performed on 1-cell through 16-cell embryos to determine if the relative amount of *chch* gene expression is increased as development progresses. This analysis revealed an increase in *chch* expression over these stages (C). Together these results show that *chch* is being zygotically transcribed prior to the mid-blastula transition.

spot in each cell. At some stages, 2 spots appear in many cells (Figure 3.2 A-D). In the late 8-cell embryo, the 2 spots align with the cleavage planes of the cells. The punctate stain co-localizes with DAPI stain demonstrating that *chch* transcripts are within the nucleus (data not shown).

To determine whether the nuclear stain corresponds to new transcripts, zygotic transcription was blocked in wild-type embryos using Actinomycin D. Embryos were microinjected with Actinomycin D and *chch* expression was examined at the 64-cell stage by RNA *in situ* hybridization (Figure 3.3 A-B). Following Actinomycin D treatment, the nuclear stain was lost. As a further test to confirm early zygotic transcription of *chch*, real-time PCR was performed on 1-cell, 8-cell and 16-cell embryos to determine if the relative amount of *chch* transcripts increases as development progresses. This analysis revealed an increase in *chch* expression over these stages (Figure 3.3 C). Taken together, these data demonstrate that *chch* is transcribed prior to the mid-blastula transition and is likely also supplied as a maternal mRNA.

At sphere and shield stages, *chch* is widely expressed but some cells express higher levels of *chch* (Figure 3.2 E-G). Expression was observed in forerunner cells (Figure 3.2 F) but a clear pattern of specific regions of the embryo with high *chch* expression could not be discerned. During somitogenesis, *chch* is weakly expressed throughout the embryo, but robust expression in the ventral-most cells of the embryo adjacent to the yolk is observed (Figure 3.2 J-M). *chch* is also expressed on the surface of the yolk, in presumptive mucous cells and keratinocytes (Figure 3.2 K), although expression was not detected in these cell types in other regions of the embryo. By 30 hpf *chch* transcripts are observe in anterior neural tissue and ventral cells adjacent to the yolk (Figure 3.2 M-M'). Expression remains weak and indistinct until 96 hpf when expression is observed in the pharynx, ethmoid plate and gut (Figure 3.2 O-Q).

3.2.2. FGF signaling is required for *chch* expression.

Activation of FGF signaling was shown to be sufficient to induce *chch* expression in the chick (Sheng et al., 2003). However, that study did not determine whether FGF was required for *chch* expression. To determine if *chch* is regulated by FGF signaling in zebrafish, *chch*

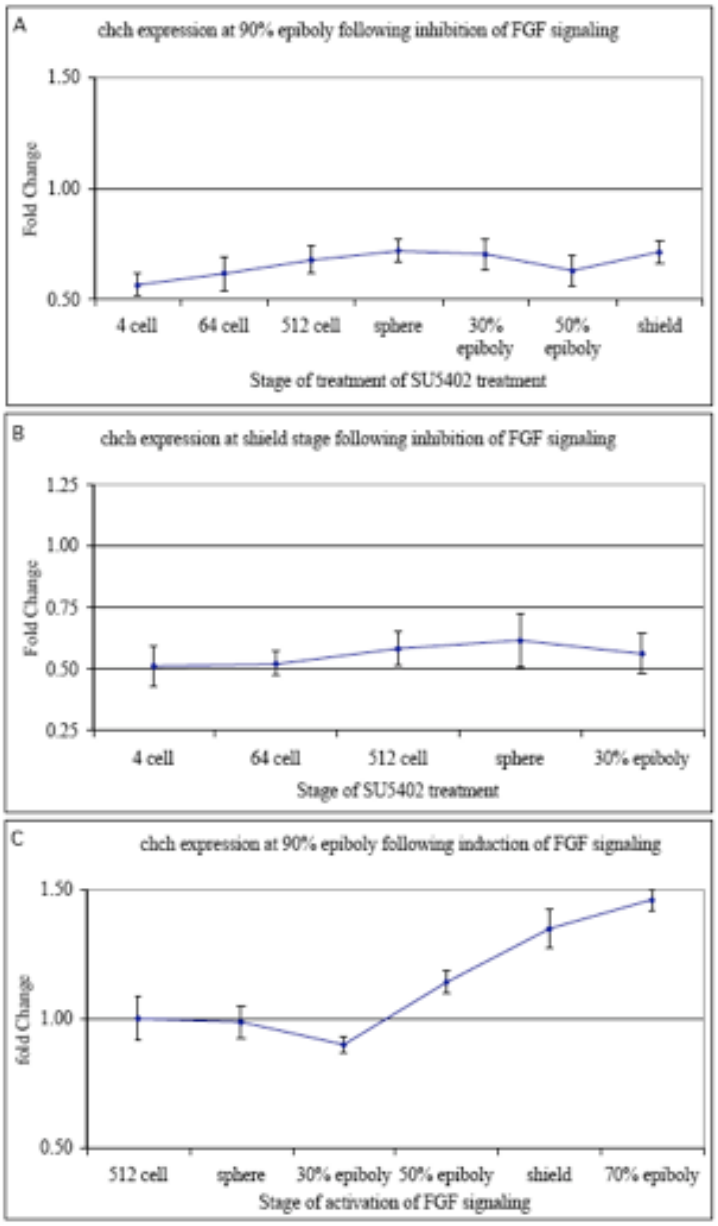

Figure 3.4. FGF signaling regulates zebrafish *chch* expression. To determine if FGF signaling regulates *chch* gene expression, *chch* expression was assayed by real-time PCR following inhibition (A-B) or activation (C) of FGF signaling. Wild-type embryos were placed in were treated for 2 hours in SU5402 to block FGF signaling at the indicated stage (x-axis) and collected at 90% epiboly (A) or shield stage (B) for real-time PCR. FGF signaling was induced by the addition of AP20187 to iFGFR1 mRNA injected embryos. Embryos were placed in the AP20187 at the indicated stage (x-axis) for 15 minutes then washed and collected at 90% epiboly for real-time PCR (C). The fold change in *chch* transcript levels (y-axis) is graphed relative to untreated control embryos (which is set at 1).

expression following inhibition or activation of FGF signaling was examined. FGF signaling was inhibited using a pharmacological inhibitor of FGF, SU5402 (Mohammadi et al., 1996). Embryos were placed into 60μM SU5402 for 2 hours at a series of time points between the 4-cell and shield stages. Treated embryos were washed in embryo medium and allowed to develop until late gastrulation, when *chch* expression was assayed by quantitative real-time PCR (Figure 3.4 A). Inhibiting FGF signaling during cleavage, blastula and gastrula stages, results in about a 40% decrease in *chch* gene expression by late gastrulation.

To determine whether *chch* expression recovered between the stage when SU5402 was washed out and expression was assayed, a similar experiment was performed that examined *chch* expression at shield stage (6 hpf) (Figure 3.4 B). These treatments resulted in about a 40% decrease in *chch* transcript levels by shield stage suggesting that recovery of *chch* expression does not occur.

To determine whether activation of FGF signaling is sufficient to induce *chch* expression and to address the time window for this response, FGF signaling was activated using an inducible FGF type I receptor (iFGFR-1) (Pownall et al., 2003; Welm et al., 2002). This construct becomes active with the addition of a synthetic molecule, AP20187, which results in FGF receptor dimerization and activation. Wild-type embryos were injected with iFGFR-1 mRNA and the effect of FGF activation on *chch* expression was examined by real-time PCR during late gastrulation (Figure 3.4 C). *chch* transcript levels were not altered when FGF signaling was activated prior to shield stage. When FGF signaling was activated after shield stage, there was a 25% increase in *chch* mRNA levels and nearly a 50% increase when FGF was activated at 70% epiboly (mid-gastrulation). Since the half-life of *chch* transcripts is not known and message could be rapidly degraded, *chch* induction at shield stage after blastula stage induction of FGF signaling with iFGFR-1 was also assayed. Induction of *chch* mRNA at shield stage was not observed (data not shown) suggesting that the failure to observe induction of *chch* mRNA following early activation of FGF signaling is not due to rapid turnover of message.

3.3 Discussion:

In the chick, *chch* expression was shown in the prospective neural plate starting at stage 4 and remaining until stage 13 (Sheng et al., 2003). This is in contrast to what is shown here, where expression of zebrafish *chch* is not limited to the neural plate, but rather is expressed throughout early development. Prior to somitogenesis *chch* is widely expressed. While it is maternally expressed, it also begins to be zygotically transcribed prior to the mid-blastula transition. Early zygotic transcription of a gene has been thought to be rare, but examples have been characterized in Xenopus (Yang et al., 2002). Recently, a set of over one hundred zebrafish genes that are transcribed prior to the mid-blastula transition were identified by microarray analysis (Mathavan et al., 2005), although *chch* was not identified in this screen.

Unlike in the chick specific *chch* expression in the neural plate during gastrulation is not detected. During blastula and early gastrula stages, *chch* is expressed throughout the embryo, although there is increased expression in the forerunner cells suggesting a role in mediating cell movements. This would be consistent with one of its proposed functions in the chick (Sheng et al., 2003). By somitogenesis, *chch* expression becomes reduced throughout the embryo, except in the ventral regions of the embryo. After 24hrs, *chch* expression remains in anterior neural tissue and ventral cells next to the yolk. The pharynx expression bares similarity to the expression of chch in the pharyngeal endoderm in Nematostella (Matus et al., 2007).

Similar to the chick, zebrafish *chch* is regulated by FGF signaling. Since inhibition of FGF activity at various developmental stages has similar effects on *chch* expression, continuous FGF signaling may be required for maintenance of *chch* expression rather than initiation of expression. The *chch* transcripts observed may have been generated prior to application of the FGF inhibitor or may stem from FGF independent regulation of *chch* expression. One set of candidates that may also regulate *chch* is members of the Oct3/4 class of pou domain proteins. Recently, XLPOU91 was shown to regulator of *chch* in Xenopus (Snir et al., 2006). One function of this FGF mediated *chch* regulation could be to mediate gastrulation cell movements, mesodermal induction or neural induction, all of which require FGF signals.

The results shown here show that in zebrafish, *chch* is widely expressed prior to somitogenesis. While it is maternally expressed, it also begins to be zygotically transcribed prior to the mid-blastula transition. Unlike in the chick, there is not detectable specific

expression of *chch* in the neural plate during gastrulation. However, *chch* expression in the pharynx, which bares similarity to the expression of chch in the pharyngeal endoderm in Nematostella is detected. Finally, this work demonstrates that in zebrafish, wild-type *chch* expression requires FGF signaling but that activation of FGF signaling with iFGFR1 can induce *chch* expression during gastrula stages but not blastula stages.

3.4 Materials and methods:

3.4.1 Zebrafish stocks and embryo maintenance.

Adult TL wild-type zebrafish were maintained at 28.5°C. Embryos were produced by natural matings of adult fish, collected and raised at 28.5°C in embryo medium until desired stage according to Kimmel et al. (Kimmel et al., 1995).

3.4.2 Cloning of Churchill.

The Churchill coding sequence was cloned into the StuI site of the pCS2 plasmid. The primer sequences used for cloning were:

chch: ATGTGTACCGGTTGTGTCCA/CTAGAAGAGAGGTGCTGTTTG

3.4.3 Whole mount RNA in situ hybridization and photography.

Embryos of the desired stage were fixed in 4% paraformaldehyde in phosphate-buffered saline (PBS) overnight at 4°C then stored in 100% methanol at -20°C. RNA *in situ* hybridizations were done as previously described (Thisse et al., 1993). Constructs for *chch* in situ, probes containing the 5'UTR and the coding sequence or the 3'UTR alone were used to synthesize probes. After in situ hybridization, embryos were washed in benzyl benzoate/benzyl salicylate (40:1), and photographed using a Zeiss Axiocam mounted on a Zeiss Axioplan microscope. Prior to sectioning embryos were imbedded in JB-4 resin (Ted Pella).

3.4.4 Pharmacological treatments.

FGF signaling was pharmacologically inhibited by placing embryos of the appropriate stage into 60 μM SU5402 (Calbiochem, La Jolla, CA.) for 2 hours. Upon removal from SU5402, embryos were washed in embryo media and allowed to develop until collected for real-time PCR. FGF signaling was activated with an inducible FGF receptor 1 (iFGFR-1) construct. Embryos were microinjected with 2.5pg iFGFR-1 mRNA and activated at the appropriate stage with the addition of 1.25 μM AP20187 (ARIAD Pharmaceuticals, www.airaid.com/regulationkits) resulting in constitutive activation of the receptor. Embryos were left in AP20187 for 15 minutes then washed 3 times in embryo media for 5 minutes and allowed to develop until the appropriate stage. Transcription was inhibited by microinjection with 400pM Actinomycin D (Sigma-Aldrich) or DMSO as a control and collected at the desired stage for in situ hybridization.

3.4.5 Analysis of gene expression by real-time PCR.

Embryos were collected at the appropriate stage and placed in TRIzol reagent (Invitrogen) for RNA extraction. cDNA was synthesized from .5 μg mRNA with the SuperScript First-Strand Synthesis System for RT-PCR (Invitrogen). Real-time PCR was performed and analyzed as previously described (Londin et al., 2005), primer sequences used for

chch: TGTGTCCAGAAGCAATATCC/TCCTCCTCATCTTCATTCAC.

Chapter 4: Churchill regulates cell movements and mesoderm specification by repressing Nodal signaling

This chapter has been published in BMC Developmental Biology 2007, 7:120

4.1 Introduction:

The establishment of the vertebrate body plan depends on a carefully orchestrated series of position-dependent cell interactions that determine the nature and proportion of cells that will populate each of the three germ layers. The movement of cells or their resistance to move, influences the inductive signals they will encounter. These signals initiate developmental programs that generate various differentiated cell types.

The series of dynamic cell movements during gastrulation positions cells to receive signals that will direct them to a given fate. In zebrafish, these movements include epiboly, internalization and convergence and extension movements. Epiboly is the process of spreading and thinning of the embryo during blastula and gastrula stages. Mesendodermal precursor cells are located at the margin in a thickened region termed the germ ring. These precursors are internalized resulting in the formation of an outer epiblast layer and inner hypoblast layer (Kimmel et al., 1990). The convergence and extension movements results the movement of cells towards the dorsal side of the embryo, while elongating along the anterior-posterior axis of the embryo also on the dorsal side (Warga and Kimmel, 1990).

As the germ layers are specified, there is an antagonistic relationship between mesoderm and neural induction. Expansion of the mesoderm comes at the expense of the ectoderm; conversely, repression of mesoderm results in an expansion of the ectoderm (Feldman et al., 2002; Feldman et al., 2000; Gritsman et al., 1999; Thisse et al., 2000). FGF signaling has critical roles in specification and patterning of the mesoderm and neural ectoderm in mice, frogs, fish and the chick (Alvarez et al., 1998; Amaya et al., 1991; Furthauer et al., 2004; Griffin et al., 1995; Hongo et al., 1999; Londin et al., 2005; Storey et al., 1998; Sun et al., 1999; Yamaguchi et al., 1994).

In many species, neural and mesoderm induction occur at similar times and in adjacent cell populations. How can FGF function in the seemingly contradictory roles as an

inducer of mesoderm and neural tissue? One possibility is that different FGF effectors are present in the mesoderm and ectoderm to regulate its activity. One candidate FGF effector is the zinc finger transcription factor Churchill (*chch*) (Sheng et al., 2003).

chch overexpression in *Xenopus* embryos results in suppression of the mesodermal marker *brachyury* (Sheng et al., 2003). Morpholino knockdown of *chch* in the chick epiblast results in inappropriate migration of epiblast cells through the primitive streak (Sheng et al., 2003). *chch* morpholino-injected cells emerged from the primitive streak and gave rise to paraxial mesoderm. This suggests that *chch* is required to limit ingression of the epiblast allowing those cells to become neural tissue. In addition, the chick experiments implicate Smad-interacting protein-1 (Sip1) as a direct target of *chch* and suggest that Sip1 is the major *chch* effector involved in blocking ingression of the epiblast (Sheng et al., 2003).

Although the effect of *chch* in the assays in the frog and chick is the same (to limit mesoderm), the mechanisms of action in these two experiments likely differ. One difference is that cell movement is not thought to be required for mesoderm induction in the animal cap assay. The chick experiments do not address the question of whether the migration of *chch*-inhibited epiblast cells causes them to be exposed to mesoderm-inducing signals or whether they migrate because they have already acquired mesodermal properties. In order to elucidate the mechanisms of action of *chch*, a series of experiments were performed to study the requirement for *chch* in the zebrafish and to address the roles of *chch* in cell migration and cell fate.

Here, *chch* is shown to limit mesodermal gene expression in zebrafish. During gastrulation, inhibition of *chch* results in an increase in transcript levels of mesodermal genes and a decrease in the levels of ectodermal transcripts. In cell transplant experiments, cells with compromised *chch* activity are more motile than wild-type cells when transplanted to the epiblast of wild-type hosts. These cells leave the epiblast and migrate into the germ ring to acquire mesodermal cell fates, and both migration of *chch*-compromised donor cells and acquisition of mesodermal character depend on Nodal signaling. Finally, *chch* is required to repress the transcriptional response to Nodal signaling. Together, these findings demonstrate that *chch* regulates cell fate by limiting the response to Nodal signals.

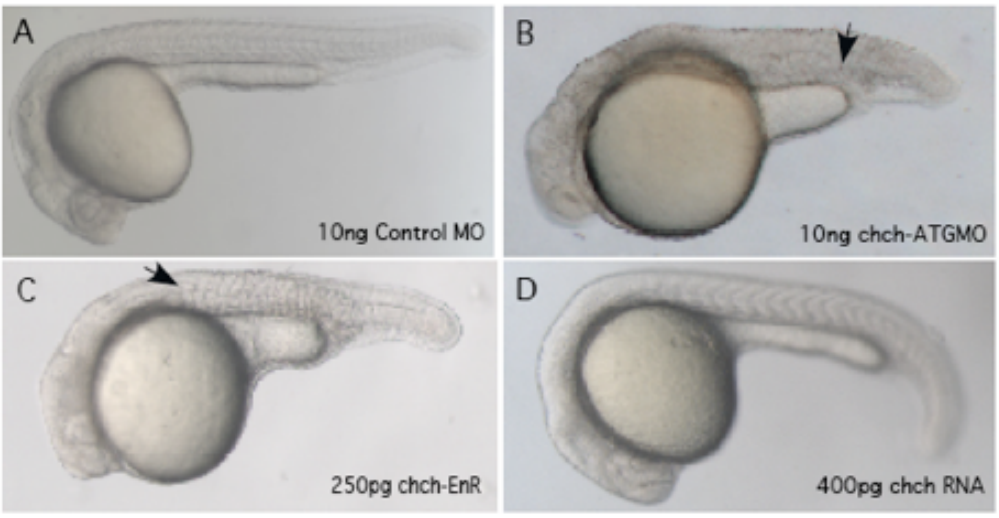

Figure 4.1. *chch* inhibition results in axial and somite defects. The effect of inhibiting *chch* was examined using a morpholino and a dominant-negative construct. Microinjection of *chch*-ATGMO results in a broad, misshapen notochord (arrow) and misshapen somites and a shortened axis (B). Microinjection of *chch*-EnR, results in a similar phenotype as the morpholino, a broad, misshapen notochord, and enlarged and misshapen somites formed (C). *chch* mRNA overexpression produces embryos that are wild-type in appearance (D). Arrowheads point to the notochord. All embryos are 24 hpf.

4.2 Results

4.2.1 *chch* inhibition produces axial and somite defects.

The zebrafish *chch* sequence was previously reported (Sheng et al., 2003) but the zebrafish *chch* has not been further characterized. Similar to the chick, zebrafish *chch* is regulated by FGF signaling, but unlike in the chick expression is widespread and not limited to the prospective neural plate (Londin et al., 2007a). To examine the function of *chch* in zebrafish, *chch* activity was inhibited with a morpholino directed against the translation start site and a dominant-negative mRNA. This morpholino will inhibit translation of *chch* protein. Microinjection of *chch*-ATGMO produces embryos with enlarged and misshapen somites (Figure 4.1 B). In addition, these embryos have a short body axis and poorly formed anterior neural structures (Figure 4.1 B).

Since *chch* functions as a transcriptional activator (Sheng et al., 2003), a dominant-negative construct by fusing the zebrafish *chch* coding sequence to the *drosophila* engrailed repressor domain (*chch*-EnR) was generated. The addition of the engrailed repressor domain will produce a powerful dominant-negative construct by recruiting transcriptional repressors to the promoter. Microinjection of *chch*-EnR mRNA pronounced a similar phenotype to the morpholino; highly disorganized somites, a wide notochord and short axis were observed (Figure 4.1 C). Taken together, these results demonstrate that *chch* is essential for proper formation of the body axis and suggest that *chch* deficiency may result in convergence extension defects.

4.2.2 Churchill is required for notochord morphogenesis.

To determine the role of *chch* on axial mesoderm specification, the effect of chch inhibition on *ntl* gene expression during late gastrulation (Figure 4.2 A-E) and early somitogenesis (Figure 4.2 F-M) was examined. During late gastrulation, microinjection of *chch*-EnR results in a broad notochord domain as evident by examination of *ntl* expression (Figure 4.2 B). Furthermore, closure of the yolk plug is abnormal in *chch*-EnR embryos (Figure 4.2 B').

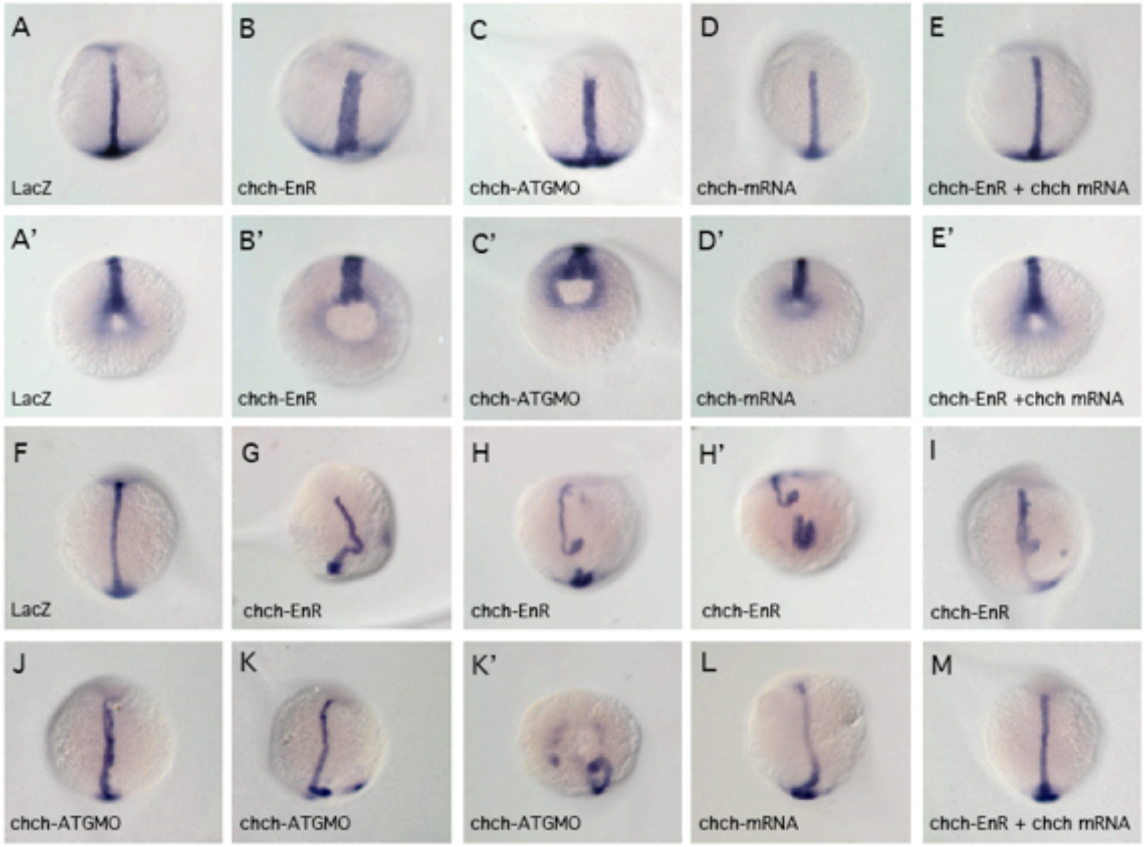

Figure 4.2. *chch* is required for notochord morphogenesis. Expression of the notochord marker *no-tail* was examined by RNA *in situ* hybridization during late gastrulation (90% epiboly) in embryos microinjected with the *chch*-ATG MO, *chch*-EnR mRNA or *chch* mRNA. Overexpression of *chch*-EnR mRNA results in a broad notochord (B) and altered yolk plug closure (B'). Treatment of wild-type embryos with *chch*-ATG MO results in a slight widening of the notochord and altered yolk plug closure (C-C'). Conversely, *chch*-mRNA has little effect during late gastrulation (D-D'). The notochord and yolk plug closure defects produced by *chch*-EnR injection can be rescued by co-expression of *chch*-mRNA (E-E'). Dorsal views are shown, A'-E' are vegetal or dorsal-vegetal views of the embryos in A-E.

Table 4.1. Co-expression of *chch*-EnR mRNA and *chch*-mRNA rescues the *chch*-EnR mRNA phenotype.

Bud Stage:					
Injection:	**# Wild type**	**Wide notochord**	**Split notochord**	**Thin notochord**	**Shortened notochord**
Control	24/24 (100%)	0	0	0	0
250pg ChCh-EnR	14/60 (23%)	30/60 (50%)	16/60 (26%)	0	0
400pg ChCh-RNA	30/42 (71%)	0	0	5/42 (11%)	7/42 (16%)
Co-injection	26/42 (61%)	7/42 (16%)	4/42 (9%)	5/42 (11%)	0
10 somites:					
Injection:	**# Wild type**	**Wide notochord**	**Split or bent notochord**	**Thin and curved notochord**	
Control	30/30 (100%)	0	0	0	
250pg ChCh-EnR	16/51 (31%)	11/51 (19%)	24/51 (47%)	0	
400pg ChCh-RNA	36/54 (66%)	0	0	18/54 (33%)	
Co-injection	36/52 (69%)	6/52 (11%)	6/52 (11%)	4/52 (7%)	

chch-ATGMO treatment produces a similar but less severe effect on the notochord and yolk plug closure than the chch-EnR construct (Figure 4.2 C-C'). Conversely, overexpression of *chch* mRNA has no effect on notochord morphogenesis or yolk plug closure (Figure 4.2 D-D'). Co-expression of either *chch*-EnR or *chch*-ATG MO with *chch*-mRNA results in the rescue of the effects on the notochord and yolk plug closure (Figure 4.2 E-E', Table 4.1 and data not shown). This demonstrates that the effects of the *chch*-EnR mRNA result from blocking *chch* function. A variety of axial defects in *chch* deficient embryos at the mid-somitogenesis (Figure 4.2 F-M) were observed. These included severe bends, splits and duplications. The dominant-negative construct has a more severe phenotype than the morpholino, suggesting that it more effectively blocks *chch* function. Together, these results demonstrate that *chch* is required for notochord morphogenesis.

To determine if *chch* is required at the early stages of notochord development, dorsal mesodermal markers during early gastrulation by *in situ* hybridization and real-time PCR following *chch* inhibition was examined. At this stage, both chordin (*chd)* and floating head *(flh)* are expressed within the shield. Following inhibition of *chch*, neither marker showed altered expression by RNA *in situ* hybridization (Figure 4.3 A-D) or real-time PCR (Figure 4.3 O). Other organizer-specific markers such as noggin and goosecoid were also examined (data not shown) and did not show a change in expression. These data suggest that repressing *chch* function does not alter initial specification of dorsal mesoderm but acts on subsequent steps in notochord development.

4.2.3 *chch* regulates mesoderm specification.

To determine if expression of other mesodermal genes is altered when *chch* function is reduced, pan-mesodermal markers at the start of gastrulation was examined. *In situ* hybridization and real-time PCR were used to assay expression of *no-tail* (*ntl*), *spadetail* (*spt)* and *tbx6*. All of these markers showed significant increases in expression at shield stage. Mesodermal gene expression was expanded towards the animal pole of these embryos (Figure 4.3 E-H and data not shown). This expansion of the mesodermal markers corresponds to a 2-2.25-fold increase in transcript levels when assayed by real-time PCR

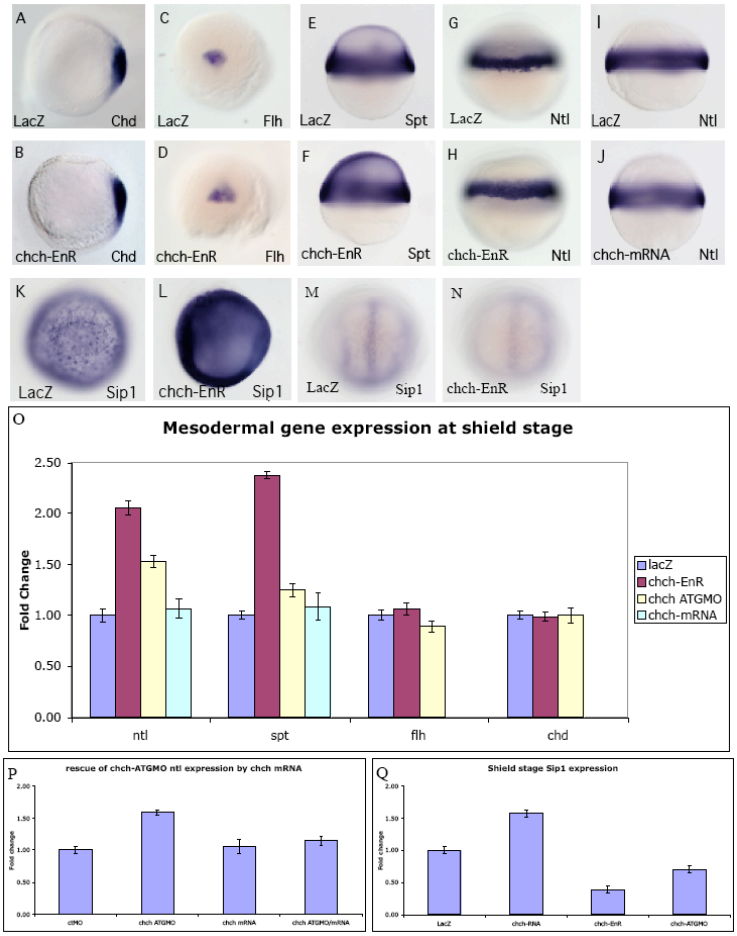

Figure 4.3. *chch* represses mesodermal markers. Mesodermal markers were examined by RNA *in situ* hybridization and real-time PCR in embryos microinjected with *chch*-EnR mRNA. Inhibition of *chch* does not alter expression of dorsal mesodermal genes *chd* (A, B) or *flh* (C, D). Expression of mesodermal markers at shield stage, including *spt* (E-F) and *ntl* (G-H) are expanded slightly in *chch*-inhibited embryos. Overexpression of *chch* mRNA does not alter *no-tail* expression at shield stage (I-J). *chch* inhibition results in a decrease in Sip1 gene expression at bud stage (M-N), while *chch* activation results in Sip1 induction at shield stage (K-L). Real-time PCR analysis of mesodermal markers in *chch*-inhibited embryos (O). The fold change in transcript levels (y-axis) is graphed relative to control embryos following overexpression of *chch*-EnR mRNA, *chch*-ATGMO and *chch* mRNA. This analysis reveals that the domains of mesodermal genes are expanded at shield stage while dorsal mesodermal genes are unaffected. Conversely, overexpression of *chch* mRNA does not result in alteration of early mesodermal gene expression. The induction of *ntl* expression following *chch* inhibition with the ATGMO can be rescued by co-expression of *chch* mRNA (P). Real-time PCR analysis of *Sip1* mRNA in *chch, chch*-EnR and *chch*-ATGMO treated embryos (Q). Induction of *chch* results in a 50% increase in Sip1 expression, conversely, inhibition of *chch* results in a 70% reduction of Sip1 expression. The fold change in Sip1 transcript levels (y-axis) is graphed relative to control embryos. (A-N produced by Laurie Mentzer)

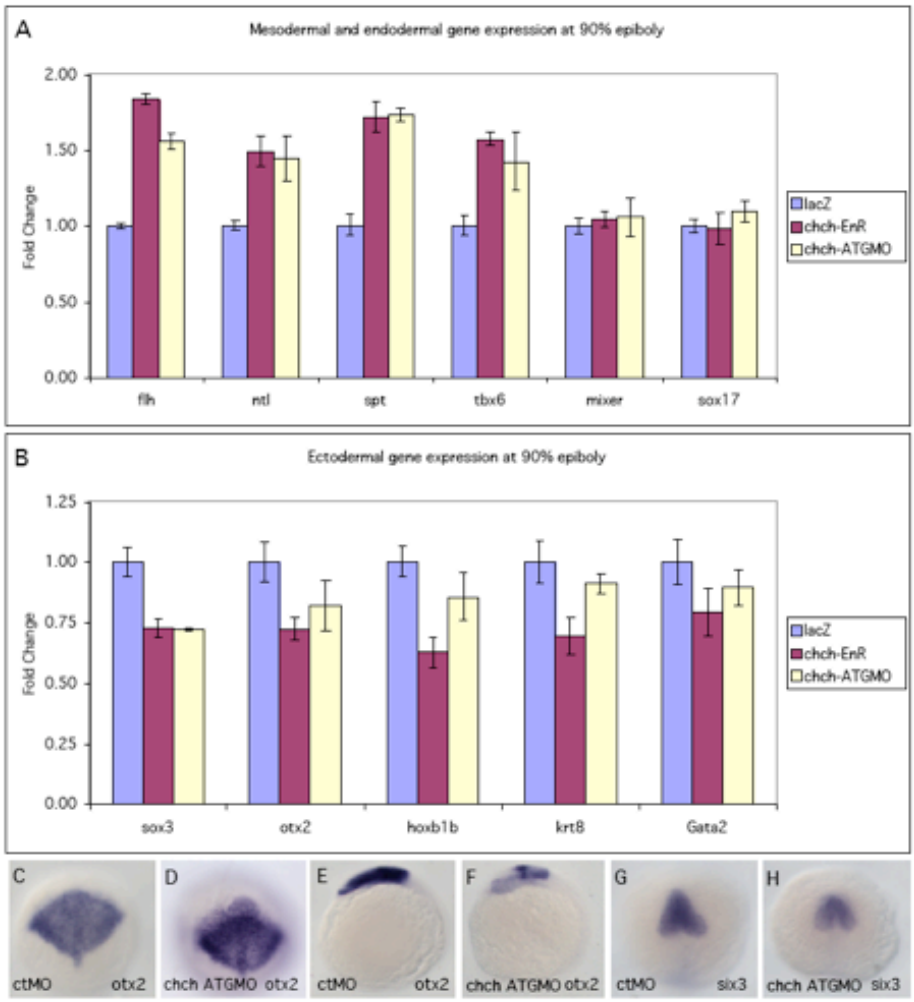

Figure 4.4. *chch* inhibition results in decreased ectodermal gene expression. Real-time PCR analysis of mesodermal, ectodermal and endodermal markers during late gastrulation in *chch*-compromised embryos. The mesodermal markers *flh, ntl*, *spt,* and *tbx6* (A), endodermal markers, *mixer* and *sox17b* (A) and ectodermal markers *otx2*, *hoxb1b*, *sox3*, *krt8* and *gata2* (B) were examined following microinjection of *chch*-EnR mRNA and *chch*-ATGMO. Mesodermal markers are increased, endodermal are unaffected while ectodermal marker levels are decreased. Expression of the neural genes *otx2* at 90% epiboly (C-D) and 6-somites (E-F) and *Six3* at 6-somites (G-H). C-D, G-H are dorsal views. E-F are lateral views.

(Figure 4.3 O). Surprisingly, overexpression of *chch*-mRNA did not alter mesodermal marker expression (Figure 4.3 I-J, O). These data demonstrates that *chch* is required to limit the mesodermal domain. However, unlike in *Xenopus*, ectopic *chch* is insufficient to block *brachyury* expression (Sheng et al., 2003).

Smad-interacting protein 1 (Sip1) is a direct target of *chch* in the chick (Sheng et al., 2003) and a direct repressor of *Xenopus brachyury* (Lerchner et al., 2000). Therefore, I asked whether the inability of ectopic zebrafish *chch* to repress *no-tail* stemmed from a failure to induce Sip1 expression. Since a zebrafish Sip1 *in situ* hybridization probe has not been previously described, a mRNA *in situ* probe and was generated by cloning from the Sip1 genomic locus (Ensembl gene Id: ENSDARG00000059564). At shield stage, overexpression of *chch*-mRNA results in large increases in Sip1 transcript levels (Figure 4.3 L, P). Conversely, inhibition of *chch* results in about a 70% decrease in Sip1 expression (Figure 4.3 N, Q). Together, these results reveal that zebrafish Sip1 is regulated by *chch*. Therefore, despite robust induction of Sip1, overexpression of zebrafish *chch* is not sufficient to alter *no-tail* expression.

We next assayed whether the increase in mesodermal gene expression following *chch* inhibition came at the expense of other germ layers. By late gastrulation, mesodermal markers in *chch*-inhibited embryos show a 50-75% increase compared to control embryos when assayed by real-time PCR (Figure 4.4 A). Conversely, the endodermal markers, *mixer* and *sox17*, do not show altered mRNA levels at late gastrulation following inhibition of *chch* activity (Figure 4.4 A). This contrasts ectodermal gene expression at late gastrulation. By RNA *in situ* hybridization, the expression domains of the neural gene *otx2* were not obviously altered (Figure 4.4 C-D) by late-gastrulation. However, real-time PCR analysis revealed that mRNA levels of both neural and epidermal markers were consistently decreased in *chch* morphants and *chch*-EnR treated embryos. The anterior neural marker *otx2*, the posterior neural marker *hoxb1b*, the pan-neural marker *sox3* and the epidermal markers *krt8* and *gata2* all showed decreased transcript levels (Figure 4.4 B). By early somitogenesis, the anterior neural markers *otx2* and *six3* both had reduced expression domains in *chch* morphants (Figure 4.4 E-H). Overexpression of *chch* mRNA did not result in a change in ectodermal or endodermal gene expression during late gastrulation (data not shown).

While there was an expansion of the expression domains of mesodermal markers at shield stage when *chch* function was abrogated, there was not a detectable spatial decrease in ectodermal marker expression. However, the quantitative real-time PCR data demonstrates a consistent decrease in the levels of expression of ectodermal markers during gastrulation. The ectodermal deficits may be too subtle to be detected by *in situ* hybridization or the expression domains recover by the time were able to assayed them. These findings suggest that *chch* regulates mesodermal cell fate during early development.

4.2.4 *chch* inhibition results in aberrant cell movements and cell fate changes.

The next question to be examined was whether repression of *chch* alters cell movements by tracking the behavior of *chch* compromised cells in a wild-type host. Sphere stage (mid-blastula) cells from ctMO or *chch*-ATGMO injected donor embryos were transplanted to the animal pole of similar stage wild-type hosts. Donor cell movements were observed at 40% epiboly, germ ring, shield stage and after 24hpf (Figure 4.5 B-M). Control donor cells undergo limited movement and spreading (Figure 4.5 B-D). In contrast, *chch*-inhibited cells moved vegetally and spread much faster (Figure 4.5 F-H).

To determine whether the vegetal movement of *chch* inhibited cells resulted in a fate change, the position of the donor cells after 24 hpf was examined. As expected, when transplanted to the animal pole, ctMO-donor cells generally became incorporated into anterior neural ectoderm (42/52 embryos, table 4.2, Figure 4.5 E). In a few embryos, ctMO-donor cells were found in the superficial cell layers in 3/42 embryos (7.1%, table 4.2) or in both neural tissue and superficial cell layers of the trunk 7/52 embryos (13.5%, table4.2). *chch* morphant donor cells often behaved much differently. When transplanted to the animal pole of a wild-type host, 44/72 embryos, *chch* morphant donor cells were observed in anterior neural structures (Figure 4.5 I, table 4.2). In the remaining embryos, the cells were spread over the trunk in superficial regions of the embryos in 15/72 embryos (20.8%) or in both neural tissue and superficial cell layers of the trunk in 12/72 embryos (16.7%, table 4.2). Importantly, the movement phenotype produced by the *chch*-ATGMO could be rescued by co-injection with *chch* mRNA (Figure 4.5 J-M). Unlike *chch* morphant donor cells which were restricted to the superficial layers of the trunk in 15/72 (20.8%) transplants, cells from

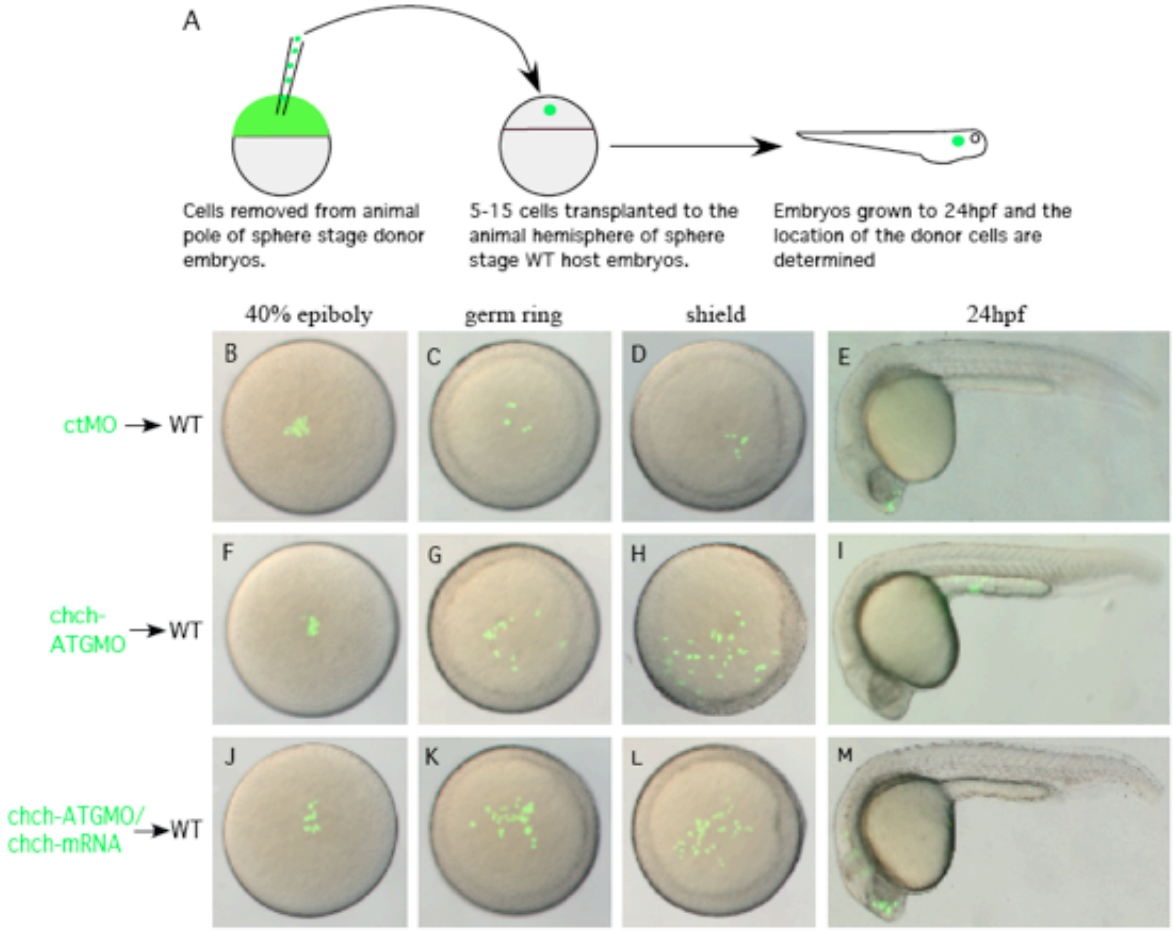

Figure 4.5. *chch* inhibition results in inappropriate cell movements. (A) A schematic representation of the transplantation scheme. ctMO or *chch*-ATGMO mRNA-injected donor cells were transplanted to the hemisphere of a sphere stage wild-type host. Embryos were photographed at 40% epiboly (B, F, J), germ ring (C, G, K) shield stage (D, H, L), and 24 hpf (E, I, M). The *chch* morphant cells (F-I) undergo greater spreading than the control cells and move toward the margin. At 24 hpf control cells are often found in anterior neural tissue (E) while the *chch* morphant cells are more frequently found in superficial cell layers of the trunk (I). The abnormal movement of *chch* morphant cells to superficial cell layers of the trunk is rescued by the injection of *chch*-mRNA (J-M).

Table 4.2. Transplantation of *chch* inhibited cells during mid-blastula stages results in inappropriate cell movements

		Location of cells at 24hpf			
Treatment	N	**Neural tissue**	**Superficial cells spread over the trunk**	**Neural and superficial cells spread over the trunk**	**Mesoderm**
ctMO	52	42	3	7	0
chch-ATG2MO	72	44	15	12	1
chch-ATG2MO/ *chch mRNA*	41	33	0	8	0

chch-ATGMO + *chch* mRNA injected donors were never restricted to the superficial layers of the trunk (0/41 embryos, Figure 4.5 J-M, table 4.2). However, in 8/41 (19.5%) embryos, cells were observed in superficial layers of the trunk and in anterior neural tissue (table 1), a rate comparable to the control transplant. Cells from *chch*-EnR mRNA injected donors also underwent similar spreading behavior as the *chch* morphant cells (data not shown).

These results show that *chch* inhibition results in inappropriate cell movements. To determine if the increase in mesodermal gene expression observed in *chch*-inhibited embryos (Figure 4.2) results from inappropriate cell movements, cell transplant experiments were performed to assay the behavior of *chch*-EnR and *chch*-ATGMO cells in wild-type hosts. Since transplantation of sphere stage (mid-blastula) *chch* compromised donor cells to sphere stage wild-type host resulted in movement of *chch* compromised donor cells to superficial cell layers, a series of heterochronic transplants to determine if the vegetal migration could result in a mesodermal fate change was performed. Here, sphere (mid-blastula) stage LacZ mRNA, *chch*-ATGMO or *chch*-EnR mRNA injected cells were transplanted to the animal hemisphere of 30% epiboly (late-blastula) stage embryos. Donor cell position was documented at 40% epiboly (5 hpf), shield stage (6 hpf) and 24 hpf (Figure 4.6 and table 4.3).

When LacZ cells were transplanted into the animal hemisphere of late-blastula embryos, donor cells remained within the ectoderm in 77/79 hosts (Figure 4.6 B-D, table 4.3). Cells with compromised *chch* function behaved dramatically different in this assay (Figure 4.6 E-G). In 44/110 (40.0%) transplants, *chch*-EnR donor cells migrated from the epiblast to the germ ring by shield stage (table 4.3). The effects of the *chch*-ATGMO were less pronounced but in 8/51 (15.7%) transplants, morphant cells migrated from the epiblast to the germ ring (Figure 4.6 K-M). Cells from donor embryos that had been co-injected with *chch*-EnR mRNA and *chch* mRNA tended to remain in the animal hemisphere (Figure 4.6 H-J, table 4.3). In these transplants in only 5/38 (13.2%) hosts, was migration of donor cells to the germ ring observed. This demonstrates that the migration of *chch* deficient donor cells can be rescued with *chch* mRNA and indicates that the defect stems from knockdown of *chch* function.

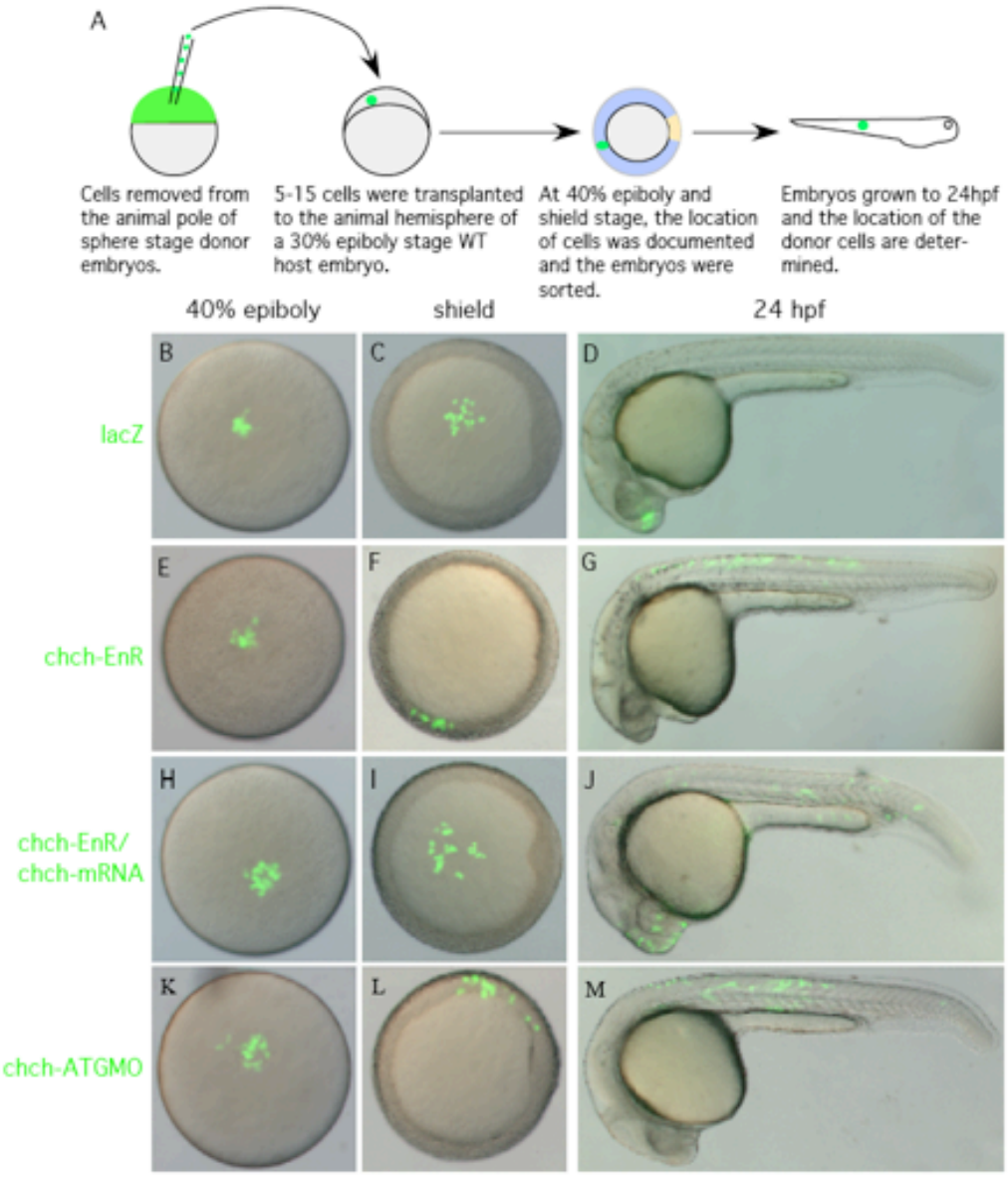

Figure 4.6. *chch*-inhibited cells leave the epiblast and enter the germ ring and become mesoderm. (A) A schematic representation of the transplantation scheme. Cells from sphere stage LacZ, *chch*-EnR mRNA or *chch*-ATGMO injected donors were transplanted to the animal hemisphere of 30% epiboly (late blastula) wild-type embryos. Embryos were photographed at 40% epiboly (B, E, H, K), at the start of gastrulation (shield) (C, F, I, L) and after 24 hpf (D, G, J, M). As expected, LacZ cells remain within the ectoderm and take on ectodermal fates at 24 hpf (B-D). In contrast, *chch* inhibited cells often migrate from the presumptive ectoderm to the germ ring (E-G, K-M). These cells are often later found in the somites (G). The abnormal movement of *chch*-EnR cells into the germ ring is rescue by co-injection of *chch* mRNA (H-J).

Table 4.3. *chch*-inhibited cells undergo inappropriate movements during gastrulation and results in cells in the mesoderm.

		Location of Cells at shield				
Injected mRNA	**N[a]**	**Dorsal Ectoderm**	**Ventral ectoderm**	**Shield**	**Lateral mesoderm**	**Ventral mesoderm**
LacZ	79	52	25	0	2	0
chch-EnR	110	38	28	10	20	14
chch-EnR/ *chch*-mRNA	38	20	13	0	2	3
chch-ATGMO	51	26	17	1	5	2

[a]-Host embryos with cells in the presumptive ectoderm at 40% epiboly

Location of cells at shield stage	**Injected mRNA**	**N[b]**	**Location of cells at 24hpf**				
			Neural tissue	**Epidermis**	**Notochord**	**Anterior somites**	**Posterior somites**
Shield	LacZ	0	0	0	0	0	0
	chch-EnR	10	2	0	6	2	0
	chch-EnR/ *chch*-mRNA	0	0	0	0	0	0
	chch-ATGMO	1	0	0	1	0	0
Lateral Mesoderm	LacZ	1	0	0	0	1	0
	chch-EnR	20	2	0	4	12	2
	chch-EnR/ *chch*-mRNA	2	0	0	0	2	0
	chch-ATGMO	5	0	0	0	2	3
Ventral Mesoderm	LacZ	0	0	0	0	0	0
	chch-EnR	14	1	1	0	10	2
	chch-EnR/ *chch*-mRNA	3	0	0	0	2	1
	chch-ATGMO	2	0	0	0	1	1

[b]-Same embryos were scored at 40% epiboly, shield stage and 24hrs

To determine whether movement of *chch*-compromised cells to the germ ring correlated with a fate change in these cells, their locations at 24 hpf was determined. Of the *chch*-EnR donor cells that migrated to the germ ring, 38/44 were found in mesodermal structures at 24 hpf. Likewise, 8/8 *chch* morphant donor cells that migrated to the germ ring were later found in mesodermal structures. This demonstrates that *chch* compromised cells transplanted distant from the margin at 30% epiboly generated mesoderm while LacZ donor cells did not. In 6/44 transplants, *chch*-EnR donor cells migrated to the germ ring but did not give rise to mesoderm. This suggests that movement of these cells may not entirely be linked to acquisition of mesodermal character.

The location of the *chch* compromised donor cells after 24 hpf was often not characteristic of their position at shield stage. The *chch*-EnR cells that migrated out of the ectoderm and into the germ ring also acquired unexpected fates and were found in surprising locations. Cells located in the ventral germ ring would be expected give rise to posterior somites. Instead, these cells were found in more anterior somites (first 15 somites, 10/14 embryos) or were observed in the ectoderm (2/14 embryos) (table 4.3). Cells located lateral to the shield would be expected to assume anterior somite fates. While a majority of these cells did give rise to anterior somites (12/20 embryos), cells were also located within the notochord (4/20 embryos) and neural tissue (2/20 embryos) (table 4.3). Together, these results suggest that inhibiting *chch* results in several kinds of inappropriate cell movements including movement of presumptive ectodermal cells into the germ ring.

4.2.5 Migration and fate change of chch-compromised cells requires Nodal signaling.

The initial transplant experiments do not reveal whether the fate changes observed in *chch*-compromised donor cells result from a failure to limit cell movement or whether a fate change precedes the improper movement. Three models could account for the movement of *chch*-compromised donor cells to the germ ring and subsequent acquisition of mesodermal character observed: 1) *chch*-compromised donor cells may autonomously express mesodermal markers which drives both movement and acquisition of mesodermal character;

2) inappropriate movement of *chch*-compromised donor cells to the margin may result in exposure of donor cells to mesoderm inducing signals; or 3) *chch*-compromised donor cells may exhibit increased sensitivity to non-autonomous signals that drive migration and/or acquisition of mesodermal character. Since induction of trunk mesoderm requires Nodal signaling (Feldman et al., 1998; Gritsman et al., 1999), blocking Nodal signaling after transplantation of *chch*-compromised cells would allow these models to be distinguished. If the first model is correct, migration of *chch* compromised cells and fate change will occur regardless of the state of Nodal signaling. If inappropriate movement allows *chch* compromised donor cells to come under the influence of the high levels of Nodal ligands present in the germ ring (model 2), donor cell migration would be observed, but these cells would be unable to respond to mesoderm inducing signals. If the third model is correct, both migration and acquisition of mesodermal character will be blocked in *chch*-compromised donor cells when Nodal signaling is abrogated.

To test these hypotheses, cell transplantation experiments were performed with *chch*-EnR donor cells placed into the animal hemisphere of wild-type hosts. *chch*-EnR donors instead of *chch* morphant donors were used because these cells had a greater tendency to migrate from the epiblast to the germ ring (table 4.3). Both donors and hosts were maintained in SB431542 to block Nodal signaling prior to transplantation and returned to SB431542 containing media following transplantation. SB431542 inhibits Alk4, Alk5 and Alk7 kinase activity and it has been shown to phenocopy Nodal pathway mutants (Ho et al., 2006; Sun et al., 2006).

As expected, LacZ cells transplanted from the animal hemisphere of a sphere stage (4 hpf) embryo to the animal hemisphere of a wild-type host at a late blastula stage (4.7 hpf) remained in the animal hemisphere (22/22 embryos) and by 1 dpf were observed in anterior neural tissue (Figure 4.7 A-A' and table 4.4). Treatment with SB431542 did not alter the behavior of these cells (Figure 4.7 B-B'). Conversely, in the same transplant scheme, *chch*-inhibited cells often migrated to the germ ring and became incorporated into mesodermal structures at 1dpf (Figure 4.7 C-C' and table 4.4). Surprisingly, when Nodal signaling was blocked, *chch*-EnR donor cells remained in the animal hemisphere (32/32 embryos) and were observed in anterior neural structures at 1 dpf (24/32 hosts, Figure 4.7 D-D' and table 4.4). In

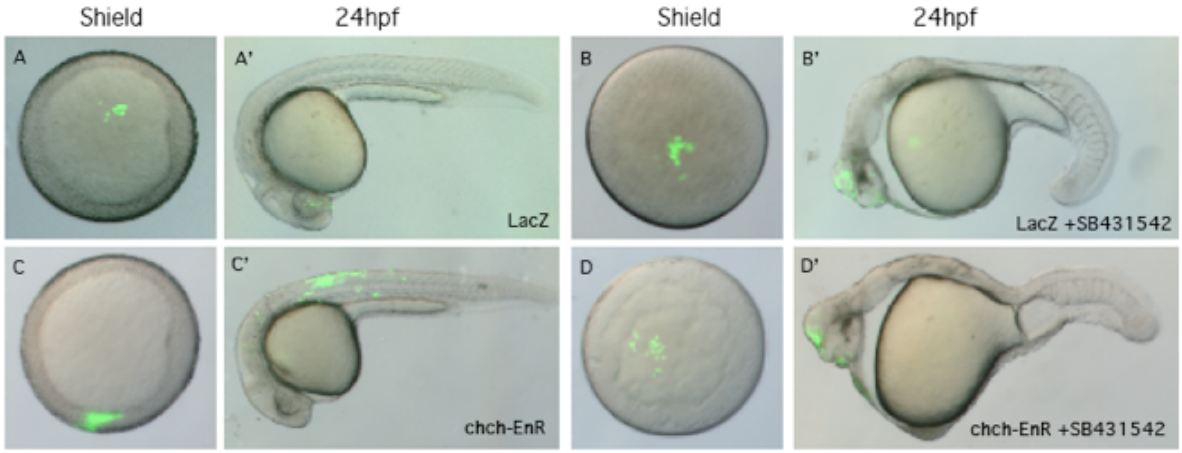

Figure 4.7. Alk receptor signaling is required for both migration and acquisition of mesodermal character of *chch*-EnR transplanted cells. Transplanted LacZ cells were present in the animal pole at shield stage (A) and were found in anterior neural tissue after 24 hpf (A'). 400 μM SB431542 (Sigma-Aldrich), which inhibits Alk receptors did not alter LacZ donor cell behavior (B-B'). Conversely, *chch*-EnR donor cells moved from the animal hemisphere to the germ ring by shield stage (C) and were observed in mesodermal structures after 24 hpf (C'). SB431542 treatment results in blocking movement of *chch*-EnR cells. The donor cells remain in the animal hemisphere at shield stage (D) and are found in anterior neural structures after 24 hpf (D'). This result suggests that signaling via Alk receptors is required for both migration and acquisition of mesodermal character of *chch*-EnR donor cells.

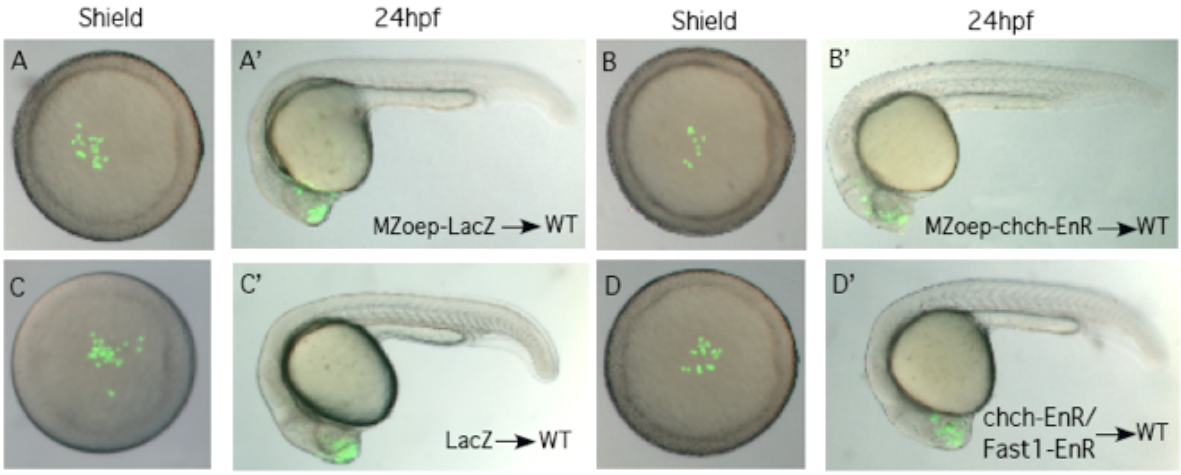

Figure 4.8. *chch*-compromised cells migrate to the germ ring and become mesoderm in response to Nodal signals. Transplanted *MZoep*-LacZ cells to the animal hemisphere of a wild-type host remain within the animal hemisphere at shield stage (A) and are observed in anterior neural structures after 24 hpf (A'). Similar behavior was observed for transplanted *MZoep*- *chch*-EnR cells in wild-type hosts (B-B'). Similarly, when donor cells express 12.5 pg xFast1-EnR, along with *chch*-EnR, migration to the margin is blocked and donor cells are observed in anterior neural structures after 24 hpf (D-D'). Together, these results demonstrate that the migration of the *chch* inhibited cells to the germ ring and acquisition of mesodermal character depends upon Nodal signaling.

Table 4.4. Transplantation of *chch*-EnR cells requires nodal signaling for cell movements and fate changes.

			Location of cells at shield		Location of Cells at 24hpf				
Donor cells	**Host embryos**	**n**	**Animal pole**	**Germ ring**	**Neural**	**Epidermis**	**Somites**	**Notochord**	**Yolk (Superficial)**
LacZ	Wild-type	22	22	0	19	3	0	0	0
LacZ	Wild-type + SB431542	25	25	0	25	0	0	0	0
chch-EnR	Wild-type	32	19	13	11	1	17	2	0
chch-EnR	Wild-type + SB431542	32	32	0	24	0	0	0	8
MZoep-LacZ	Wild-type	36	35	1	29	7	0	0	0
Mzoep-chch-EnR	Wild-type	48	48	0	41	6	1	0	0
LacZ	Wild-type	26	26	0	23	3	0	0	0
chch-EnR/xFsast1-EnR	Wild-type	38	38	0	26	6	0	0	6

the remaining 8/32 cases, donor cells were scattered in superficial layers of the yolk (likely epidermis). The behavior of this subset of cells differs from LacZ donors and non-SB431542 treated *chch*-EnR donors and may stem from an incomplete block of Nodal signaling. These findings demonstrate that signaling via Alk receptors is required for both migration to the germ ring and acquisition of mesodermal character of the *chch*-EnR donor cells. Since SB431542 treatment blocked Alk signaling in both donor and host cells, it could not be infered which cells required Alk-mediated signaling from these experiments.

To establish the whether Nodal signaling is required in the donor or host cells two manipulations to repress Nodal signaling in the donor cells were employed. These experiments utilized *MZoep* mutants which lack Oep, an EGF-CFC protein that functions as a co-receptor for Nodal signals (Gritsman et al., 1999) or dominant-negative xFAST1-EnR mRNA. *MZoep* embryos are completely non-responsive to Nodal signals. Fast1 (or FoxH1) is a transcription factor that responds to Nodal and FAST1-EnR constructs are effective in blocking Nodal signaling in fish and frogs (Pogoda et al., 2000; Watanabe and Whitman, 1999).

Donor cells were removed at 4 hpf either from the animal pole of an *MZoep* embryo injected with *chch*-EnR mRNA or from a wild-type donor injected with *chch*-EnR and xFast1-EnR mRNA. First, control or *chch*-inhibited *MZoep* cells were transplanted to the animal hemisphere of a wild-type host embryo at a late blastula stage (4.7 hpf). LacZ injected *MZoep* cells behaved similarly to wild-type cells. These donor cells did not leave the animal hemisphere and were observed in anterior neural structures at 1 dpf (Figure 4.8 A-A'). Similar to the SB431542 experiment, *chch*-EnR-*MZoep* cells remained in the animal hemisphere (48/48 embryos), and were observed in anterior neural tissues at 24 hpf (Figure 4.8 B-B' and table 4.4) demonstrating that Oep is required for both migration and fate change of the *chch*-EnR donor cells.

Next, transplanted cells from donor embryos co-injected with *chch*-EnR and xFast1-EnR to wild-type hosts. Following transplantation of LacZ cells, little movement of donor cells was observed at 6 hpf and donor cells were found in anterior neural structures at 1 dpf (Figure 4.8 C-C' and table 4.4). Similarly, transplanted *chch*-EnR/xFast1-EnR co-injected donor cells (Figure 4.8 D-D' and table 4.4) remained in the animal hemisphere and gave rise

to anterior neural tissue (26/38 embryos), epidermis (6/32 embryos) or were on the superficial surface of the yolk (6/32 embryos). This result suggests that xFast1-EnR prevents *chch*-EnR cells from adopting mesodermal fates. However, some *chch*-EnR/xFast1-EnR co-injected donor cells behave differently than the LacZ donors and are found spread across the yolk at 1dpf. These donor cells likely retain some responses to Nodal since some Nodal signaling events are independent of xFast1 and are instead mediated by Mixer-related molecules (Kunwar et al., 2003).

Since *chch*-compromised cells fail to migrate to the germ ring and assume mesodermal fates if Alk, Oep or Fast1 function is abrogated, suggesting that both migration and fate change depends on Nodal signaling. In the xFast1-EnR and SB431542 experiments, *chch*-EnR cells underwent aberrant movements but were not later observed in mesodermal structures suggesting that migration and fate change can be uncoupled.

4.2.6 *chch*-EnR embryos have an enhanced response to Nodal.

The above results suggest that the *chch*-EnR cells placed in the animal hemisphere respond to a Nodal signal but wild-type cells do not. Since Nodal ligands are expressed at the margin during late blastula and early gastrula stages, the hypothesis that *chch*-compromised cells have increased responsiveness to low levels of Nodal was tested. Wild-type embryos were microinjected with *chch*-EnR mRNA, 0.5 pg or 2.5 pg of *sqt* mRNA, *chch*-EnR mRNA and *sqt* mRNA or LacZ mRNA. Embryos were collected at shield stage and the levels of five genes whose expression depends on Nodal signaling were measured by real-time PCR. These genes included the dorsal markers, *chd*, *gsc*, *flh*, as well as the pan-mesodermal marker *ntl* and the endodermal marker *mixer* (Figure 4.9). All of these markers show no change or modest changes in embryos injected with *chch*-EnR mRNA and a dose-dependent response to *sqt* mRNA (Figure 4.7 A-E). Synergistic increases were observed when both *chch*-EnR mRNA and *sqt* mRNA were co-injected. For example, microinjection of 2.5 pg of *sqt* mRNA resulted in a 3.5 fold increase in *chd* mRNA levels (Figure 4.7 A). When *chch*-EnR mRNA was co-injected with 2.5 pg of *sqt,* a greater then 7-fold increase in *chd* mRNA levels were measured.

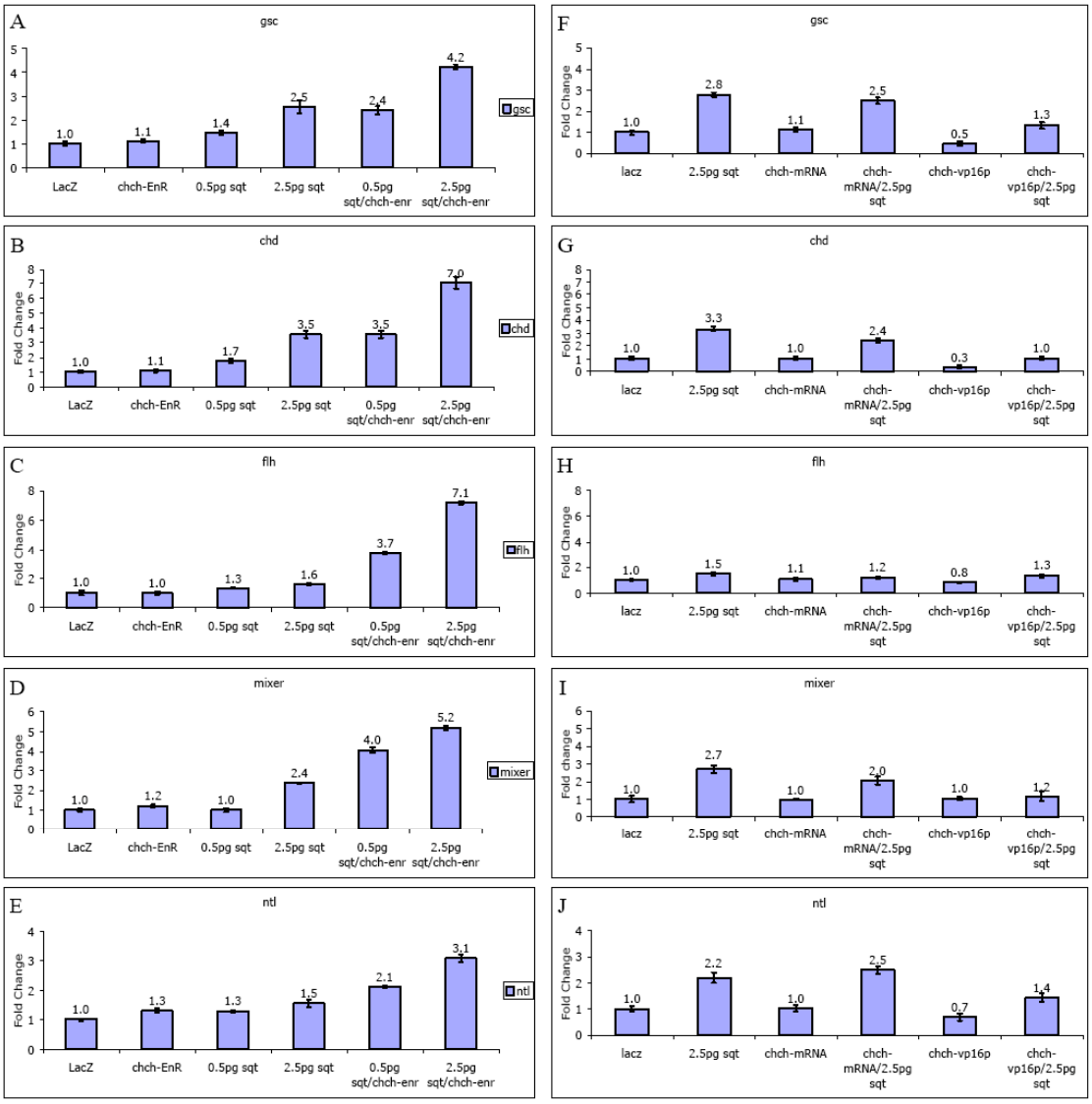

Figure 4.9. *chch* suppresses the transcriptional response to Nodal signaling. Embryos were microinjected with either 250 pg *chch*-EnR mRNA, 0.5 pg *sqt* mRNA, 2.5 pg *sqt* mRNA, or co-injected with 250 pg *chch*-EnR mRNA and 0.5 pg or 2.5 pg *sqt* mRNA and were analyzed at shield stage by real-time PCR with the dorsal markers *gsc* (A), *chd* (B), and *flh* (C), the endodermal marker *mixer* (D) and the pan-mesodermal marker *ntl* (E). All of these markers show little change in gene expression in embryos injected with *chch*-EnR mRNA and a dose dependent response to *sqt* mRNA. When both *chch*-EnR and *sqt* mRNA were co-injected, synergistic increases in marker expression were observed. These results demonstrate that *chch* suppresses the response to Nodal signaling. Conversely, microinjection of *chch*-VP-16 mRNA suppresses the transcriptional response to Nodal signaling. Embryos were microinjected with 2.5pg *sqt*, 500pg *chch* mRNA, 500pg *chch*-VP16 mRNA, or co-injected with *sqt* and *chch* mRNA or *chch*-VP16 mRNA. Embryos were collected at shield stage and analyzed by real-time PCR with *gsc* (F), *chd* (G), *flh* (H), *mixer* (I), and *ntl* (J). Co-injection of *chch*-VP16 mRNA along with *sqt* mRNA suppresses the transcriptional response to *sqt.*

Overexpression of *chch* mRNA had little effect in suppressing the effects of *sqt* overexpression on the same markers when assayed by real-time PCR at shield stage (Figure 4.7 F-J). However, overexpression of zebrafish *chch* fused to the VP16 transcriptional activator domain (*chch*-VP16) was able to suppress the effects of Nodal activation (Figure 4.7 F-J). The endogenous levels of *chd*, *gsc* and *ntl* were also suppressed by microinjection of *chch*-VP16 mRNA. Levels of *mixer* and *flh* were unaltered by microinjection of either *chch* mRNA or *chch*-VP16 mRNA. Together, these results demonstrate that *chch* functions to suppress the response to Nodal signaling.

4.3 Discussion:

Here, the function of the zinc finger transcription factor Churchill in zebrafish was characterized. The data presented showed that *chch* is required to repress expression of markers of non-axial mesoderm, while both neural and presumptive epidermal markers are diminished in *chch*-compromised embryos. In transplant assays, cells with compromised *chch* function undergo atypical cell movements when placed in the animal hemisphere and acquire fates inappropriate for their position in the early gastrula. Unlike control cells, these donor cells often migrate to the margin and are later observed in mesodermal derivatives. The movement and corresponding fate change of the transplanted *chch* compromised cells can be suppressed by blocking Nodal signaling in the donor cells, and finally, *chch* suppresses the transcriptional response to Nodal signaling.

4.3.1 *chch* limits expression of mesodermal markers.

In *Xenopus*, *chch* overexpression is sufficient to repress *Xbra* expression (Sheng et al., 2003). This data demonstrate that when *chch* function is repressed, mesodermal gene expression is expanded during gastrulation (Figure 4.3) and the expansion corresponds to a decrease in the levels of ectodermal markers (Figure 4.4). The effects on ectoderm are relatively modest during gastrulation but later anterior neural defects were observed.

In contrast to *Xenopus*, no detectable repression of *ntl* (*brachyur*y) was observed when *chch* is overexpressed (Figure 4.3 I-J). Since the concentration of *chch* mRNA used in

the overexpression experiments was sufficient to rescue both the morpholino and dominant-negative phenotypes, these levels are likely physiologically relevant. Overexpression of higher doses of *chch* mRNA failed to alter early *ntl* expression (data not shown). However, repression of *ntl* following microinjection of *chch*-VP16 mRNA (Figure 4.9) was observed. The different effects of *chch* overexpression on *brachyury* expression may reflect experimental differences or divergence in regulation of *brachyury* between fish and frogs. One possibility is that an essential *chch* or Sip1 cofactor is widely expressed in *Xenopus* but has restricted expression in zebrafish.

4.3.2 *chch* regulates cell movement.

Here, cells with compromised *chch* function undergo inappropriate cell movements. When placed into a wild-type embryo at a late blastula stage, these cells often leave the epiblast, migrate to the germ ring and become mesoderm (Figure 4.6). This result is consistent with the *chch* study in the chick, where *chch* was shown to be required to repress ingression of epiblast cells into the primitive streak (Sheng et al., 2003). These data suggest an evolutionarily conserved function for *chch* in the regulation of cell movement during gastrulation.

A key question is whether the *chch* compromised cells that leave the epiblast and enter the germ ring, become mesoderm because *chch* regulates migration and they are subsequently exposed to mesoderm-inducing signals in the germ ring or whether they migrate to the germ ring because they have already established mesodermal identity; is movement directing fate or is fate controlling movement?

The transplant experiments in which the responsiveness of the donor cells to Nodal signaling was manipulated, revealed that *chch*-EnR cells do not autonomously become mesoderm but require activation of the Nodal pathway to migrate to the germ ring and adopt mesodermal fates. When Nodal signaling is blocked, *chch*-compromised cells fail to migrate to the germ ring and do not assume mesodermal fates (Figures 4.7, 4.8). Analysis of zebrafish Nodal mutants has shown that Nodal signaling is required for internalization of mesodermal precursors (Carmany-Rampey and Schier, 2001). These results suggest that Nodal may also play a role in cell movement toward the margin prior to internalization. The

Nodal family member responsible for this activity has not been established, although Sqt is a strong candidate because it is expressed at these stages and has been shown to act as a long-range signal (Chen and Schier, 2001). Alternatively, the movement of *chch*-compromised donor cells may be influenced by another Nodal family member, perhaps Vg1 which is also expressed early and requires Oep function (Cheng et al., 2003; Helde and Grunwald, 1993).

It is important to note that not all cells that underwent unusual movements ended up in the mesoderm. This implies that movement can be uncoupled from acquisition of mesodermal character. Since not all of the donor cells showed the same movements, the differences may have resulted in variations in the initial positions of cells or subtle differences in *chch* activity in the donor cells. In addition to an enhanced responsiveness to Nodal signals, *chch*-compromised cells might also be sensitive to other TGF-β signals including BMPs, which could account for alterations in cell behavior. More detailed analysis of the behavior of *chch*-deficient cells will be necessary to determine additional roles for *chch* in regulating cell movements during gastrulation.

4.3.3 *chch* represses the transcriptional response to Nodal signals.

It was found that the transcriptional response to the Nodal ligand *sqt* is enhanced in embryos expressing *chch*-EnR mRNA. The mRNA levels of five Nodal target genes were synergistically increased when *sqt* and *chch*-EnR mRNA where co-injected (Figure 4.9). Three of these targets, *chd*, *fh* and *gsc* are expressed in the dorsal mesoderm. The fourth, *mixer*, is an endodermal marker. However, in contrast to pan-mesodermal markers like *ntl* (Figures 4.3 and 4.8) and *spt* (Figure 4.3), the transcript levels of these markers were largely unaltered by *chch*-EnR mRNA or *chch*-ATGMO microinjection. This suggests that endogenous *chch* does not play a role in suppressing the high levels of Nodal signaling that are required for specification of dorsal mesoderm and endoderm but represses the response to lower Nodal levels.

This data suggests that the increased expression of mesodermal markers observed when *chch* is repressed results from an enhanced response to Nodal. Microinjection of morpholinos directed against the extracellular Nodal antagonist, Lefty, also result in expansion of mesodermal markers (Agathon et al., 2001; Chen and Schier, 2002; Feldman et

al., 2002). The *chch* target Sip1 likely mediates the effect of *chch* on Nodal signaling. Sip1 has not been previously characterized in zebrafish, although here, zebrafish Sip1 is regulated by *chch* (Figure 4.3 K-N, Q). Sip1 represses TGF-β signaling by binding to activated forms of Smad1/5 and Smad2/3 (Postigo, 2003; Postigo et al., 2003) and is a direct repressor of *Xbra* (Verschueren et al., 1999). The decrease in Sip1 expression following *chch* inhibition could result in a failure to check Nodal signaling, which results in mesoderm expansion. However, Sip1 morpholinos do not alter Xbra expression in *Xenopus* (Nitta et al., 2004). The increase in mesodermal gene expression observed in *chch*-compromised embryos (Figure 4.2) is consistent with an enhanced sensitivity to TGF-β signals. In addition to suppressing *Xbra* and TGF-β signaling, Sip1 is also a direct repressor of *E-cadherin* (Comijn et al., 2001). While migration of *chch*-compromised cells to the germ ring depends on Nodal signaling, alterations in *E-cadherin* levels may also influence the unusual movements of these cells.

This study of the zinc finger transcription regulator, *chch*, is the first analysis of the function of this gene in zebrafish. Roles for *chch* in regulating cell movements within the gastrula that are consistent with the initial data on *chch* in the chick and *Xenopus* were identified. Significantly, several novel functions for *chch* were identified. This data suggests a broader role for *chch* then was previously demonstrated and provides key insight into the mechanism of action of *chch*. From this analysis the following can be conclude: (1) that *chch* is required to limit mesodermal gene expression; (2) *chch* limits Nodal-dependant movement of presumptive ectodermal cells (3) *chch* limits the response of cells to Nodal signaling. These findings provide a basis to begin to elucidate the dynamic roles for *chch* in regulating cell movement and fate during early development.

4.4 Materials and methods

4.4.1 Constructs and morpholinos:

The Churchill coding sequence was cloned into the StuI site of the pCS2 plasmid or a pCS2-EnR (ChCh-EnR). Morpholinos were synthesized by GeneTools (Philomath, OR): ChCh-ATGMO-5'- GCTTCTGGACACAACCGGTACACAT

4.4.2 RNA in situ hybridization and photography:

RNA *in situ* hybridization, probes and photography techniques were previously described (Londin et al., 2005). For time-lapse photography, embryos were mounted in 2.5% methylcellulose, 1% low melt-agarose, and photographed every 5 minutes.

4.4.3 Real-time PCR:

PCR and primers were previously described (Londin et al., 2005) with the addition of:

chch: TGTGTCCAGAAGCAATATCC/TCCTCCTCATCTTCATTCAC;

Sip1: CACTCAGCTGGAGAGACATA/TGCTCCTTTAGATGGTGTTT;

mixer: CAGAATCGAGAATTCAGGTC/TGTGGTAAACTGGTGCATAA.

4.4.4 Cell transplantations:

Embryos were microinjected with either LacZ mRNA for a control or ChCh-EnR mRNA for the experimentals along with 5 mg/ml Fluorescein dextran (Molecular Probes). For the isochronic transplants, cells from sphere stage embryos were transplanted to a sphere stage host embryo. For the heterochronic transplants, sphere stage cells were transplanted to the animal hemisphere of 30% epiboly embryos. Each transplant consisted of 5-15 cells. The location of the transplanted cells documented at the indicated times.

Chapter 5: Conclusions and future directions

FGF signaling plays many key roles during development. Figure 5.1 shows a model for FGF signaling in regulating neural and mesodermal cell fates. Both neural and mesodermal are fated in close proximity and at similar times during development. The FGF signaling pathway is important in determining these two different cell fates and its activity needs to be carefully regulated.

5.1 FGF signaling is required for neural induction:

An important step for neural induction to occur is the inhibition of BMP protein activity within the dorsal ectoderm. The work presented here shows that FGF signaling plays a key role in zebrafish neural induction (chapter 2). Inhibition of FGF signaling results in early neural specification deficits, however the anterior neural domain recovers in a Nodal dependent fashion by early somitogenesis (Figure 2.6). FGF signaling acts at multiple levels to repress BMP signaling. It acts prior to gastrulation to diminish BMP transcription (Figure 2.4) and later to induce *chordin* expression (Figure 2.5). The combined activities of FGF, Chordin and Nodal signaling targets are required for proper neural tissue to occur. Previous studies in the chick showed that FGFs may attenuate BMP signaling through repression of *bmp* gene transcription (Streit et al., 2000; Wilson and Edlund, 2001; Wilson et al., 2000). The work presented here demonstrates that a similar mechanism exists in zebrafish suggesting that FGF inhibition of *bmp* gene transcription may be a conserved role in neural induction. Importantly we found that repression of BMP transcription by FGF does not require protein synthesis (Figure 2.8).

These results show that FGF signaling is acting at multiple levels in neural induction (Figure 5.1). Questions about its exact function still exist. First, the primary construct used to inhibit FGF signaling here and in other studies is a dominant negative FGFR1 (XFD). FGFR1 blocks neural induction by the organizer (Launay et al., 1996), chordin (Sasai et al.,

1995), and notochord tissue (Barnett et al., 1998). It is possible that FGF signaling may be mediated through FGFRs other than FGFR1. FGFR4 was shown to have a greater role in anterior neural induction than FGFR1 (Hongo et al., 1999). FGF8 stimulates neuronal differentiation preferentially through FGFR4 (Hardcastle et al., 2000), while FGF signaling through FGFR1 is required for neural crest formation (Monsoro-Burq et al., 2003). Additionally, the two receptors activate different downstream pathways suggesting distinct functions in neural induction. FGFR1 preferentially activates the Ras-MAPK pathway, which is involved in posteriorization of an already neuralized ectoderm (Ribisi et al., 2000; Umbhauer et al., 1995). Conversely, FGFR4 signals through PLCγ in neural induction (Umbhauer et al., 1995). Further work is needed to determine the differences between the different receptors. While FGF is having a role in neural induction, the different receptors have varying effects on neural gene expression.

A second question is whether FGFs can induce neural gene expression independently of BMP inhibition. Studies in other animal models, suggest that FGF signaling can act independent of BMP signaling to directly induce neural gene expression. The work presented here does show that FGFs are acting prior to the onset of gastrulation in neural induction, although a BMP independent effect is not shown. In basal chordates, such as ascidians, FGFs rather than BMP inhibition are the endogenous factors responsible for generating the nervous system (Bertrand et al., 2003; Darras and Nishida, 2001; Hudson et al., 2003). Some studies in *Xenopus* showed that FGFs could directly induce neural tissue in animal caps. However, these studies relied a sensitized background in which BMP signaling was partially attenuated (Kengaku and Okamoto, 1995; Lamb and Harland, 1995; Ribisi et al., 2000). These studies relied on using animal caps where the one-to four-cell stage embryo is injected animally with a RNA then grown to blastula or gastrula stage when the animal cap is cut and allowed to develop in isolation from the rest of the embryo. Since these studies had artificially inhibited BMP signaling prior to the FGF signal, it is not clear if FGF is acting directly on neural induction or if the effect seen was due to BMP inhibition. Although, it was shown that posterior neural fates can be generated by FGF in regions of high BMP activity (Kudoh et al., 2004).

In the chick, studies have shown that neural induction can occur independent of *BMP* mRNA expression. Here, low levels of FGF signals act directly on neural genes independent

of affecting BMP expression (Streit et al., 2000; Wilson et al., 2000). Conversely, high levels of FGF signals act to induce neural genes through repression of *bmp* mRNA expression. Thus, when FGF signals are attenuated at low levels, neural gene expression is blocked, but can be rescued with the addition of BMP antagonists (Wilson et al., 2000). To date, a direct role for FGF signaling in zebrafish expression of neural genes has not yet been identified and is subject to future research. A cell transplant experimentation to test this experiment can be performed. Here, iFGFR-1 cells can be transplanted to the ventral ectodermal region, a region of high BMP expression. FGF expression in these cells can be activated by with the addition of AP20187 and determined if neural genes can be expressed within these cells. Since the cells are in a region of the embryo with high BMP gene activity, the induction of neural gene expression would suggest that it can occur independently of the BMP activity.

5.2. Zebrafish *chch* is regulates neural and mesodermal gene expression and cellular migration:

In addition to neural induction, FGF signaling also has well defined roles in mesoderm induction (Kimelman and Kirschner, 1987). FGF acts downstream of Nodal signaling to induce mesoderm targets in zebrafish embryos (Mathieu et al., 2004). In addition, FGF signaling can directly induce the expression of *Xbra* expression (Kimelman and Kirschner, 1987). How the FGF signal can be regulated to induce both neural and mesodermal cell fates is an important question in developmental biology. Insights into this answer came with the identification of the transcription factor, *churchill (chch)* (Sheng et al., 2003). *chch*, a small zinc finger transcription factor, was shown to act as a switch that modulates the activity of FGF between mesoderm and neural induction (Sheng et al., 2003). *chch* overexpression in *Xenopus* embryos results in suppression of the mesodermal marker *brachyury* (Sheng et al., 2003), while *chch* morpholino knockdown in the chick epiblast results in inappropriate migration of epiblast cells through the primitive streak (Sheng et al., 2003). Although the effect of *chch* in the frog and chick assays is the same (to limit mesoderm), the mechanisms of action in these two experiments likely differ. In order to elucidate the mechanisms of action of *chch*, a series of experiments were performed to study

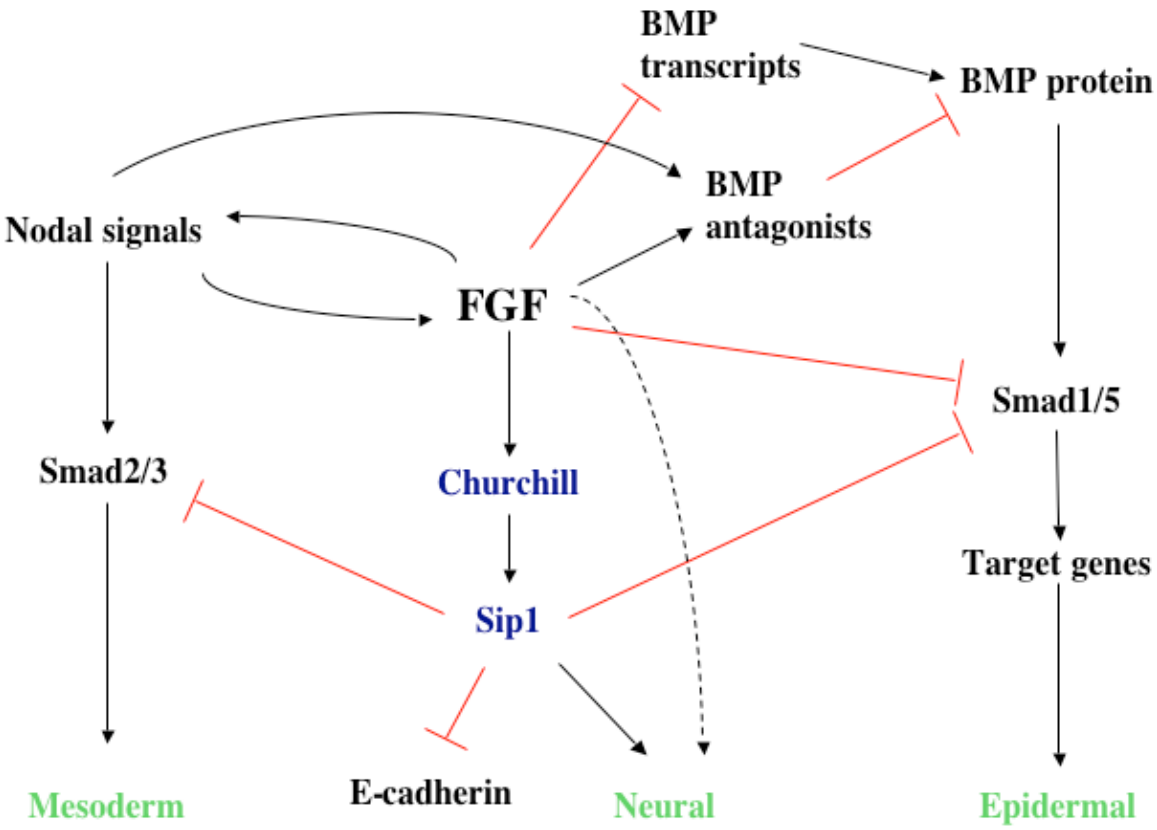

Figure 5.1. Schematic representation of the role and regulation of FGF signaling in zebrafish neural and mesodermal development. FGF signaling acts to induce neural and mesodermal tissues. FGF inhibits BMP signaling through inhibition of blastula stage BMP transcripts and induction of gastrula stage BMP antagonists (Londin et al., 2005). There is evidence that FGF signaling can directly induce the expression of neural gene expression, but additional experiments are required to determine FGFs role in this capacity. Nodal signals induce FGF signaling to allow for mesoderm induction (Mathieu et al., 2004). FGF induction of *chch* (Londin et al., 2007a) regulates the FGF signaling between mesodermal and neural induction. In ascidians, FGF can directly induce the expression of neural genes independent of BMP inhibition (Bertrand et al., 2003), although it is not know if a similar effect exists in vertebrates (dotted line). Through the regulation of the *Sip1* gene, *chch* acts to inhibit mesoderm, cell movements and induce neural gene expression (Londin et al., 2007b; Sheng et al., 2003). *Sip1* inhibits Smad signaling in both the BMP and Nodal pathways (Postigo, 2003; Postigo et al., 2003) as well as *E-cadherin* expression. Sip1 can also directly inhibit epidermal gene expression (Comijn et al., 2001; Nitta et al., 2007; van Grunsven et al., 2000). Further experiments are required to determine *Sip1s* role in zebrafish.

the requirement for *chch* in the zebrafish and to address the roles of *chch* in cell migration and cell fate (chapters 3-4, and Figure 5.1).

The work presented here shows similarities and differences with previously identified functions of *chch*. First, differences in the patterns of expression are observed. In the chick, *chch* is expressed in the prospective neural plate starting at stage 4 and remaining until stage 13 (Sheng et al., 2003). In contrast, here zebrafish *chch* is expressed throughout early development. *chch* is maternally expressed, and also begins to be zygotically transcribed prior to the mid-blastula transition. It is not yet known if the early zygotically transcribed mRNA is translated or what the purpose of this mRNA is. During blastula and gastrula stages, *chch* is widely expressed and may function to regulate cell movements of forerunner cells. After gastrulation, *chch* becomes restricted to ventral regions of the embryo and later expression remains within the anterior neural tissue (Figure 3.2). These expression differences may represent species-specific differences. Finally, similar to the chick, I have shown that FGF signaling is required for *chch* expression, but additional factors in regulating *chch* expression (Figure 3.4) (Londin et al., 2007a).

In the chick and *Xenopus*, *chch* overexpression results in a decrease in mesodermal gene expression (Sheng et al., 2003) with no change in ectodermal gene expression. Conversely, *chch* inhibition in zebrafish results in expansion of mesodermal genes with a corresponding decrease in neural gene expression (figure 4.3-4.4). In contrast to the chick and *Xenopus* (Sheng et al., 2003), *chch* overexpression in zebrafish does not alter mesodermal gene expression. The different effects of *chch* overexpression on *brachyury* expression may reflect experimental differences or divergence in regulation of *brachyury* between fish and frogs. The concentration of *chch* mRNA used in the overexpression experiments was sufficient to rescue both the morpholino and dominant-negative phenotypes, suggesting that these levels are likely physiologically relevant. One possibility is that *chch* requires a cofactor for its activity that is widely expressed in *Xenopus* but has restricted expression in zebrafish.

As in the chick (Sheng et al., 2003), zebrafish *chch* also regulates cell movements (Figures 4.5-4.7). In the chick, *chch* represses ingression of epiblast cells into the primitive streak (Sheng et al., 2003). *chch* compromised cells undergo inappropriate cell movements. When placed into a wild-type embryo at a late blastula stage, these cells often leave the

epiblast, migrate to the germ ring and become mesoderm (Figure 4.6). This result is consistent with the chick, suggesting an evolutionarily conserved function for *chch* in the regulation of cell movement during gastrulation. This work expands on this finding by showing that the *chch* inhibited cells are migrating in response to a Nodal signal (Figures 4.6-4.8). Nodal signals are highly expressed within the germ ring where mesodermal genes are expressed. *chch* expression within the ectoderm will prevent these cells from migrating towards Nodal signals, allowing them to remain within and become incorporated into the ectoderm. This result is similar to in the chick where *chch* overexpressed cells remain within the epiblast and become incorporated into the ectoderm (Sheng et al., 2003).

Recently, the structure and DNA binding activity of *chch* was questioned (Lee et al., 2007). At the time of its discovery, *chch* was thought to be a transcription factor contain two zinc fingers (Sheng et al., 2003). The basis for this was determined by its protein sequence and by a DNA binding assay. The original *chch* study and the work performed here both showed that *chch* acts as a transcription factor with *Sip1* being its primary target. Sheng et al (Sheng et al., 2003) showed that *chch* binds to a consensus sequence of (CGGG(G/A/T)(G/A/C)) which is present in the *Sip1* promoter region. Similarly in zebrafish, inhibition or overexpression of *chch* results in a change of *Sip1* expression (Appendix).

The work by Lee et al (Lee et al., 2007) showed contradictory results to the originally presented structural analysis of *chch*. By performing solution NMR, this group demonstrated that the *chch* protein consists of a solvent-exposed β-sheet, which becomes stabilized by the coordination of three zinc ions and not two zinc finger domains. Additionally, they showed no evidence that *chch* binds to DNA. It is possible that *chch* may require a co-factor for its binding activity, which would explain why overexpression of zebrafish *chch* does not result in a change in mesodermal or neural gene expression. Further experimentation is needed to resolve this issue of the DNA binding activity of *chch*.

5.3. *chch* regulates Smad interacting protein 1:

While it is clear that *chch* is playing an important regulating mesodermal and neural cell fates as well as cell movements, a mechanism for its function is not known. What is

known is that *chch* regulates the expression of Smad interacting protein 1 (Sip1) in zebrafish (Figures 4.3 K-N, P-Q and 5.1) and in the chick (Sheng et al., 2003; Snir et al., 2006).

Sip1 is a large protein that has multiple conserved domains: a homeodomain (HD), a C-terminal binding protein (CtBP) binding site (CBS), two two-handed zinc finger domains (one at the N-terminus and one at the C-terminus), and a Smad binding domain (SBD). The different domains will allow the protein to interact with different co-factors and DNA giving various functions. In fact, *Sip1* has been documented primarily as a transcriptional repressor (Comijn et al., 2001; van Grunsven et al., 2003; van Grunsven et al., 2007; Vandewalle et al., 2005; Verschueren et al., 1999), but it can also act as an activator (Long et al., 2005; Yoshimoto et al., 2005). *Sip1* can recruit histone deacetylases by a mechanism involving the binding of the CBS to CtBP resulting in repression of gene transcription (Furusawa et al., 1999; Postigo and Dean, 1999). Conversely, *Sip1* can interact with the coactivators p300 and p/CAF to induce gene expression particularly those involved in neural induction (Eisaki et al., 2000; Papin et al., 2002; van Grunsven et al., 2006).

Many functions for *Sip1* have been previously identified. This association occurs only when Smad1 is activated by phosphorylation (Postigo, 2003; Verschueren et al., 1999), suggesting that *Sip1* functions as a regulator of BMP signaling in the cell. Additionally, it has been documented to act as both a transcriptional activator and repressor with roles in mesodermal (Lerchner et al., 2000; Papin et al., 2002), and neural induction (Nitta et al., 2007; Nitta et al., 2004) as well as in regulating cell movements. Mutational analysis of the different domains showed that each domain regulates the different functions of *Sip1's* activity. Repression of *E-cadherin* occurs independently of CtBP binding (van Grunsven et al., 2003), although deletion of SBD, decrease the repressor activity on the *E-cadherin* promoter (Comijn et al., 2001). The N-terminus zinc finger domain of the *Xenopus Sip1* is important for neural induction, but not for the suppression of *Xbra* expression (Nitta et al., 2007).

Through extensive studies in *Xenopus* and mouse, *Sip1* has been shown to have various functions in neural and mesodermal patterning, but is *Sip1* acting to regulate *chch's* function? In fact, several lines of evidence do suggest *Sip1* is acting in this manner. First, both work shown here (Figure 4.3 K-N, P-Q) and by others (Sheng et al., 2003; Snir et al., 2006) show a requirement of *chch* for *Sip1's* function. *chch* overexpression results in

increases in *Sip1* expression while inhibition of *chch's* function abrogates *Sip1* expression (Figure 4.3). These facts make *Sip1* a highly attractive protein as a regulator for chch's function.

Signaling events through *chch* play a role in regulating neural gene expression (Figure 4.4 and Sheng et al., 2003). The mechanism of *chch's* action in this role can come through *Sip1*. First through a regulation of BMP signaling is a possible mechanism. *Sip1* represses TGF-β signaling by binding activated Smad1/5 (BMP) (Postigo, 2003; Postigo et al., 2003). *Sip1* inhibits BMP signaling and drives the putative epidermis towards a neural fate (Eisaki et al., 2000; Nitta et al., 2004; van Grunsven et al., 2006). Overexpression of *Sip1* in Xenopus suppresses the transcription of BMP and genes downstream of BMP signaling (Eisaki et al., 2000; Postigo, 2003; van Grunsven et al., 2006). Second, Xenopus *Sip1* has been shown to directly repress epidermal gene expression, suggesting that *Sip1* is involved in inhibiting BMP signaling and inducing neural cell fate (Comijn et al., 2001; Nitta et al., 2004; van Grunsven et al., 2000). Third, overexpression of *Sip1* induces neural markers in animal caps resulting in a hyperneuralized phenotype (Eisaki et al., 2000). Mouse *Sip1* homozygotic mutants are embryonic lethal and show severe neural crest defects (Van de Putte et al., 2003). *chch* induced *Sip1* expression within the dorsal ectoderm can inhibit BMP signaling by blocking Smad signaling. The ultimate result is an inhibition of BMP signaling allowing the dorsal ectoderm to take on its default neural state.

Following *chch* inhibition, an increase in mesodermal gene expression is observed (Figures 4.2-4.4). This result can come through a failure to induce *Sip1* expression. The lack of *Sip1* present will lead to unchecked amounts of Nodal signaling with an ultimate increase in mesodermal gene expression. In addition to inhibiting the BMP pathway, *Sip1* also inhibits Nodal signaling by binding activated forms of Smad2/3 (Postigo, 2003; Postigo et al., 2003). Knockdown studies in *Xenopus* using *Sip1* morpholinos, show that like in the mouse, *Sip1* is essential for neural differentiation. Additionally, *Sip1* overexpression in the *Xenopus* embryo represses *brachyury (Xbra)* transcription (Lerchner et al., 2000; Papin et al., 2002), where there are *Sip1* binding sites in the *Xbra* promoter (Lerchner et al., 2000). Further *Xbra* regulation is through the repression of the Smad1/5 pathway. Further evidence for this comes from the fact that *chch* is regulating a transcriptional response to Nodal signaling (Figure 4.9). *chch* inhibition in conjunction with *sqt* overexpression results in a

synergistic response on Nodal target genes. *Sip1* inhibition of Smad2/3 signaling results in a blockage of Nodal signaling and the loss of *Sip1*, results in an amplified effect of Nodal signaling.

chch's role in cell movements was previously examined (Sheng et al., 2003) as well as further examined here (Figures 4.5-4.8). The *chch*-inhibited cells exhibit increased motility (Figure 4.5) acting in response to Nodal signaling (Figure 4.6-4.8), a function of that can act through *Sip1*. In addition to suppressing *Xbra* and TGF-β signaling, *Sip1* is also a direct repressor of *E-Cadherin* (Comijn et al., 2001). While migration of *chch*-compromised cells to the germ ring depends on Nodal signaling, alterations in *E-cadherin* levels may also influence the unusual movements of these cells. *E-cadherin* in also highly expressed in the EVL. De-repression of *E-cadherin* may also play a central role in sorting of *chch*-compromised cells in the sphere stage transplant experiments (Figure 4.6). *chch's* regulation of *Sip1* can have two effects on cell movements. First, the induction of *Sip1* can affect *E-cadherin* levels, resulting in the increased motility of the cells. The second method can be through the regulation of Nodal signaling where, *chch* senses the levels of Nodal signaling, and possibly *Sip1* prevents a response to Nodal signals within the cell. The ultimate response is to prevent cells from migrating.

The multiple determined roles of *Sip1* make it an attractive gene to regulate *chch's* function. To date, *Sip1* has not been characterized in zebrafish and examination of the zebrafish genome does show that a *Sip1* homologue exists. Furthermore, preliminary examination of this Sip1 does show that it is regulated by chch (see appendix A). Additional experiments are needed to further determine the role and function of *Sip1* in zebrafish development.

5.4. Future directions:

Taken together, the results presented in this thesis show a complex role for FGF signaling in determining neural and mesodermal cell fate. FGF signaling functions to inhibit bmp gene transcription and induce the expression of BMP antagonist genes to induce neural genes within the prospective neural plate (chapter 2). The transcription factor *chch* functions to regulate cell movements as well as to inhibit mesodermal gene expression. These

functions of *chch* act to regulate FGFs function between patterning neural and mesodermal cell fates (Figure 5.1). Further experimentation is needed to identify additional roles of FGF signaling in neural and mesodermal patterning. In particular, there is evidence in other species suggesting that FGF signaling is acting to induce neural gene expression independent of BMP inhibition. This has not yet been shown in zebrafish but does remain as an additional mechanism in zebrafish.

Additionally, the work shown on the function of *chch* is just the beginning in understanding its full function. The precise role on regulating FGF and Nodal signaling needs to be further examined. It is not yet know if *chch* is actually sensing the levels of Nodal signaling and preventing cells from migrating towards those signals. While *chch* regulates cell movements in response to Nodal signaling, the Nodal family ligand responsible for this activity is not yet established. *Sqt* is a strong candidate due to its expression and range of activity, other Nodal ligands such as spt or Vg1 may also have an effect. Similarly, *chch* may also limit cell movements in response to other TGF-β signaling factors, such as BMP signaling. Furthermore, the increased migratory behavior of the *chch*-inhibited cells may be due to the fact that the cells have become induced to mesoderm prior to migration. It is not yet known if the cell fate change is determining the migration or if the migration of the cells results in a cell fate change.

Finally, the role of *Sip1* needs further examination in zebrafish. While many roles for Sip1 have been shown in other model organisms, little work has been done in zebrafish. In particular, the function of the two Sip1 genes will have to be examined very carefully.

References:

Agathon, A., Thisse, B. and Thisse, C. (2001). Morpholino knock-down of antivin1 and antivin2 upregulates nodal signaling. *Genesis* **30**, 178-82.

Agathon, A., Thisse, C. and Thisse, B. (2003). The molecular nature of the zebrafish tail organizer. *Nature* **424**, 448-52.

Alvarez, I. S., Araujo, M. and Nieto, M. A. (1998). Neural induction in whole chick embryo cultures by FGF. *Dev Biol* **199**, 42-54.

Amaya, E., Musci, T. J. and Kirschner, M. W. (1991). Expression of a dominant negative mutant of the FGF receptor disrupts mesoderm formation in Xenopus embryos. *Cell* **66**, 257-70.

Babb, S. G. and Marrs, J. A. (2004). E-cadherin regulates cell movements and tissue formation in early zebrafish embryos. *Dev Dyn* **230**, 263-77.

Bachiller, D., Klingensmith, J., Kemp, C., Belo, J. A., Anderson, R. M., May, S. R., McMahon, J. A., McMahon, A. P., Harland, R. M., Rossant, J. and De Robertis, E. M. (2000). The organizer factors Chordin and Noggin are required for mouse forebrain development. *Nature* **403**, 658-61.

Barnett, M. W., Old, R. W. and Jones, E. A. (1998). Neural induction and patterning by fibroblast growth factor, notochord and somite tissue in Xenopus. *Dev Growth Differ* **40**, 47-57.

Barth, K. A., Kishimoto, Y., Rohr, K. B., Seydler, C., Schulte-Merker, S. and Wilson, S. W. (1999). Bmp activity establishes a gradient of positional information throughout the entire neural plate. *Development* **126**, 4977-87.

Bertocchini, F. and Stern, C. D. (2002). The hypoblast of the chick embryo positions the primitive streak by antagonizing nodal signaling. *Dev Cell* **3**, 735-44.

Bertrand, V., Hudson, C., Caillol, D., Popovici, C. and Lemaire, P. (2003). Neural tissue in ascidian embryos is induced by FGF9/16/20, acting via a combination of maternal GATA and Ets transcription factors. *Cell* **115**, 615-27.

Bottcher, R. T., Pollet, N., Delius, H. and Niehrs, C. (2004). The transmembrane protein XFLRT3 forms a complex with FGF receptors and promotes FGF signalling. *Nat Cell Biol* **6**, 38-44.

Carmany-Rampey, A. and Schier, A. F. (2001). Single-cell internalization during zebrafish gastrulation. *Curr Biol* **11**, 1261-5.

Cebria, F., Kobayashi, C., Umesono, Y., Nakazawa, M., Mineta, K., Ikeo, K., Gojobori, T., Itoh, M., Taira, M., Sanchez Alvarado, A. and Agata, K. (2002). FGFR-related gene nou-darake restricts brain tissues to the head region of planarians. *Nature* **419**, 620-4.

Chen, Y. and Schier, A. F. (2001). The zebrafish Nodal signal Squint functions as a morphogen. *Nature* **411**, 607-10.

Chen, Y. and Schier, A. F. (2002). Lefty proteins are long-range inhibitors of squint-mediated nodal signaling. *Curr Biol* **12**, 2124-8.

Cheng, S. K., Olale, F., Bennett, J. T., Brivanlou, A. H. and Schier, A. F. (2003). EGF-CFC proteins are essential coreceptors for the TGF-beta signals Vg1 and GDF1. *Genes Dev* **17**, 31-6.

Ciruna, B. and Rossant, J. (2001). FGF signaling regulates mesoderm cell fate specification and morphogenetic movement at the primitive streak. *Dev Cell* **1**, 37-49.

Ciruna, B. G., Schwartz, L., Harpal, K., Yamaguchi, T. P. and Rossant, J. (1997). Chimeric analysis of fibroblast growth factor receptor-1 (Fgfr1) function: a role for FGFR1 in morphogenetic movement through the primitive streak. *Development* **124**, 2829-41.

Comijn, J., Berx, G., Vermassen, P., Verschueren, K., van Grunsven, L., Bruyneel, E., Mareel, M., Huylebroeck, D. and van Roy, F. (2001). The two-handed E box binding zinc finger protein SIP1 downregulates E-cadherin and induces invasion. *Mol Cell* **7**, 1267-78.

Conlon, F. L. and Smith, J. C. (1999). Interference with brachyury function inhibits convergent extension, causes apoptosis, and reveals separate requirements in the FGF and activin signalling pathways. *Dev Biol* **213**, 85-100.

Cornell, R. A. and Kimelman, D. (1994a). Activin-mediated mesoderm induction requires FGF. *Development* **120**, 453-62.

Cornell, R. A. and Kimelman, D. (1994b). Combinatorial signaling in development. *Bioessays* **16**, 577-81.

Darras, S. and Nishida, H. (2001). The BMP/CHORDIN antagonism controls sensory pigment cell specification and differentiation in the ascidian embryo. *Dev Biol* **236**, 271-88.

Delaune, E., Lemaire, P. and Kodjabachian, L. (2004). Neural induction in Xenopus requires early FGF signalling in addition to BMP inhibition. *Development*.

Detrich, H. W., 3rd, Kieran, M. W., Chan, F. Y., Barone, L. M., Yee, K., Rundstadler, J. A., Pratt, S., Ransom, D. and Zon, L. I. (1995). Intraembryonic hematopoietic cell migration during vertebrate development. *Proc Natl Acad Sci U S A* **92**, 10713-7.

Dougan, S. T., Warga, R. M., Kane, D. A., Schier, A. F. and Talbot, W. S. (2003). The role of the zebrafish nodal-related genes squint and cyclops in patterning of mesendoderm. *Development* **130**, 1837-51.

Driever, W., Solnica-Krezel, L., Schier, A. F., Neuhauss, S. C., Malicki, J., Stemple, D. L., Stainier, D. Y., Zwartkruis, F., Abdelilah, S., Rangini, Z., Belak, J. and Boggs, C. (1996). A genetic screen for mutations affecting embryogenesis in zebrafish. *Development* **123**, 37-46.

Eisaki, A., Kuroda, H., Fukui, A. and Asashima, M. (2000). XSIP1, a member of two-handed zinc finger proteins, induced anterior neural markers in Xenopus laevis animal cap. *Biochem Biophys Res Commun* **271**, 151-7.

Fainsod, A., Deissler, K., Yelin, R., Marom, K., Epstein, M., Pillemer, G., Steinbeisser, H. and Blum, M. (1997). The dorsalizing and neural inducing gene follistatin is an antagonist of BMP-4. *Mech Dev* **63**, 39-50.

Fekany-Lee, K., Gonzalez, E., Miller-Bertoglio, V. and Solnica-Krezel, L. (2000). The homeobox gene bozozok promotes anterior neuroectoderm formation in zebrafish through negative regulation of BMP2/4 and Wnt pathways. *Development* **127**, 2333-45.

Feldman, B., Concha, M. L., Saude, L., Parsons, M. J., Adams, R. J., Wilson, S. W. and Stemple, D. L. (2002). Lefty antagonism of Squint is essential for normal gastrulation. *Curr Biol* **12**, 2129-35.

Feldman, B., Dougan, S. T., Schier, A. F. and Talbot, W. S. (2000). Nodal-related signals establish mesendodermal fate and trunk neural identity in zebrafish. *Curr Biol* **10**, 531-4.

Feldman, B., Gates, M. A., Egan, E. S., Dougan, S. T., Rennebeck, G., Sirotkin, H. I., Schier, A. F. and Talbot, W. S. (1998). Zebrafish organizer development and germ-layer formation require nodal-related signals. *Nature* **395**, 181-5.

Feng, X. H. and Derynck, R. (2005). Specificity and versatility in tgf-beta signaling through Smads. *Annu Rev Cell Dev Biol* **21**, 659-93.

Furthauer, M., Thisse, C. and Thisse, B. (1997). A role for FGF-8 in the dorsoventral patterning of the zebrafish gastrula. *Development* **124**, 4253-64.

Furthauer, M., Van Celst, J., Thisse, C. and Thisse, B. (2004). Fgf signalling controls the dorsoventral patterning of the zebrafish embryo. *Development* **131**, 2853-64.

Furusawa, T., Moribe, H., Kondoh, H. and Higashi, Y. (1999). Identification of CtBP1 and CtBP2 as corepressors of zinc finger-homeodomain factor deltaEF1. *Mol Cell Biol* **19**, 8581-90.

Gomez-Skarmeta, J., de La Calle-Mustienes, E. and Modolell, J. (2001). The Wnt-activated Xiro1 gene encodes a repressor that is essential for neural development and downregulates Bmp4. *Development* **128**, 551-60.

Griffin, K., Patient, R. and Holder, N. (1995). Analysis of FGF function in normal and no tail zebrafish embryos reveals separate mechanisms for formation of the trunk and the tail. *Development* **121**, 2983-94.

Griffin, K. J., Amacher, S. L., Kimmel, C. B. and Kimelman, D. (1998). Molecular identification of spadetail: regulation of zebrafish trunk and tail mesoderm formation by T-box genes. *Development* **125**, 3379-88.

Grinblat, Y., Gamse, J., Patel, M. and Sive, H. (1998). Determination of the zebrafish forebrain: induction and patterning. *Development* **125**, 4403-16.

Grinblat, Y. and Sive, H. (2001). zic Gene expression marks anteroposterior pattern in the presumptive neurectoderm of the zebrafish gastrula. *Dev Dyn* **222**, 688-93.

Gritsman, K., Zhang, J., Cheng, S., Heckscher, E., Talbot, W. S. and Schier, A. F. (1999). The EGF-CFC protein one-eyed pinhead is essential for nodal signaling. *Cell* **97**, 121-32.

Haffter, P., Granato, M., Brand, M., Mullins, M. C., Hammerschmidt, M., Kane, D. A., Odenthal, J., van Eeden, F. J., Jiang, Y. J., Heisenberg, C. P., Kelsh, R. N., Furutani-Seiki, M., Vogelsang, E., Beuchle, D., Schach, U., Fabian, C. and Nusslein-Volhard, C. (1996). The identification of genes with unique and essential functions in the development of the zebrafish, Danio rerio. *Development* **123**, 1-36.

Halpern, M. E., Ho, R. K., Walker, C. and Kimmel, C. B. (1993). Induction of muscle pioneers and floor plate is distinguished by the zebrafish no tail mutation. *Cell* **75**, 99-111.

Hammerschmidt, M., Pelegri, F., Mullins, M. C., Kane, D. A., van Eeden, F. J., Granato, M., Brand, M., Furutani-Seiki, M., Haffter, P., Heisenberg, C. P., Jiang, Y. J., Kelsh, R. N., Odenthal, J., Warga, R. M. and Nusslein-Volhard, C. (1996). dino and mercedes, two genes regulating dorsal development in the zebrafish embryo. *Development* **123**, 95-102.

Hardcastle, Z., Chalmers, A. D. and Papalopulu, N. (2000). FGF-8 stimulates neuronal differentiation through FGFR-4a and interferes with mesoderm induction in Xenopus embryos. *Curr Biol* **10**, 1511-4.

Helde, K. A. and Grunwald, D. J. (1993). The DVR-1 (Vg1) transcript of zebrafish is maternally supplied and distributed throughout the embryo. *Dev Biol* **159**, 418-26.

Helde, K. A., Wilson, E. T., Cretekos, C. J. and Grunwald, D. J. (1994). Contribution of early cells to the fate map of the zebrafish gastrula. *Science* **265**, 517-20.

Hemmati-Brivanlou, A., Kelly, O. G. and Melton, D. A. (1994). Follistatin, an antagonist of activin, is expressed in the Spemann organizer and displays direct neuralizing activity. *Cell* **77**, 283-95.

Hemmati-Brivanlou, A. and Melton, D. (1997). Vertebrate neural induction. *Annu Rev Neurosci* **20**, 43-60.

Hild, M., Dick, A., Rauch, G. J., Meier, A., Bouwmeester, T., Haffter, P. and Hammerschmidt, M. (1999). The smad5 mutation somitabun blocks Bmp2b signaling during early dorsoventral patterning of the zebrafish embryo. *Development* **126**, 2149-59.

Ho, D. M., Chan, J., Bayliss, P. and Whitman, M. (2006). Inhibitor-resistant type I receptors reveal specific requirements for TGF-beta signaling in vivo. *Dev Biol* **295**, 730-42.

Ho, R. K. and Kane, D. A. (1990). Cell-autonomous action of zebrafish spt-1 mutation in specific mesodermal precursors. *Nature* **348**, 728-30.

Ho, R. K. and Kimmel, C. B. (1993). Commitment of cell fate in the early zebrafish embryo. *Science* **261**, 109-11.

Holowacz, T. and Sokol, S. (1999). FGF is required for posterior neural patterning but not for neural induction. *Dev Biol* **205**, 296-308.

Hongo, I., Kengaku, M. and Okamoto, H. (1999). FGF signaling and the anterior neural induction in Xenopus. *Dev Biol* **216**, 561-81.

Hudson, C., Darras, S., Caillol, D., Yasuo, H. and Lemaire, P. (2003). A conserved role for the MEK signalling pathway in neural tissue specification and posteriorisation in the invertebrate chordate, the ascidian Ciona intestinalis. *Development* **130**, 147-59.

Hug, B., Walter, V. and Grunwald, D. J. (1997). tbx6, a Brachyury-related gene expressed by ventral mesendodermal precursors in the zebrafish embryo. *Dev Biol* **183**, 61-73.

Joly, J. S., Joly, C., Schulte-Merker, S., Boulekbache, H. and Condamine, H. (1993). The ventral and posterior expression of the zebrafish homeobox gene eve1 is perturbed in dorsalized and mutant embryos. *Development* **119**, 1261-75.

Jones, C. M., Lyons, K. M., Lapan, P. M., Wright, C. V. and Hogan, B. L. (1992). DVR-4 (bone morphogenetic protein-4) as a posterior-ventralizing factor in Xenopus mesoderm induction. *Development* **115**, 639-47.

Kane, D. A., McFarland, K. N. and Warga, R. M. (2005). Mutations in half baked/E-cadherin block cell behaviors that are necessary for teleost epiboly. *Development* **132**, 1105-16.

Kengaku, M. and Okamoto, H. (1995). bFGF as a possible morphogen for the anteroposterior axis of the central nervous system in Xenopus. *Development* **121**, 3121-30.

Kiefer, P., Strahle, U. and Dickson, C. (1996). The zebrafish Fgf-3 gene: cDNA sequence, transcript structure and genomic organization. *Gene* **168**, 211-5.

Kimelman, D. (2006). Mesoderm induction: from caps to chips. *Nat Rev Genet* **7**, 360-72.

Kimelman, D. and Kirschner, M. (1987). Synergistic induction of mesoderm by FGF and TGF-beta and the identification of an mRNA coding for FGF in the early Xenopus embryo. *Cell* **51**, 869-77.

Kimmel, C. B. (1989). Genetics and early development of zebrafish. *Trends Genet* **5**, 283-8.

Kimmel, C. B., Ballard, W. W., Kimmel, S. R., Ullmann, B. and Schilling, T. F. (1995). Stages of embryonic development of the zebrafish. *Dev Dyn* **203**, 253-310.

Kimmel, C. B., Warga, R. M. and Schilling, T. F. (1990). Origin and organization of the zebrafish fate map. *Development* **108**, 581-94.

Kishimoto, Y., Lee, K. H., Zon, L., Hammerschmidt, M. and Schulte-Merker, S. (1997). The molecular nature of zebrafish swirl: BMP2 function is essential during early dorsoventral patterning. *Development* **124**, 4457-66.

Kitisin, K., Saha, T., Blake, T., Golestaneh, N., Deng, M., Kim, C., Tang, Y., Shetty, K., Mishra, B. and Mishra, L. (2007). Tgf-Beta signaling in development. *Sci STKE* **2007**, cm1.

Klingensmith, J., Ang, S. L., Bachiller, D. and Rossant, J. (1999). Neural induction and patterning in the mouse in the absence of the node and its derivatives. *Dev Biol* **216**, 535-49.

Koshida, S., Shinya, M., Nikaido, M., Ueno, N., Schulte-Merker, S., Kuroiwa, A. and Takeda, H. (2002). Inhibition of BMP activity by the FGF signal promotes posterior neural development in zebrafish. *Dev Biol* **244**, 9-20.

Krauss, S., Johansen, T., Korzh, V. and Fjose, A. (1991). Expression of the zebrafish paired box gene pax[zf-b] during early neurogenesis. *Development* **113**, 1193-206.

Kretzschmar, M., Doody, J. and Massague, J. (1997). Opposing BMP and EGF signalling pathways converge on the TGF-beta family mediator Smad1. *Nature* **389**, 618-22.

Kroll, K. L. and Amaya, E. (1996). Transgenic Xenopus embryos from sperm nuclear transplantations reveal FGF signaling requirements during gastrulation. *Development* **122**, 3173-83.

Kubota, Y. and Ito, K. (2000). Chemotactic migration of mesencephalic neural crest cells in the mouse. *Dev Dyn* **217**, 170-9.

Kudoh, T., Concha, M. L., Houart, C., Dawid, I. B. and Wilson, S. W. (2004). Combinatorial Fgf and Bmp signalling patterns the gastrula ectoderm into prospective neural and epidermal domains. *Development* **131**, 3581-92.

Kudoh, T., Wilson, S. W. and Dawid, I. B. (2002). Distinct roles for Fgf, Wnt and retinoic acid in posteriorizing the neural ectoderm. *Development* **129**, 4335-46.

Kunwar, P. S., Zimmerman, S., Bennett, J. T., Chen, Y., Whitman, M. and Schier, A. F. (2003). Mixer/Bon and FoxH1/Sur have overlapping and divergent roles in Nodal signaling and mesendoderm induction. *Development* **130**, 5589-99.

Kuroda, H., Wessely, O. and De Robertis, E. M. (2004). Neural induction in Xenopus: requirement for ectodermal and endomesodermal signals via Chordin, Noggin, beta-Catenin, and Cerberus. *PLoS Biol* **2**, E92.

Kwan, K. M. and Kirschner, M. W. (2003). Xbra functions as a switch between cell migration and convergent extension in the Xenopus gastrula. *Development* **130**, 1961-72.

LaBonne, C., Burke, B. and Whitman, M. (1995). Role of MAP kinase in mesoderm induction and axial patterning during Xenopus development. *Development* **121**, 1475-86.

LaBonne, C. and Whitman, M. (1994). Mesoderm induction by activin requires FGF-mediated intracellular signals. *Development* **120**, 463-72.

Lamb, T. M. and Harland, R. M. (1995). Fibroblast growth factor is a direct neural inducer, which combined with noggin generates anterior-posterior neural pattern. *Development* **121**, 3627-36.

Launay, C., Fromentoux, V., Shi, D. L. and Boucaut, J. C. (1996). A truncated FGF receptor blocks neural induction by endogenous Xenopus inducers. *Development* **122**, 869-80.

Lee, B. M., Buck-Koehntop, B. A., Martinez-Yamout, M. A., Dyson, H. J. and Wright, P. E. (2007). Embryonic neural inducing factor churchill is not a DNA-binding zinc finger

protein: solution structure reveals a solvent-exposed beta-sheet and zinc binuclear cluster. *J Mol Biol* **371**, 1274-89.

Lemaire, P., Bertrand, V. and Hudson, C. (2002). Early steps in the formation of neural tissue in ascidian embryos. *Dev Biol* **252**, 151-69.

Leptin, M. (2005). Gastrulation movements: the logic and the nuts and bolts. *Dev Cell* **8**, 305-20.

Lerchner, W., Latinkic, B. V., Remacle, J. E., Huylebroeck, D. and Smith, J. C. (2000). Region-specific activation of the Xenopus brachyury promoter involves active repression in ectoderm and endoderm: a study using transgenic frog embryos. *Development* **127**, 2729-39.

Leung, T., Bischof, J., Soll, I., Niessing, D., Zhang, D., Ma, J., Jackle, H. and Driever, W. (2003). bozozok directly represses bmp2b transcription and mediates the earliest dorsoventral asymmetry of bmp2b expression in zebrafish. *Development* **130**, 3639-49.

Londin, E. R., Mentzer, L., Gates, K. P. and Sirotkin, H. I. (2007a). Expression and regulation of the zinc finger transcription factor Churchill during zebrafish development. *Gene Ex pr. Pattern* **Do1:10.1016/j.modgep.2007.04.002**.

Londin, E. R., Mentzer, L. and Sirotkin, H. I. (2007b). Churchill regulates cell movement and mesoderm specification by repressing Nodal signaling. *BMC Developmental Biology* **7:120**.

Londin, E. R., Niemiec, J. and Sirotkin, H. I. (2005). Chordin, FGF signaling, and mesodermal factors cooperate in zebrafish neural induction. *Dev Biol* **279**, 1-19.

Long, J., Zuo, D. and Park, M. (2005). Pc2-mediated sumoylation of Smad-interacting protein 1 attenuates transcriptional repression of E-cadherin. *J Biol Chem* **280**, 35477-89.

Massague, J. (2003). Integration of Smad and MAPK pathways: a link and a linker revisited. *Genes Dev* **17**, 2993-7.

Mathavan, S., Lee, S. G., Mak, A., Miller, L. D., Murthy, K. R., Govindarajan, K. R., Tong, Y., Wu, Y. L., Lam, S. H., Yang, H., Ruan, Y., Korzh, V., Gong, Z., Liu, E. T. and Lufkin, T. (2005). Transcriptome analysis of zebrafish embryogenesis using microarrays. *PLoS Genet* **1**, 260-76.

Mathieu, J., Griffin, K., Herbomel, P., Dickmeis, T., Strahle, U., Kimelman, D., Rosa, F. M. and Peyrieras, N. (2004). Nodal and Fgf pathways interact through a positive regulatory loop and synergize to maintain mesodermal cell populations. *Development* **131**, 629-41.

Matsumoto, K., Nishihara, S., Kamimura, M., Shiraishi, T., Otoguro, T., Uehara, M., Maeda, Y., Ogura, K., Lumsden, A. and Ogura, T. (2004). The prepattern transcription

factor Irx2, a target of the FGF8/MAP kinase cascade, is involved in cerebellum formation. *Nat Neurosci* **7**, 605-12.

Matus, D. Q., Thomsen, G. H. and Martindale, M. Q. (2007). FGF signaling in gastrulation and neural development in Nematostella vectensis, an anthozoan cnidarian. *Dev Genes Evol*.

Melby, A. E., Beach, C., Mullins, M. and Kimelman, D. (2000). Patterning the early zebrafish by the opposing actions of bozozok and vox/vent. *Dev Biol* **224**, 275-85.

Miller-Bertoglio, V. E., Fisher, S., Sanchez, A., Mullins, M. C. and Halpern, M. E. (1997). Differential regulation of chordin expression domains in mutant zebrafish. *Dev Biol* **192**, 537-50.

Mitchell, T. S. and Sheets, M. D. (2001). The FGFR pathway is required for the trunk-inducing functions of Spemann's organizer. *Dev Biol* **237**, 295-305.

Mohammadi, M., Schlessinger, J. and Hubbard, S. R. (1996). Structure of the FGF receptor tyrosine kinase domain reveals a novel autoinhibitory mechanism. *Cell* **86**, 577-87.

Monsoro-Burq, A. H., Fletcher, R. B. and Harland, R. M. (2003). Neural crest induction by paraxial mesoderm in Xenopus embryos requires FGF signals. *Development* **130**, 3111-24.

Montero, J. A. and Heisenberg, C. P. (2004). Gastrulation dynamics: cells move into focus. *Trends Cell Biol* **14**, 620-7.

Mori, H., Miyazaki, Y., Morita, T., Nitta, H. and Mishina, M. (1994). Different spatio-temporal expressions of three otx homeoprotein transcripts during zebrafish embryogenesis. *Brain Res Mol Brain Res* **27**, 221-31.

Morita, T., Nitta, H., Kiyama, Y., Mori, H. and Mishina, M. (1995). Differential expression of two zebrafish emx homeoprotein mRNAs in the developing brain. *Neurosci Lett* **198**, 131-4.

Munoz-Sanjuan, I. and Brivanlou, A. H. (2002). Neural induction, the default model and embryonic stem cells. *Nat Rev Neurosci* **3**, 271-80.

Myers, D. C., Sepich, D. S. and Solnica-Krezel, L. (2002a). Bmp activity gradient regulates convergent extension during zebrafish gastrulation. *Dev Biol* **243**, 81-98.

Myers, D. C., Sepich, D. S. and Solnica-Krezel, L. (2002b). Convergence and extension in vertebrate gastrulae: cell movements according to or in search of identity? *Trends Genet* **18**, 447-55.

Nasevicius, A. and Ekker, S. C. (2000). Effective targeted gene 'knockdown' in zebrafish. *Nat Genet* **26**, 216-20.

Neave, B., Holder, N. and Patient, R. (1997). A graded response to BMP-4 spatially coordinates patterning of the mesoderm and ectoderm in the zebrafish. *Mech Dev* **62**, 183-95.

Neave, B., Rodaway, A., Wilson, S. W., Patient, R. and Holder, N. (1995). Expression of zebrafish GATA 3 (gta3) during gastrulation and neurulation suggests a role in the specification of cell fate. *Mech Dev* **51**, 169-82.

Nieuwkoop, P. D. (1952). Activation and organization of the central nervous system in amphibians, parts I-III. *J. Exp. Zool.* **120**, 1-108.

Nikaido, M., Tada, M., Saji, T. and Ueno, N. (1997). Conservation of BMP signaling in zebrafish mesoderm patterning. *Mech Dev* **61**, 75-88.

Nitta, K. R., Takahashi, S., Haramoto, Y., Fukuda, M., Tanegashima, K., Onuma, Y. and Asashima, M. (2007). The N-terminus zinc finger domain of Xenopus SIP1 is important for neural induction, but not for suppression of Xbra expression. *Int J Dev Biol* **51**, 321-5.

Nitta, K. R., Tanegashima, K., Takahashi, S. and Asashima, M. (2004). XSIP1 is essential for early neural gene expression and neural differentiation by suppression of BMP signaling. *Dev Biol* **275**, 258-67.

Oelgeschlager, M., Kuroda, H., Reversade, B. and De Robertis, E. M. (2003). Chordin is required for the Spemann organizer transplantation phenomenon in Xenopus embryos. *Dev Cell* **4**, 219-30.

Oxtoby, E. and Jowett, T. (1993). Cloning of the zebrafish krox-20 gene (krx-20) and its expression during hindbrain development. *Nucleic Acids Res* **21**, 1087-95.

Papin, C., van Grunsven, L. A., Verschueren, K., Huylebroeck, D. and Smith, J. C. (2002). Dynamic regulation of Brachyury expression in the amphibian embryo by XSIP1. *Mech Dev* **111**, 37-46.

Pera, E. M., Ikeda, A., Eivers, E. and De Robertis, E. M. (2003). Integration of IGF, FGF, and anti-BMP signals via Smad1 phosphorylation in neural induction. *Genes Dev* **17**, 3023-8.

Perea-Gomez, A., Vella, F. D., Shawlot, W., Oulad-Abdelghani, M., Chazaud, C., Meno, C., Pfister, V., Chen, L., Robertson, E., Hamada, H., Behringer, R. R. and Ang, S. L. (2002). Nodal antagonists in the anterior visceral endoderm prevent the formation of multiple primitive streaks. *Dev Cell* **3**, 745-56.

Piccolo, S., Agius, E., Leyns, L., Bhattacharyya, S., Grunz, H., Bouwmeester, T. and De Robertis, E. M. (1999). The head inducer Cerberus is a multifunctional antagonist of Nodal, BMP and Wnt signals. *Nature* **397**, 707-10.

Piccolo, S., Sasai, Y., Lu, B. and De Robertis, E. M. (1996). Dorsoventral patterning in Xenopus: inhibition of ventral signals by direct binding of chordin to BMP-4. *Cell* **86**, 589-98.

Pogoda, H. M., Solnica-Krezel, L., Driever, W. and Meyer, D. (2000). The zebrafish forkhead transcription factor FoxH1/Fast1 is a modulator of nodal signaling required for organizer formation. *Curr Biol* **10**, 1041-9.

Postigo, A. A. (2003). Opposing functions of ZEB proteins in the regulation of the TGFbeta/BMP signaling pathway. *Embo J* **22**, 2443-52.

Postigo, A. A. and Dean, D. C. (1999). ZEB represses transcription through interaction with the corepressor CtBP. *Proc Natl Acad Sci U S A* **96**, 6683-8.

Postigo, A. A., Depp, J. L., Taylor, J. J. and Kroll, K. L. (2003). Regulation of Smad signaling through a differential recruitment of coactivators and corepressors by ZEB proteins. *Embo J* **22**, 2453-62.

Pownall, M. E., Welm, B. E., Freeman, K. W., Spencer, D. M., Rosen, J. M. and Isaacs, H. V. (2003). An inducible system for the study of FGF signalling in early amphibian development. *Dev Biol* **256**, 89-99.

Pyati, U. J., Webb, A. E. and Kimelman, D. (2005). Transgenic zebrafish reveal stage-specific roles for Bmp signaling in ventral and posterior mesoderm development. *Development* **132**, 2333-43.

Rentzsch, F., Bakkers, J., Kramer, C. and Hammerschmidt, M. (2004). Fgf signaling induces posterior neuroectoderm independently of Bmp signaling inhibition. *Dev Dyn* **231**, 750-7.

Ribisi, S., Jr., Mariani, F. V., Aamar, E., Lamb, T. M., Frank, D. and Harland, R. M. (2000). Ras-mediated FGF signaling is required for the formation of posterior but not anterior neural tissue in Xenopus laevis. *Dev Biol* **227**, 183-96.

Sasai, Y., Lu, B., Steinbeisser, H. and De Robertis, E. M. (1995). Regulation of neural induction by the Chd and Bmp-4 antagonistic patterning signals in Xenopus. *Nature* **376**, 333-6.

Saude, L., Woolley, K., Martin, P., Driever, W. and Stemple, D. L. (2000). Axis-inducing activities and cell fates of the zebrafish organizer. *Development* **127**, 3407-17.

Schier, A. F. (2003). Nodal signaling in vertebrate development. *Annu Rev Cell Dev Biol* **19**, 589-621.

Schier, A. F., Neuhauss, S. C., Helde, K. A., Talbot, W. S. and Driever, W. (1997). The one-eyed pinhead gene functions in mesoderm and endoderm formation in zebrafish and interacts with no tail. *Development* **124**, 327-42.

Schier, A. F. and Talbot, W. S. (2005). Molecular genetics of axis formation in zebrafish. *Annu Rev Genet* **39**, 561-613.

Schmid, B., Furthauer, M., Connors, S. A., Trout, J., Thisse, B., Thisse, C. and Mullins, M. C. (2000). Equivalent genetic roles for bmp7/snailhouse and bmp2b/swirl in dorsoventral pattern formation. *Development* **127**, 957-67.

Schulte-Merker, S., Lee, K. J., McMahon, A. P. and Hammerschmidt, M. (1997). The zebrafish organizer requires chordino. *Nature* **387**, 862-3.

Schulte-Merker, S., van Eeden, F. J., Halpern, M. E., Kimmel, C. B. and Nusslein-Volhard, C. (1994). no tail (ntl) is the zebrafish homologue of the mouse T (Brachyury) gene. *Development* **120**, 1009-15.

Sheng, G., dos Reis, M. and Stern, C. D. (2003). Churchill, a zinc finger transcriptional activator, regulates the transition between gastrulation and neurulation. *Cell* **115**, 603-13.

Sidi, S., Goutel, C., Peyrieras, N. and Rosa, F. M. (2003). Maternal induction of ventral fate by zebrafish radar. *Proc Natl Acad Sci U S A* **100**, 3315-20.

Sirotkin, H. I., Dougan, S. T., Schier, A. F. and Talbot, W. S. (2000a). bozozok and squint act in parallel to specify dorsal mesoderm and anterior neuroectoderm in zebrafish. *Development* **127**, 2583-92.

Sirotkin, H. I., Gates, M. A., Kelly, P. D., Schier, A. F. and Talbot, W. S. (2000b). Fast1 is required for the development of dorsal axial structures in zebrafish. *Curr Biol* **10**, 1051-4.

Slack, J. M., Darlington, B. G., Heath, J. K. and Godsave, S. F. (1987). Mesoderm induction in early Xenopus embryos by heparin-binding growth factors. *Nature* **326**, 197-200.

Smith, W. C. and Harland, R. M. (1992). Expression cloning of noggin, a new dorsalizing factor localized to the Spemann organizer in Xenopus embryos. *Cell* **70**, 829-40.

Snir, M., Ofir, R., Elias, S. and Frank, D. (2006). Xenopus laevis POU91 protein, an Oct3/4 homologue, regulates competence transitions from mesoderm to neural cell fates. *Embo J* **25**, 3664-74.

Solnica-Krezel, L. (2006). Gastrulation in zebrafish -- all just about adhesion? *Curr Opin Genet Dev* **16**, 433-41.

Solnica-Krezel, L. and Driever, W. (1994). Microtubule arrays of the zebrafish yolk cell: organization and function during epiboly. *Development* **120**, 2443-55.

Spemann, H., Mangold, H. (1924). Induction of embryonic primordia by implantation of organizers from different species. *Roux's Arch Entw Mech* **100**, 500-638.

Stern, C. D. (2002). Induction and initial patterning of the nervous system - the chick embryo enters the scene. *Curr Opin Genet Dev* **12**, 447-51.

Stern, C. D. (2005). Neural induction: old problem, new findings, yet more questions. *Development* **132**, 2007-21.

Stern, C. D. (2006). Neural induction: 10 years on since the 'default model'. *Curr Opin Cell Biol* **18**, 692-7.

Stern, C. D., Jaques, K. F., Lim, T. M., Fraser, S. E. and Keynes, R. J. (1991). Segmental lineage restrictions in the chick embryo spinal cord depend on the adjacent somites. *Development* **113**, 239-44.

Storey, K. G., Goriely, A., Sargent, C. M., Brown, J. M., Burns, H. D., Abud, H. M. and Heath, J. K. (1998). Early posterior neural tissue is induced by FGF in the chick embryo. *Development* **125**, 473-84.

Strahle, U., Jesuthasan, S., Blader, P., Garcia-Villalba, P., Hatta, K. and Ingham, P. W. (1997). one-eyed pinhead is required for development of the ventral midline of the zebrafish (Danio rerio) neural tube. *Genes Funct* **1**, 131-48.

Streisinger, G., Walker, C., Dower, N., Knauber, D. and Singer, F. (1981). Production of clones of homozygous diploid zebra fish (Brachydanio rerio). *Nature* **291**, 293-6.

Streit, A., Berliner, A. J., Papanayotou, C., Sirulnik, A. and Stern, C. D. (2000). Initiation of neural induction by FGF signalling before gastrulation. *Nature* **406**, 74-8.

Streit, A., Lee, K. J., Woo, I., Roberts, C., Jessell, T. M. and Stern, C. D. (1998). Chordin regulates primitive streak development and the stability of induced neural cells, but is not sufficient for neural induction in the chick embryo. *Development* **125**, 507-19.

Strong, C. F., Barnett, M. W., Hartman, D., Jones, E. A. and Stott, D. (2000). Xbra3 induces mesoderm and neural tissue in Xenopus laevis. *Dev Biol* **222**, 405-19.

Sun, X., Meyers, E. N., Lewandoski, M. and Martin, G. R. (1999). Targeted disruption of Fgf8 causes failure of cell migration in the gastrulating mouse embryo. *Genes Dev* **13**, 1834-46.

Sun, Z., Jin, P., Tian, T., Gu, Y., Chen, Y. G. and Meng, A. (2006). Activation and roles of ALK4/ALK7-mediated maternal TGFbeta signals in zebrafish embryo. *Biochem Biophys Res Commun* **345**, 694-703.

Thisse, B., Wright, C. V. and Thisse, C. (2000). Activin- and Nodal-related factors control antero-posterior patterning of the zebrafish embryo. *Nature* **403**, 425-8.

Thisse, C., Thisse, B., Schilling, T. F. and Postlethwait, J. H. (1993). Structure of the zebrafish snail1 gene and its expression in wild-type, spadetail and no tail mutant embryos. *Development* **119**, 1203-15.

Udvadia, A. J. and Linney, E. (2003). Windows into development: historic, current, and future perspectives on transgenic zebrafish. *Dev Biol* **256**, 1-17.

Umbhauer, M., Marshall, C. J., Mason, C. S., Old, R. W. and Smith, J. C. (1995). Mesoderm induction in Xenopus caused by activation of MAP kinase. *Nature* **376**, 58-62.

Van de Putte, T., Maruhashi, M., Francis, A., Nelles, L., Kondoh, H., Huylebroeck, D. and Higashi, Y. (2003). Mice lacking ZFHX1B, the gene that codes for Smad-interacting protein-1, reveal a role for multiple neural crest cell defects in the etiology of Hirschsprung disease-mental retardation syndrome. *Am J Hum Genet* **72**, 465-70.

van Grunsven, L. A., Michiels, C., Van de Putte, T., Nelles, L., Wuytens, G., Verschueren, K. and Huylebroeck, D. (2003). Interaction between Smad-interacting protein-1 and the corepressor C-terminal binding protein is dispensable for transcriptional repression of E-cadherin. *J Biol Chem* **278**, 26135-45.

van Grunsven, L. A., Papin, C., Avalosse, B., Opdecamp, K., Huylebroeck, D., Smith, J. C. and Bellefroid, E. J. (2000). XSIP1, a Xenopus zinc finger/homeodomain encoding gene highly expressed during early neural development. *Mech Dev* **94**, 189-93.

van Grunsven, L. A., Taelman, V., Michiels, C., Opdecamp, K., Huylebroeck, D. and Bellefroid, E. J. (2006). deltaEF1 and SIP1 are differentially expressed and have overlapping activities during Xenopus embryogenesis. *Dev Dyn* **235**, 1491-500.

van Grunsven, L. A., Taelman, V., Michiels, C., Verstappen, G., Souopgui, J., Nichane, M., Moens, E., Opdecamp, K., Vanhomwegen, J., Kricha, S., Huylebroeck, D. and Bellefroid, E. J. (2007). XSip1 neuralizing activity involves the co-repressor CtBP and occurs through BMP dependent and independent mechanisms. *Dev Biol* **306**, 34-49.

Vandewalle, C., Comijn, J., De Craene, B., Vermassen, P., Bruyneel, E., Andersen, H., Tulchinsky, E., Van Roy, F. and Berx, G. (2005). SIP1/ZEB2 induces EMT by repressing genes of different epithelial cell-cell junctions. *Nucleic Acids Res* **33**, 6566-78.

Verschueren, K., Remacle, J. E., Collart, C., Kraft, H., Baker, B. S., Tylzanowski, P., Nelles, L., Wuytens, G., Su, M. T., Bodmer, R., Smith, J. C. and Huylebroeck, D. (1999).

SIP1, a novel zinc finger/homeodomain repressor, interacts with Smad proteins and binds to 5'-CACCT sequences in candidate target genes. *J Biol Chem* **274**, 20489-98.

Warga, R. M. and Kimmel, C. B. (1990). Cell movements during epiboly and gastrulation in zebrafish. *Development* **108**, 569-80.

Watanabe, M. and Whitman, M. (1999). FAST-1 is a key maternal effector of mesoderm inducers in the early Xenopus embryo. *Development* **126**, 5621-34.

Welm, B. E., Freeman, K. W., Chen, M., Contreras, A., Spencer, D. M. and Rosen, J. M. (2002). Inducible dimerization of FGFR1: development of a mouse model to analyze progressive transformation of the mammary gland. *J Cell Biol* **157**, 703-14.

Wilson, S. I. and Edlund, T. (2001). Neural induction: toward a unifying mechanism. *Nat Neurosci* **4 Suppl**, 1161-8.

Wilson, S. I., Graziano, E., Harland, R., Jessell, T. M. and Edlund, T. (2000). An early requirement for FGF signalling in the acquisition of neural cell fate in the chick embryo. *Curr Biol* **10**, 421-9.

Wilson, S. I., Rydstrom, A., Trimborn, T., Willert, K., Nusse, R., Jessell, T. M. and Edlund, T. (2001). The status of Wnt signalling regulates neural and epidermal fates in the chick embryo. *Nature* **411**, 325-30.

Woo, K. and Fraser, S. E. (1995). Order and coherence in the fate map of the zebrafish nervous system. *Development* **121**, 2595-609.

Woo, K. and Fraser, S. E. (1997). Specification of the zebrafish nervous system by nonaxial signals. *Science* **277**, 254-7.

Yamaguchi, T. P., Harpal, K., Henkemeyer, M. and Rossant, J. (1994). fgfr-1 is required for embryonic growth and mesodermal patterning during mouse gastrulation. *Genes Dev* **8**, 3032-44.

Yamamoto, A., Amacher, S. L., Kim, S. H., Geissert, D., Kimmel, C. B. and De Robertis, E. M. (1998). Zebrafish paraxial protocadherin is a downstream target of spadetail involved in morphogenesis of gastrula mesoderm. *Development* **125**, 3389-97.

Yang, J., Tan, C., Darken, R. S., Wilson, P. A. and Klein, P. S. (2002). Beta-catenin/Tcf-regulated transcription prior to the midblastula transition. *Development* **129**, 5743-52.

Yoshimoto, A., Saigou, Y., Higashi, Y. and Kondoh, H. (2005). Regulation of ocular lens development by Smad-interacting protein 1 involving Foxe3 activation. *Development* **132**, 4437-48.

Zhao, J., Cao, Y., Zhao, C., Postlethwait, J. and Meng, A. (2003). An SP1-like transcription factor Spr2 acts downstream of Fgf signaling to mediate mesoderm induction. *Embo J* **22**, 6078-88.

Zimmerman, L. B., De Jesus-Escobar, J. M. and Harland, R. M. (1996). The Spemann organizer signal noggin binds and inactivates bone morphogenetic protein 4. *Cell* **86**, 599-606.

Appendix A: Smad interacting protein 1 (Sip1) as a regulatory protein for *churchill* function-preliminary results

A.1 Introduction:

The transcription factor *Churchill* (*chch*) was identified to regulate FGFs function between neural and mesodermal induction. The work presented here showed that *chch* is widely expressed during early zebrafish development and is regulated by FGF signaling (chapter 3) (Londin et al., 2007a). *chch*-deficient cells are more motile than wild-type cells suggesting a role to limit cell movements (chapter 4) (Londin et al., 2007b). Additionally, *chch*-deficient cells often leave the epiblast, migrate to the germ ring and are later found in mesodermal structures in a movement that parallels the expansion of mesoderm and decrease in ectodermal markers that is observed (chapter 4) (Londin et al., 2007b). Both the movement of *chch*-compromised cells to the germ ring and acquisition of mesodermal character depends upon the ability of the donor cells to respond to Nodal signals (chapter 4) (Londin et al., 2007b). Finally, *chch* is required to limit the transcriptional response to Nodal (chapter 4) (Londin et al., 2007b). Together these data establish a broad role for *chch* in regulating both cell movement and Nodal signaling during early development.

One known transcriptional target of *chch,* Smad interacting protein 1 (*Sip1*), is thought to mediate its function (Londin et al., 2007b; Sheng et al., 2003). *Sip1* was originally identified in a screen for proteins that associate with Smad1 (Verschueren et al., 1999). *Sip1* represses TGF-β signaling by binding to activated forms of Smad1/5 (Nodal) and Smad2/3 (BMP) (Postigo, 2003; Postigo et al., 2003). Studies in *Xenopus* and mouse have shown that it can act as both a transcriptional activator and repressor with roles in mesodermal and neural induction as well as in regulating cell movements. (See chapter 5.3 for a more in depth description of *Sip1s* function.)

To date, *Sip1* has not been characterized in zebrafish, although there are two zebrafish homologues present, and it is regulated by *chch* (figure 4.3). Here, I show some preliminary results on the identification and characterization of a zebrafish *Sip1* orthologue. Unlike in the mouse and *Xenopus*, zebrafish contain two *Sip1* homologues, with each homologue having a splice variant present. *Sip1* inhibition results in a gain of mesodermal gene expression but does not appear to act synergistically with Nodal signaling. While, *Sip1* does regulate *E-cadherin* expression, no movement phenotype was observed in cell transplant assays with *Sip1* inhibited embryos. These preliminary results suggest that *Sip1* is may mediated *chch's* response although additional work is needed to further elucidate its role.

A.2 Preliminary results

To date, Sip1 has not yet been characterized in zebrafish. To identify a zebrafish homologue, the zebrafish genome was blast searched using *Xenopus* and mouse Sip1 protein sequences. These results identified two *Sip1* homologues in zebrafish (Figure A.1) termed Sip1a and Sip1b (Unpublished from Iann Sheppards lab, Emory Univerisy). The identified genes do contain similar structural features as the *Xenopus* and mouse Sip1 genes, including a homeodomain (HD), a C-terminal binding protein (CtBP) binding site (CBS), two two-handed zinc finger domains (one at the N-terminus and one at the C-terminus), and a Smad binding domain (SBD). In addition to the two full length genes identified, a splice variant of each gene was also identified (Figure A.1). Both of these splice variants result in the loss of the sixth zinc finger domain. The two *Sip1* homologues may have arisen out of a duplication of the zebrafish genome. It is not yet know whether the two genes have similar functions or if each function to regulate different activities of *Sip1*. The importance of the splice variants is also not yet known. Both of these issues are subject to further experimentation.

Both Sip1 genes are expressed throughout early development (Figure A.2 and data not shown). To determine if the two *Sip1a* splice forms are expressed at similar levels during development, their expression levels were monitored by real-time PCR. Primers were used that would specifically amplify the presence or lack of presence of the sixth zinc finger domain (Figure A.2). By comparing the relative expression levels of the *Sip1a* homologues, showed that during the first 48hrs of development, there is 2-3 times more of the full length gene present than the spliced variant. The reason for this difference is not yet known, and a similar comparison needs to be performed for *Sip1b*.

Next, the effects of inhibting *Sip1a* function by microinjection of a morpholino to the ATG site of the Sip1a gene (Sip1aMO) (Figure A.3) was examined by real-time PCR. Inhibition of Sip1a expression results in modest increases in mesodermal (*ntl, chd,* and *gsc)* and endocermal (*mixer*) gene expression at shield stage. The modest observed on these markers may be due to the presence of *Sip1b*. Inhibiting both Sip1a and Sip1b together may result in more robust effects on mesodermal markers. Conversely, overexpression of a *Xenopus Sip1a*-mRNA (*xSip1a*) does not result in an effect on mesodermal and endodermal gene expression (Figure A.3). Co-expressing the *Sip1a*MO along with *xSip1a*-mRNA results in a rescue of the mesodermal markers *ntl* and *gsc* and the endodermal marker *mixer*. Interestingly, *chd* expression is further decreased upon co expression of the *Sip1a*MO and *xSip1a*-mRNA. Here, there may be different regulation of the *chd* gene than other mesodermal markers.

chch inhibition results in increases in mesodermal gene expression (Figure 4.3-4.4). Real-time PCR was used to assay whether overexpression of *Sip1a*-mRNA can rescue the effects of *chch*-EnR (Figure A.4). At shield stage, *ntl* gene expression is increased following *chch* inhibition. Conversely, overexpression of either 20pg or 2pg *Sip1a*-mRNA has modest effects on *ntl* gene expression. Co-expression of *chch*-EnR along with *Sip1a*-mRNA does result in a rescue of the effect on *ntl* gene expression, although this rescue is only observed when 20pg of *Sip1a*-mRNA is used and not 2pg *Sip1a*-mRNA. Taken together, these results do show that *Sip1a*-mRNA can rescue a chch inhibtion phenotype. These results provide show that like *chch*, *Sip1* also regulates *ntl* gene expression (Figure 4.3).

Figure A.1. Alignment of Sip1 protein sequences. A protein alignment of the two Sip1 genes, Sip1a and Sip1b, along with the splice isoforms of the two genes. The splice isoforms are missing amino acids 1025-1041, representing the missing sixth zinc finger. (cloning performed by Laurie Mentzer)

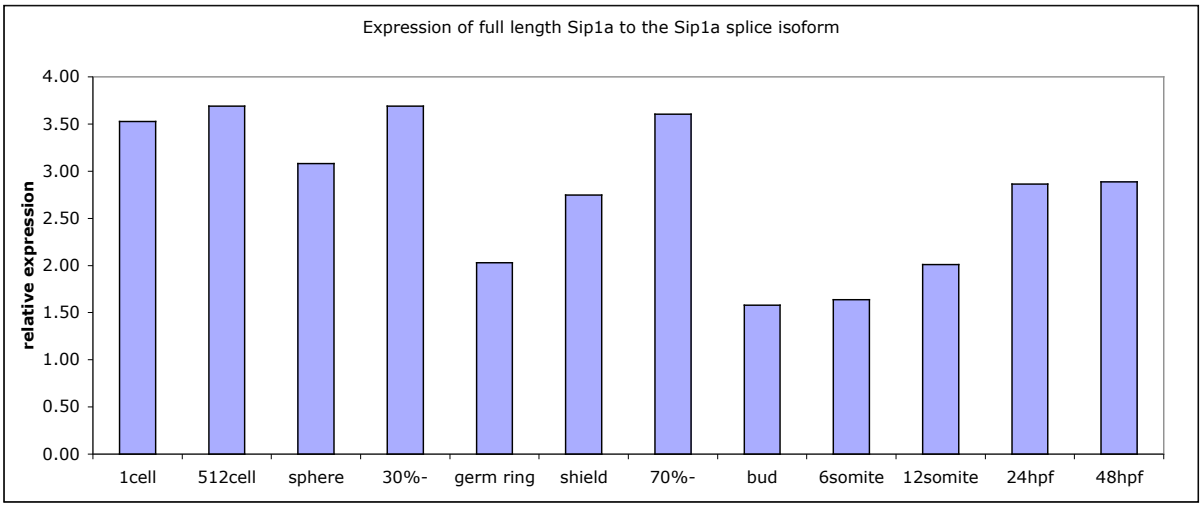

Figure A.2. Expression of the full length Sip1a relative to the *Sip1a* splice isoform. Two sets of real-time PCR primers were used which are specific for the two *Sip1a* forms of the mRNA. Analysis was monitored throughout the first 48hrs of development. This data shows that there is more than 3 times as much of the full-length Sip1a during cleavage and blastula stages. During early gastrulation, there is 2 times more of the full length Sip1a mRNA and the levels increase during gastrulation. The full length Sip1a gene remains highly elevated over the splice isoform during somitogenesis and pharyngula stages.

chch was shown to regulate a transcriptional response to Nodal signaling (Figure 4.9). Sip1 may regulate *chch's* function through inhibition of Smad1/5 proteins (Postigo et al., 2003). To determine if Sip1 is regulating *chch's* function in Nodal signaling, morpholinos to both *Sip1* genes were overexpressed along with sqt mRNA (Figure A.5). Overexpression of 2.5pg *sqt* mRNA results in a 1.5 fold increase in *ntl* expression, a 4.5 fold increase of *chd* expression, a 3.5 fold increase in *gsc* expression and a nearly 5 fold increase in *mixer* gene expression. Conversely overexpression of *Sip1a* and *Sip1b* morpholinos results in a similar effect on *ntl* expression, but only has modest effects on *chd*, *gsc* and *mixer* gene expressions, although *Sip1b* inhibition results in a large 4.5 fold increase in *mixer* expression. Co-expression of *Sip1a*/*b* morpholinos along with *sqt* results in an additive effect on mesodermal gene expression. Interestingly co-expression of *Sip1b*MO along with *sqt* results in a synergistic effect on endodermal gene expression. The different effects of the two *Sip1* genes on endodermal markers may suggest that the two genes have divergent roles on endodermal and mesodermal gene expression. These results do suggest the *Sip1* genes as mediators of *chch's* function in regulating a transcriptional response to Nodal signaling. Additionally, it would be interesting to determine the effect that *Sip1* is having on mesodermal and endodermal genes when both Sip1a and Sip1b are inhibited simultaneously. Furthermore, the effect of *Sip1* genes on the BMP pathway should be examined.

chch inhibited cells exhibit increased motility (Figure 4.5). *Sip1* is an attractive gene to regulate this function of *chch* through the regulation of the *E-cadherin* gene (van Grunsven et al., 2003). To determine if *Sip1* inhibition results in a similar movement phenotype as *chch* inhibited cells, *Sip1a*MO injected cells were transplanted to a wild type host embryo (Figure A.6). When sphere stage ctMO injected cells are transplanted to the animal pole of a sphere stage host embryo, the cells give rise to anterior neural tissue, these cells remained within the animal pole at shield stage and became incorporated into the brain after 24hpf. Conversely, *Sip1a*MO injected transplanted cells exhibited a slightly different phenotype. In 11/31 transplants, the cells had mildly spread throughout the ectoderm at shield stage at became incorporated into epidermal domains of the embryo at 24hpf. The remaining 20 embryos behaved in a similar fashion to the ctMO transplants and did not exhibit a cell movement phenotype and became incorporated into the anterior neural domain. These results do differ from those observed when *chch* inhibited cells are transplanted. The difference may be due to the presence of active Sip1b protein remaining within the cells. This gene can prevent additional cell movements observed when just *Sip1a* is inhibited. It would be interesting to determine what the effect of simultaneous inhibition of Sip1a and *Sip1b* will have. Similarly, it should be determined if *Sip1a/b* overexpression can rescue a *chch* inhibition cell movement phenotype.

A.3 Conclusion:

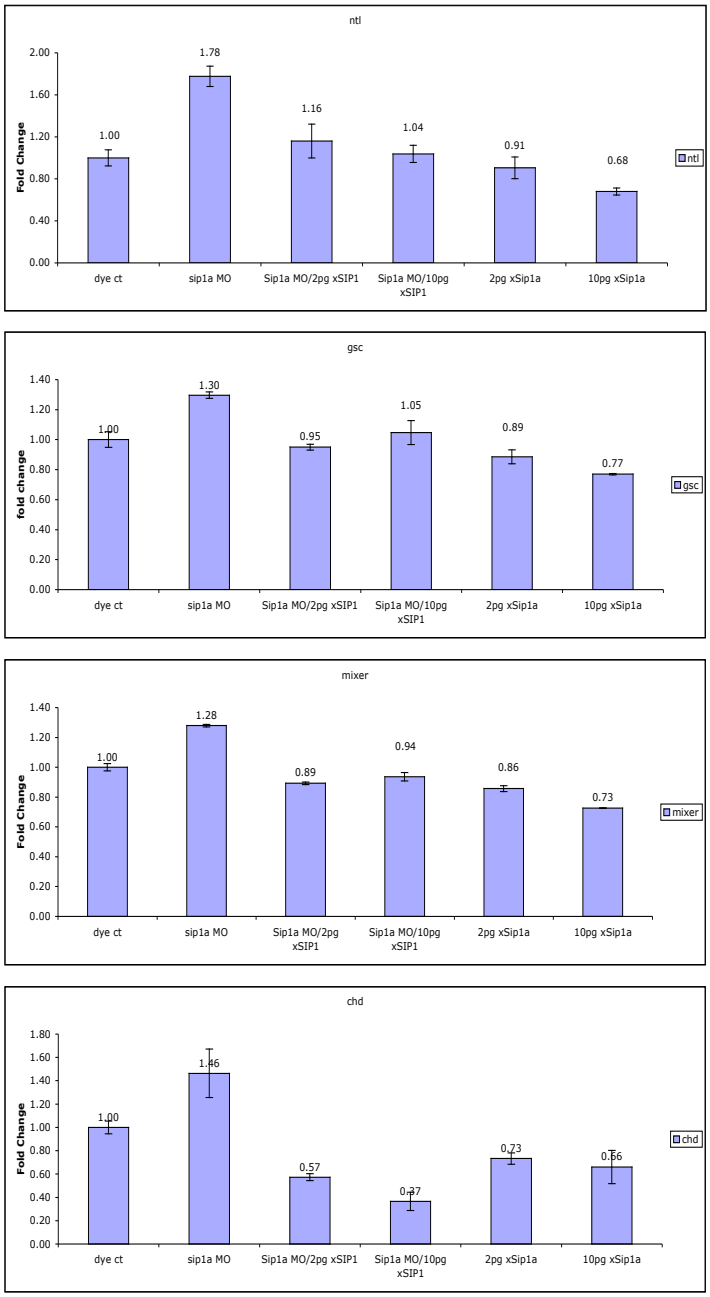

Figure A.3. The effects of *Sip1a* Morpholino injection can be rescued by *Xenopus Sip1* mRNA. Overexpression of a morpholino directed towards the Sip1a gene results in modest increases in mesodermal (*ntl*, *chd*, and *gsc)* and endodermal (*mixer*) gene expression. Conversely, overexpression of *Xenopus Sip1* (*xSip1*) mRNA results in little to no effect on mesodermal and endodermal gene expression when either 10pg or 2pg of mRNA is used. Co-injection of the *Sip1a* morpholino along with *xSip1* results in a rescue of the effects of the *Sip1a* morpholino. These results suggest that a morpholino directed towards the *Sip1a* gene has specific effects in knocking down its function. Assayed at shield stage

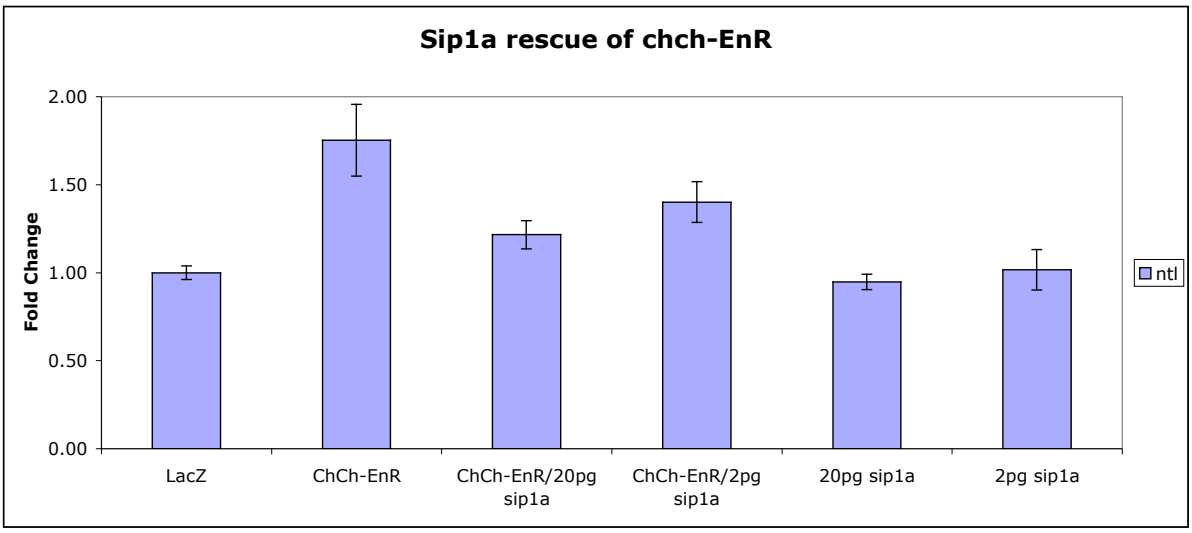

Figure A.4. *Sip1a* overexpression can rescue the effects of *chch*-EnR overexpression. Overexpression of *chch*-EnR results in a 1-fold increase in *ntl* gene expression. Overexpression of either 20pg or 2pg of *Sip1a* mRNA has no effect on ntl expression. Co-injection of both *chch*-EnR and 20pg *Sip1a* mRNA results in a rescue of the *chch*-EnR phenotype, while using 2pg of *Sip1a* mRNA only gives a partial rescue. This result suggests that *Sip1a* can rescue the effects of *chch*-EnR. Assayed at shield stage

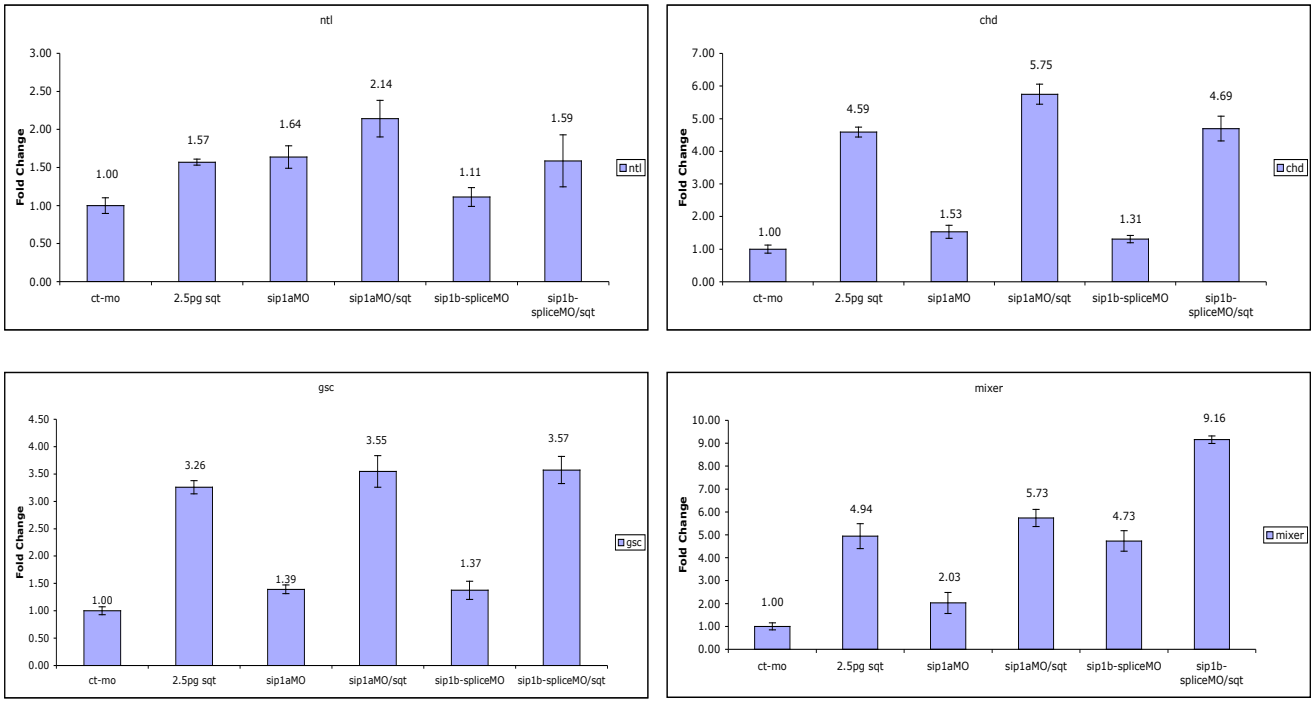

Figure A.5. ***Sip1*** **and sqt have an additive effect on mesodermal and endodermal gene expression**. Overexpression of 2.5pg *sqt* mRNA results in a 1.5 fold increase in *ntl* expression, a 4.5 fold increase of *chd* expression, a 3.5 fold increase in *gsc* expression and a nearly 5 fold increase in *mixer* gene expression. Conversely overexpression of *Sip1a* and *Sip1b* morpholinos results in a similar effect on *ntl* expression, but only has modest effects on *chd*, *gsc* and *mixer* gene expressions, although *Sip1b* inhibition results in a large 4.5 fold increase in *mixer* expression. Co-expression of *Sip1a*/*b* morpholinos along with *sqt* results in an additive effect on mesodermal gene expression. Interestingly co-expression of *Sip1b*MO along with *sqt* results in a synergistic effect on endodermal gene expression. Assayed at shield stage

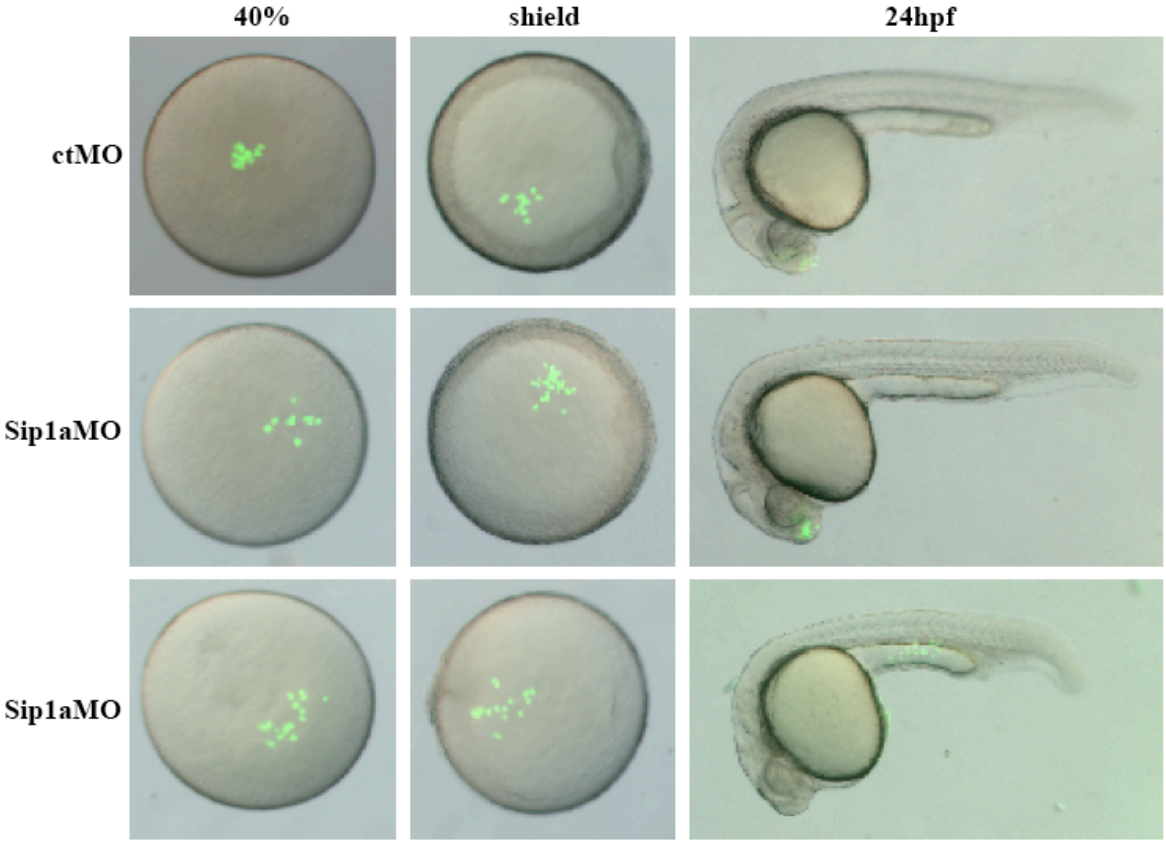

Figure A.6. Isochronic transplantation of *Sip1a* morpholino cells does not have an effect on cell movements. Either ctMO or *Sip1a*MO injected sphere stage cells were transplanted to a sphere stage host embryo. Embryos were observed at 40% epiboly, shield stage and again at 24hpf. The 20 ctMO transplants, the cells did not spread at shield stage and became incorporated into the anterior neural domain. Conversely, 11/31 *Sip1a*MO transplants had cells which mildly spread throughout the ectoderm at shield stage at became incorporated into epidermal domains of the embryo. The remaining 20 embryos behaved in a similar fashion to the ctMO transplants and did not show any effect on cell movements and the cells became incorporated into the anterior neural domain.

Smad interacting protein 1 is a transcription factor that has been identified to have various functions including inhibition of TGF-ß signaling by inhibiting activated Smad1/5 and Smad2/3. Additionally, *Sip1* has been shown to repress mesodermal gene expression and induces neural gene expression. Also, by inhibition of *E-cadherin*, *Sip1* has a role in regulating cell movements. The work presented here is preliminary results on the role of Sip1 in zebrafish development (Comijn et al., 2001; Long et al., 2005; Nitta et al., 2007; van Grunsven et al., 2003; van Grunsven et al., 2007; Vandewalle et al., 2005; Verschueren et al., 1999; Yoshimoto et al., 2005).

In contrast to mouse and *Xenopus*, zebrafish contain two *Sip1* homologues, *Sip1a* and *Sip1b*. Additionally, both of these genes have splice variants present, which have the sixth zinc finger of the protein deleted (Figure A.1). The role of the two genes as well as the splice variants is not yet known. Both *Sip1a* and *Sip1b* are expressed throughout early development. The expression of the Sip1a variants was examined by real-time PCR and showed that the while both are present, transcripts for the full length protein are present at nearly 3 times the levels as compared to the splice variant. The overall effect of this is not yet know and needs to be further examined.

Inhibiting *Sip1a* with a morpholino results in increases in mesodermal and endodermal gene expression. Furthermore, the effects can be rescued by co-expressing *Xenopus Sip1* mRNA, suggesting that the effects of the *Sip1a*MO are specific to knocking down *Sip1a* function. Since *chch* has been shown to regulate *Sip1* expression (Figure 4.3) (Londin et al., 2007b), an assay was performed to determine if *Sip1a* mRNA overexpression can rescue the effects of *chch*-EnR mRNA overexpression (Figure A.4). In fact *Sip1a* can rescue the effects of *chch*-mRNA overexpression further suggesting that *Sip1* is acting in response to *chch* function. It still has to be determined if *Sip1b* can rescue the effects of *chch* inhibition.

chch regulates a transcriptional response to Nodal signaling (Figure 4.9) (Londin et al., 2007b). To determine if this effect of *chch* is acting through *Sip1*, a similar experiment where Nodal signaling is overexpressed while *Sip1* is inhibited was performed. Both *Sip1a* and *Sip1b* inhibition results in modest effects on mesodermal gene expressions (Figure A.5), although a more dramatic endodermal effect is observed upon *Sip1b* inhibition. When *sqt* and *Sip1a/b* are co-expressed, there is an additive effect on mesodermal gene expression. *Sip1b* and *sqt* do exhibit a synergistic effect on endodermal gene expression. The effect that *Sip1a/b* are individually having on mesodermal gene expression may be occurring through an inhibition of Smad2/3 (Postigo, 2003). It is interesting that *Sip1b* has a more profound effect on endodermal gene induction, and is subject to further examination. Also, the individual effect of each *Sip1* gene is having on mesodermal gene expression is modest; the effect of inhibiting both *Sip1* genes simultaneously on mesodermal and endodermal gene expression should be examined. *Sip1* also interacts with Smad1/5 in the BMP pathway (Postigo, 2003), and the effect of inhibiting these genes on this pathway should be investigated.

Sip1 is known to inhibit *E-cadherin* expression (Comijn et al., 2001; van Grunsven et al., 2003), resulting in a regulation of cell movements. *chch* inhibition does have a clear effect on regulating cell movements (Figures 4.5-4.6) (Londin et al., 2007b), which may act through *Sip1*. To determine this, a cell transplant assay was used to determine the effect of *Sip1a* on cell movements. Here, *Sip1a* inhibition results in modest effects on cell movements (Figure A.6). This modest effect may be due to the presence of *Sip1b* present within the

embryo. The *Sip1b* gene may compensate for the loss of *Sip1a* expression. To observe an effect on cell movements, both *Sip1* genes may have to be inhibited.

These preliminary results suggest that *Sip1* does have an effect on mesodermal gene expression, although the exact role that it is having still has to be examined. The presence of two *Sip1* genes may allow for redundant activities between the two genes, confusing the identification of the genes function. In addition, the presence of splice isoforms may further confuse the identification of the genes function and they may be present to further regulate *Sip1's* function at various times during development. These two isoforms may have different activities or cooperate together to perform *Sip1s* function. Additional work is needed to further identify the role of the *Sip1* genes during development and its interaction with *chch*.

A.4 Reference:

Comijn, J., Berx, G., Vermassen, P., Verschueren, K., van Grunsven, L., Bruyneel, E., Mareel, M., Huylebroeck, D. and van Roy, F. (2001). The two-handed E box binding zinc finger protein SIP1 downregulates E-cadherin and induces invasion. *Mol Cell* 7, 1267-78.

Londin, E. R., Mentzer, L., Gates, K. P. and Sirotkin, H. I. (2007a). Expression and regulation of the zinc finger transcription factor Churchill during zebrafish development. *Gene Ex pr. Pattern* Do1:10.1016/j.modgep.2007.04.002**.**

Londin, E. R., Mentzer, L. and Sirotkin, H. I. (2007b). Churchill regulates cell movement and mesoderm specification by repressing Nodal signaling. *BMC Developmental Biology* 7:120.

Long, J., Zuo, D. and Park, M. (2005). Pc2-mediated sumoylation of Smad-interacting protein 1 attenuates transcriptional repression of E-cadherin. *J Biol Chem* 280, 35477-89.

Nitta, K. R., Takahashi, S., Haramoto, Y., Fukuda, M., Tanegashima, K., Onuma, Y. and Asashima, M. (2007). The N-terminus zinc finger domain of Xenopus SIP1 is important for neural induction, but not for suppression of Xbra expression. *Int J Dev Biol* 51, 321-5.

Postigo, A. A. (2003). Opposing functions of ZEB proteins in the regulation of the TGFbeta/BMP signaling pathway. *Embo J* 22, 2443-52**.**

Postigo, A. A., Depp, J. L., Taylor, J. J. and Kroll, K. L. (2003). Regulation of Smad signaling through a differential recruitment of coactivators and corepressors by ZEB proteins. *Embo J* 22, 2453-62.

Sheng, G., dos Reis, M. and Stern, C. D. (2003). Churchill, a zinc finger transcriptional activator, regulates the transition between gastrulation and neurulation. *Cell* 115, 603-13.

van Grunsven, L. A., Michiels, C., Van de Putte, T., Nelles, L., Wuytens, G., Verschueren, K. and Huylebroeck, D. (2003). Interaction between Smad-interacting protein-1 and the corepressor C-terminal binding protein is dispensable for transcriptional repression of E-cadherin. *J Biol Chem* 278, 26135-45.

van Grunsven, L. A., Taelman, V., Michiels, C., Verstappen, G., Souopgui, J., Nichane, M., Moens, E., Opdecamp, K., Vanhomwegen, J., Kricha, S., Huylebroeck, D. and Bellefroid, E. J. (2007). XSip1 neuralizing activity involves the co-repressor CtBP and occurs through BMP dependent and independent mechanisms. *Dev Biol* 306, 34-49.

Vandewalle, C., Comijn, J., De Craene, B., Vermassen, P., Bruyneel, E., Andersen, H., Tulchinsky, E., Van Roy, F. and Berx, G. (2005). SIP1/ZEB2 induces EMT by repressing genes of different epithelial cell-cell junctions. *Nucleic Acids Res* 33, 6566-78.

Verschueren, K., Remacle, J. E., Collart, C., Kraft, H., Baker, B. S., Tylzanowski, P., Nelles, L., Wuytens, G., Su, M. T., Bodmer, R., Smith, J. C. and Huylebroeck, D. (1999). SIP1, a novel zinc finger/homeodomain repressor, interacts with Smad proteins and binds to 5'-CACCT sequences in candidate target genes. *J Biol Chem* 274, 20489-98.

Yoshimoto, A., Saigou, Y., Higashi, Y. and Kondoh, H. (2005). Regulation of ocular lens development by Smad-interacting protein 1 involving Foxe3 activation. *Development* 132, 4437-48.